

INFORMATION TO USERS

This manuscript has been reproduced from the microfilm master. UMI films the text directly from the original or copy submitted. Thus, some thesis and dissertation copies are in typewriter face, while others may be from any type of computer printer.

The quality of this reproduction is dependent upon the quality of the copy submitted. Broken or indistinct print, colored or poor quality illustrations and photographs, print bleedthrough, substandard margins, and improper alignment can adversely affect reproduction.

In the unlikely event that the author did not send UMI a complete manuscript and there are missing pages, these will be noted. Also, if unauthorized copyright material had to be removed, a note will indicate the deletion.

Oversize materials (e.g., maps, drawings, charts) are reproduced by sectioning the original, beginning at the upper left-hand corner and continuing from left to right in equal sections with small overlaps. Each original is also photographed in one exposure and is included in reduced form at the back of the book.

Photographs included in the original manuscript have been reproduced xerographically in this copy. Higher quality 6" x 9" black and white photographic prints are available for any photographs or illustrations appearing in this copy for an additional charge. Contact UMI directly to order.

UMI

A Bell & Howell Information Company
300 North Zeeb Road, Ann Arbor, MI 48106-1346 USA
313/761-4700 800/521-0600

RECONSTRUCTION OF LATE-PLEISTOCENE
EQUILIBRIUM-LINE ALTITUDES AND PALEOENVIRONMENTS:
UINTA MOUNTAINS, UTAH AND WYOMING

A Dissertation

by

GREG C. SCHLENKER

Submitted to the Office of Graduate Studies of
Texas A&M University
in partial fulfillment of the requirements for the degree of
DOCTOR OF PHILOSOPHY

December 1995

Major Subject: Geography

UMI Number: 9615883

UMI Microform 9615883
Copyright 1996, by UMI Company. All rights reserved.

**This microform edition is protected against unauthorized
copying under Title 17, United States Code.**

UMI
300 North Zeeb Road
Ann Arbor, MI 48103

RECONSTRUCTION OF LATE-PLEISTOCENE
EQUILIBRIUM-LINE ALTITUDES AND PALEOENVIRONMENTS:
UINTA MOUNTAINS, UTAH AND WYOMING

A Dissertation

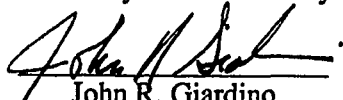
by

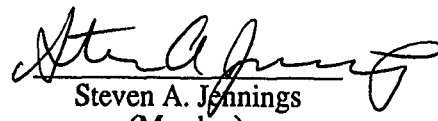
GREG C. SCHLENKER

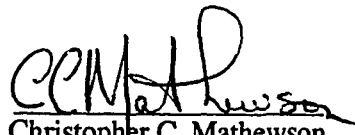
Submitted to Texas A&M University
in partial fulfillment of the requirements
for the degree of


DOCTOR OF PHILOSOPHY


Approved as to style and content by:



John R. Giardino
(Chair of Committee)


Steven A. Jennings
(Member)


Christopher C. Mathewson
(Member)


Vatche P. Tchakerian
(Member)


Michael R. Waters
(Member)


John R. Giardino
(Head of Department)

December 1995

Major Subject: Geography

ABSTRACT

**Reconstruction of Late-Pleistocene
Equilibrium-Line Altitudes and Paleoenvironments:
Uinta Mountains, Utah and Wyoming. (December 1995)
Greg C. Schlenker, B.S., Weber State College;
M.S., University of Utah
Chairman of Advisory Committee: Dr. John R. Giardino**

Climatic and paleoenvironmental changes of the Uinta Mountains are estimated by comparing oxygen isotope stage six (155 ka BP to 130 ka BP) and oxygen isotope stage two (30 ka BP to 12 ka BP) age glacial equilibrium-line altitude (ELA) trend surfaces to present (i.e., 1972 to 1990) snow accumulation trend surfaces. Whereas the present ELA was estimated from snow accumulation and regional climate data, Pleistocene full-glacial ELAs were estimated from reconstructed glacial geomorphology. Present snow accumulation and regional climatic data are also evaluated to understand relationships between snow accumulation patterns and climate variability. The evaluations reveal that snow accumulation trend surfaces have steeper gradients during moist winters and slope in the general direction of the upper-level airflow. The present and Pleistocene ELA surfaces were compared to estimate temperature, precipitation, and airflow variations. These variations include: (1) a 9.6° C to 12.2° C decrease in Pleistocene temperatures; (2) a Pleistocene snow accumulation reduction from 71 % to 68 % of present levels; and (3) Pleistocene ELA surfaces sloping to the east rather than to the northeast, suggesting a more zonal airflow than present.

The differences between the Pleistocene and present ELA surfaces indicate that major climatic variability has occurred. Temperature differences are in general agreement with estimates from other investigations in the region. Although Pleistocene precipitation is estimated to have been less than present, the moisture supply to the Uinta Mountains appears to have been influenced by paleolakes to the west in the Bonneville Basin. The Pleistocene air-flow is projected to have been more zonal than present. Where climate differences are shown to exist between the glacial episodes and present, temperature and precipitation differences between the stage six and the stage two glacial episodes are also thought to have occurred.

ACKNOWLEDGMENTS

The culmination of this research represents contributions by many people. I wish to acknowledge Randal Julander and the staff of the Salt Lake City Soil Conservation Service Office for assisting me in the acquisition of snow accumulation data. Timothy Stratman of the Texas A&M University Geographic Information Technologies Laboratory who provided ample advice and guidance on GIS applications. The staff of the Utah State University Utah Climate Center including Donald Jenson, Greg McCurdy and Dawn Drost were essential for obtaining high-altitude weather data. Brian Haslam and John Storm of the University of Utah DIGIT Laboratory were also helpful for processing the weather data.

Discussions with a number of individuals including, Donald Currey, Jeffery Keaton, David Wilkins, Derek Ryter, John Love, Bill Mulvey, Merrill Ridd, Donald Jenson and Paul Larson have all contributed to concepts explored in this dissertation. Editorial comments from Janet Nystrom were invaluable in preparation this dissertation. The members of my Advisory Committee including John Giardino, Steven Jennings, Christopher Mathewson, Vatche Tchakerian and Michael Waters are acknowledged not only for their advisory guidance, but also the patience in seeing this endeavor through.

Many friends and colleagues should take credit for their help and consideration during the duration of my studies. Individuals that I wish to name include Peter Karczewski, Rita Roybal, Barbara Chisholm-Faries, David and Marjorie Wilkins, Michael Camille and Terri Stoker. I also wish to acknowledge Jeffery Keaton and William Gordon for providing steady employment during this time. Foremost, I wish to acknowledge the support and interest that was provided by my parents, Joseph and Eunice Schlenker, and my brother Stephen Schlenker who managed to obtain his doctorate ahead of me.

TABLE OF CONTENTS

	Page
ABSTRACT.....	iii
ACKNOWLEDGMENTS.....	v
TABLE OF CONTENTS.....	vi
LIST OF TABLES.....	viii
LIST OF FIGURES.....	x
LIST OF SYMBOLS.....	xii
CHAPTER	
I INTRODUCTION.....	1
Statement Of Problem.....	1
Objective Of Research.....	2
Background.....	3
The Quaternary Period.....	3
Equilibrium-line Altitudes.....	6
The Uinta Mountains.....	8
Research Design.....	11
Trend Surface Analysis And Methodology.....	11
Data Resources.....	13
Snow Accumulation Data.....	13
Climate Data.....	14
Spatial Analysis Data.....	14
Method Of Analysis.....	15
Model Synthesis.....	15
II STUDY AREA DESCRIPTION.....	17
Location And Physiography.....	17
Study Area Climate.....	21
Study Area Vegetation.....	30
Study Area Selection.....	31
III ANALYSIS OF SNOW ACCUMULATION AND CLIMATIC VARIABILITY.....	34
Introduction.....	34
Snow Accumulation Data Resources.....	35
Analysis Of Snow Accumulation Data.....	38

CHAPTER	Page
	Analysis Of Snow Accumulation Patterns And Climate Variability..... 39
	Synthesis Of Present ELA..... 47
IV	RECONSTRUCTION OF LATE-PLEISTOCENE EQUILIBRIUM- LINE ALTITUDES: METHODS AND ANALYSIS..... 53
	Introduction..... 53
	Estimation Of Late-Pleistocene ELA..... 54
	GIS Data Resources And Data Base Construction..... 56
	Analysis Of Late-Pleistocene ELA Trend Surfaces..... 62
V	RECONSTRUCTION OF LATE-PLEISTOCENE CLIMATES..... 75
	Temperature, Snow Accumulation, And Wind Direction Estimates..... 75
	Temperature Change Estimates..... 75
	Snow Accumulation Estimates..... 79
	Wind Direction Estimates..... 87
	Summary Of Estimates..... 89
VI	LATE-PLEISTOCENE PALEOENVIRONMENTS..... 92
	Discussion Of Full-Glacial Climate Estimates..... 92
	Full-Glacial Temperature..... 92
	Full-Glacial Precipitation..... 95
	Paleolakes And The Uinta Mountains..... 98
	Full-Glacial Air Flow..... 104
	Synthesis Of Paleoenvironments..... 106
VII	CONCLUSION..... 113
	Summary Of Research Results..... 113
	Qualification Of Findings..... 118
	Future Research..... 118
	REFERENCES CITED..... 120
	APPENDIX A REGIONAL CLIMATE DATA..... 126
	APPENDIX B SNOW SURVEY DATA..... 130
	APPENDIX C SNOW ACCUMULATION TREND SURFACE STATISTICS..... 136
	APPENDIX D RECONSTRUCTED GLACIER PARAMETERS..... 139
	VITA..... 146

LIST OF TABLES

TABLE		Page
1	Climate Data For Selected Weather Stations.....	22
2	Climate Data For Selected NOAA Weather Divisions.....	24
3	Annual And Summer High Altitude Temperature Data And Lapse Rate Means For Selected National Weather Service Stations.....	28
4	Interpolated Annual And Summer High Altitude Temperature Data And Lapse Rate Means For The Uinta Mountain Study Area.....	29
5	Snow Survey Measurements Uinta Mountains 1972 To 1990.....	36
6	Annual Snow Accumulation Trend Surface Statistics 1972 To 1990.....	41
7	Annual Snow Accumulation Trend Surface Parameters And Mean Regional Winter Climate Data 1972 To 1990.....	43
8	Correlation Matrix Of 1972 To 1990 Annual Snow Accumulation Trend Surface Parameters And Mean Regional Winter Climate Data.....	44
9	Regression Analysis Of Annual Snow Accumulation Trend Surface Parameters And Mean Regional Winter Climate Data 1972 To 1990...	45
10	Estimated Present ELA From 1972 To 1990 Snow Accumulation Values.....	51
11	Oxygen Isotope Stage Six Reconstructed Glaciers.....	60
12	Oxygen Isotope Stage Two Reconstructed Glaciers.....	61
13	Full-Glacial ELA Trend Surface Statistics.....	63
14	Oxygen Isotope Stage Six ELA Parameters At 0.55 AAR.....	64
15	Oxygen Isotope Stage Two ELA Parameters At 0.55 AAR.....	65
16	Oxygen Isotope Stage Six 0.55 AAR ELA Trend Surface Residuals And Areal Parameters Of Reconstructed Glacial Extent.....	71
17	Oxygen Isotope Stage Two 0.55 AAR ELA Trend Surface Residuals And Areal Parameters Of Reconstructed Glacial Extent.....	72

TABLE	Page
18	Correlation Table Of Oxygen Isotope Stage Six And Stage Two 0.55 AAR ELA Trend Surface Residuals And Areal Parameters Of Reconstructed Glacial Extent..... 73
19	Oxygen Isotope Stage Six ELA Estimates Including Unmeasured Basins. 77
20	Full-Glacial Temperature Change Estimates..... 78
21	Oxygen Isotope Stage Six ELA Temperature Estimates..... 80
22	Oxygen Isotope Stage Two ELA Temperature Estimates..... 81
23	Estimated Oxygen Isotope Stage ELA Six Snow Accumulation And Difference From Present Snow Accumulation Estimates..... 83
24	Estimated Oxygen Isotope Stage Two ELA Snow Accumulation And Difference From Present Snow Accumulation Estimates..... 84
25	Comparison Of Full-Glacial Snow Accumulation Estimates..... 88
26	Summary Data Of Full-Glacial Temperature, Snow Accumulation, And Wind Direction Estimates..... 90
27	ELA Of Selected Locations On A 40°30' North Latitude Transect From The Pacific Ocean To The Colorado Rocky Mountains..... 102
28	Median Altitude Of Reconstructed Isotope Stage Two Glaciers In The Uinta Mountains And The Eastern Great Basin..... 111

LIST OF FIGURES

FIGURE		Page
1	Study area location.....	9
2	Research design.....	16
3	Detailed map of study area.....	18
4	Generalized topographic map of study area.....	20
5	Climographs of selected local weather stations.....	23
6	Climographs of selected NOAA weather divisions.....	25
7	Location map of selected local weather stations, NOAA divisional boundaries and National Weather Service Office stations.....	27
8	Schematic digital elevation model of the study area.....	33
9	Location map of operating snow survey sites in the Uinta Mountains.....	37
10	Mean 1972 to 1990 snow accumulation trend surface map.....	40
11	Relationship of winter accumulation and summer temperature at ELA sites world wide.....	49
12	Low and high present estimated ELA trend surfaces.....	52
13	Reconstructed oxygen isotope stage six glaciers.....	58
14	Reconstructed oxygen isotope stage two glaciers.....	59
15	Oxygen Isotope stage six 0.55 AAR ELA trend surface.....	66
16	Oxygen Isotope stage two 0.55 AAR ELA trend surface.....	67
17	Estimated oxygen isotope stage six mean snow accumulation trend surface.....	85
18	Estimated oxygen isotope stage two mean snow accumulation trend surface.....	86
19	Study area and adjacent Bonneville Basin.....	100

FIGURE		Page
20	ELA height transect from Pacific Ocean east to the Colorado Rocky Mountains along 40°30' N latitude.....	103
21	Generalized contours of median altitudes of reconstructed glaciers for sites in the Uinta Mountains and Eastern Great Basin.....	112
22	Transects of past and present ELA trend surfaces.....	115

LIST OF SYMBOLS

Lat = Degrees north latitude

Lon = Degrees west longitude

A = Snow accumulation in centimeters

Elev = Elevation in meters

R = Correlation coefficient

n = Number of cases

p = Probability statistic

r = Pearson product-moment correlation coefficient

*X*₁ = Dependent regression variable

*X*₂ and *X*₃ = Independent regression variables

*T*_{vi-viii} = Mean June through August temperature

*L*_{vi-viii} = Mean June through August lapse rate

*ZT*_{0°vi-viii} = Mean June through August 0° C isotherm altitude

ZELA = Present estimated ELA

*T*_c = Temperature change

*ELA*_m = Present estimated mean ELA

*ELA*_p = Pleistocene mean ELA

*L*_n = Normal lapse rate

*ELA*_t = Estimated temperature at ELA

*0°C*_h = Estimated 0° C isotherm altitude

Dir = Trend surface direction

Gra = Trend surface gradient

Wnd = Wind direction

CHAPTER 1

INTRODUCTION

Statement Of Problem

Climate is dynamic, and it is this dynamic nature that is responsible for changes to the earth's surface over time and space. Thus, the history of the earth has been punctuated with changes in its climate. These changes have oscillated from warm to cold and visa versa. With each of these oscillations has been long periods of relative stability (Fisher, 1981). These various oscillations have been both gradual and rapid, and in view of the complete calendar of earth history, there does not appear to be an exact predictable cyclic occurrence of change (Imbrie and Imbrie, 1979).

It has been widely recognized that the climate during the Pleistocene varied significantly from the present. Understanding both climate variability and the forces that have controlled variability in the past is an important step in understanding climatic and environmental changes occurring today. Whereas an understanding of these changes can be gained through the reconstruction of past environments, various researchers have utilized a number of differing techniques to study these changes. Although a substantial number of investigations have been conducted (Galloway, 1970; Porter, 1977; Brackenridge, 1978; Madsen and Currey, 1979; Wells, 1979; Zwick, 1980; Dohrenwend, 1984; Leonard, 1984; Spaulding and Graumlich, 1986; Zielinski and McCoy, 1987; Burbank, 1989; Leonard, 1989; Locke, 1990), the scale of Pleistocene climatic and environmental change in the western United States is not fully understood.

This dissertation conforms to the style and format of the Geological Society of America Bulletin.

Albeit, cooler temperatures are known to have prevailed during the Pleistocene full-glacial episodes, other changes to climate and environmental systems such as precipitation levels and air-mass movement are not well known. To gain a stronger understanding as to the climatic and environmental system changes that have occurred, this dissertation examines present climate and reconstructed glacial geomorphology of the Uinta Mountains to reconstruct the climate and environmental systems that existed during the Pleistocene full-glacial episodes. Thus, the problem statement for this research can be stated as a question: Can the climate and environmental systems of the late Pleistocene full-glacial episodes in the Uinta Mountains be reconstructed from present climate and environmental systems data, and late Pleistocene glacial geomorphology?

Through the examination of climate-change parameters and regional paleoenvironmental models, the intent of this dissertation was to answer three questions regarding the Pleistocene climate of the Uinta Mountains during the last two full-glacial episodes: (1) How much colder were temperatures during the full-glacial episodes? (2) Was the full-glacial precipitation significantly different from present? (3) If precipitation differed greatly, what environmental conditions would bring about this difference?

Objective of Research

The objective of this dissertation is to reconstruct the paleoenvironmental setting of the Uinta Mountains during the last two Pleistocene full-glacial episodes. Through the reconstruction of the last two Pleistocene full-glacial equilibrium-line altitudes (ELAs), and the comparison of the past ELAs with the present climatic conditions, the following full-glacial paleoclimatic parameters are reconstructed for the Uinta mountains: (1) the altitudinal variation of temperature; (2) the variation of precipitation quantity; and (3) the spatial variation of precipitation patterns. From these paleoclimatic parameters a paleoenvironmental model of full-glacial conditions of the Uinta Mountains is constructed

and evaluated to determine concurrence with global and regional climate and environmental change models (Barry, 1983; CLIMAP, 1976; COHMAP, 1988; Porter et al., 1983).

Background

The scope of this research falls into three general subject areas. These areas include: (1) the Quaternary Period and full-glacial environments; (2) the concept of ELAs and paleoclimate reconstruction; and (3) the Uinta Mountains, the area that has been selected for this study. Each of these subject areas and their importance to the objective of this dissertation are discussed in the following sections.

The Quaternary Period

The Quaternary Period spans the past 1.6 million years of geologic time and is studied on many disciplinary fronts to answer questions regarding environmental change of both the past and the present and to predict for the future. Foremost to Quaternary research is the reconstruction of past climate regimes and the explanation of the forces that have governed climate variability (Bradley, 1985). The reconstruction of past environments enables the measures of both the frequency and the range of climatic change. The explanation of climatic variability is studied to understand the duration, timing, and recurrence of these past events, as well as climate change processes. Without full comprehension of climatic variability consequent to natural processes, it is difficult to identify the effect of present human activities on climate change (Bradley, 1985). The reconstruction of Quaternary environments also explains the effect of climate variability in respect to environmental change. Through the study of past and present distributions, such as biotic or morphogenetic distributions, the past and present can be better understood in the context of environmental change. Additionally, the Quaternary Period is the most recent and well preserved segment of earth history, the reconstruction of which enables the

understanding of events and the recurrence of such events that are critical to human activity, as well as an understanding of human evolution.

The Quaternary is characterized as a period of climatic variability that has been subject to glacial and interglacial climatic episodes. The glacial episodes were marked by conditions much cooler than present, resulting in the expansion of glacial ice at locations of high latitude and high elevation (Bradley, 1985). During the Quaternary, climate and biotic boundaries are also known to have undergone meridional and elevational shifts with the transgression and regression of glacial episodes (Butzer, 1982). In concert with these boundary shifts, changes in the tropospheric circulation patterns are also believed to have occurred producing circulation patterns different from present patterns (CLIMAP, 1976; Gates, 1976; Barry 1983; COHMAP, 1988; Crowley and North, 1991). Interglacial episodes have been shown to punctuate the glacial episodes throughout the Quaternary (Bowen, 1978). The environmental conditions of the interglacial periods are believed to be much the same as those of the present and perhaps hosted climates that were warmer than present (Coope, 1974).

The Quaternary Period includes the Pleistocene and Holocene epochs. The Pleistocene, 1.6 million years BP to 10,000 BP, consisted of both glacial and interglacial periods. The Holocene interglacial, 10,000 BP to present, is thought to be the last in the series of glacial and interglacial episodes (Imbrie and Imbrie, 1979). Although not exhibiting the same highly variable conditions as the Pleistocene, the Holocene record shows evidence of significant climatic variability, from which future predictions remain unsure (Imbrie and Imbrie, 1979; Currey and James, 1982).

Long-term climatic oscillations have been documented from the isotopic record recovered from deep sea cores. Oxygen isotope ratios from the deep sea record provides an index of temperature change (Bowen, 1978). The cold and warm oscillations are defined as oxygen isotope stages, with the even numbered stages (i.e., oxygen isotope

stage six and stage two) representing glacial cycles and the odd numbered stages representing interglacial cycles. Although a relatively comprehensive record of Quaternary climate is documented within the oxygen isotope record of deep sea cores (Bowen, 1978; Imbrie and Imbrie, 1979), investigation of the less-comprehensive terrestrial settings enables the understanding of paleoclimate and environmental change at a more provincial level. Through the interpretation of diagnostic process-dependent morphogenetic landforms and fossil assemblages, the environments of the past can be reconstructed (Brackenridge, 1978; Wells, 1979). In alpine regions, the reconstruction of Quaternary glacial environments has enabled the interpretation of temperature and precipitation regimes of the past (Zielinski and McCoy, 1987; Leonard, 1989) and has even lead to explanations regarding atmospheric circulation patterns during the glaciations (Pierce, 1979; Porter et al., 1983; Hawkins, 1985).

In the Rocky Mountains two major glacial episodes are known to have occurred in the past 150,000 years (Mears, 1974, Pierce, et al., 1976). In the Rocky Mountain region these glaciations are referred to as the Bull Lake and the Pinedale episodes. The Bull Lake episode has been estimated to have occurred between 155,000 BP and 130,000 BP (Pierce et al., 1976), equivalent to oxygen isotope stage six, and the Pinedale age has been estimated to have occurred between 30,000 BP and 12,000 BP (Madole, 1986), equivalent to oxygen isotope stage two (Shackleton and Opdyke, 1973). Remnant glacial landforms reveal the extent of ice during the glacial episodes, which in turn is used to construct temperature and precipitation models (Leonard, 1989). Among the number of model construction methods is the analysis of paleoclimatic snow-lines (i.e., equilibrium-line altitudes or ELA). These snow-lines are a function of the elevation of glaciation, which is predominantly controlled by the prevailing climate.

Although evidence of past glaciation and climate change has been well documented from geomorphic phenomena, the mechanisms of Pleistocene glaciation are not entirely

known and are subject to regional variation. Nevertheless, certain parameters have been used to explain Pleistocene glaciations. Generally, a cooler temperature regime is accepted as a primary cause of Pleistocene glaciation. However, making the distinction between changes in precipitation and temperature is problematic because both parameters are climatically linked. For example, a decrease in temperature without a change in precipitation may result in a higher effective moisture regime, which in turn can be interpreted as increased precipitation. Thus, the effect of precipitation, whether increased or decreased, is difficult to measure and not well understood (Leonard, 1989). Changing atmospheric and circulation patterns are likewise difficult to ascertain. Although the Northern Hemisphere circulation pattern is believed to have depressed southward during Pleistocene glaciations (Gates, 1976), evidence for this change is sparse (Porter et al., 1983).

Equilibrium-line Altitudes

ELAs are the discrete elevations at which accumulation and ablation on the surface of a glacier is balanced (Flint, 1957; Østem, 1966; Meierding, 1982). ELAs are a function of glacier mass balance and will vary in elevation both spatially and temporally in response to environmental controls. These controls include: air-mass circulation (Pierce, 1979), proximity to moisture source (Locke, 1990), and physiographic effects (Graf, 1976). For example, where temperature and precipitation favor accumulation, equilibrium-lines are found at relatively low elevations, whereby locations that experience either warmer temperatures or lower precipitation rates will have higher ELAs. This condition is exemplified in the western United States where equilibrium-lines are found at relatively low elevations near the Pacific Coast. Inland from the coast, more continental climatic conditions prevail, and equilibrium-lines are found at progressively higher elevations (Porter et al., 1983). Furthermore, Graf (1976) has shown that present-day glaciers in the

Rocky Mountains are usually found only at locations that are geomorphically optimal for the accumulation and preservation of year-round snowpack.

The reconstruction of past ELAs is based on the height of morphogenetic phenomena such as cirques and lateral moraines, the height of glaciated summits versus unglaciated summits, and height and area ratios of formerly ice-covered areas (Meierding, 1982). These methods are discussed in detail in Chapter 4. Present ELAs can be determined from direct observations of glaciers, and at sites where present glaciers are absent, the ELA can be estimated from climate and snow accumulation data (Leonard, 1984; Zielinski and McCoy, 1987).

Reconstructed Pleistocene ELAs are used to reconstruct paleoclimatic conditions of an area or region of study. Through comparison of Pleistocene with present ELAs, explanations of both spatial and temporal climatic variability of a study area can be given. Trend surface analysis (Unwin, 1979; Krumbain and Graybill, 1965) has been commonly used to compare present and Pleistocene ELAs (Peterson and Robinson, 1969; Meierding, 1982; Mulvey, 1985; Locke, 1989; Locke, 1990). Trend surface analysis is an analytical method for evaluating change over space. By reducing spatially distributed variables to a three-dimensional best-fit surface, regional trends can be evaluated (Unwin, 1979). Paleoclimatic conditions are evaluated by differences in the height, gradient and direction of trend surfaces. Differing trend surface heights indicate temperature difference. Differing trend surface slope gradients indicate a change in the quantity of precipitation moisture (Porter, 1977), and lower trend surface gradients have been attributed to dryer conditions (Miller et al., 1975). Where trend surfaces slope in different cardinal directions, air-mass circulation or moisture source is believed to have changed significantly (Hawkins, 1985).

In many cases, Pleistocene ELA surface directions and gradients have been shown to correspond closely to present snow accumulation and ELA surface directions and gradients (Dohrenwend, 1984; Leonard, 1984). Where the direction and gradient of the

reconstructed Pleistocene ELA is shown to correspond to present snow accumulation patterns, little change between the present and Pleistocene precipitation and/or moisture source is believed to have occurred. However, in some cases investigators have shown where ELA surfaces have varied significantly between the present and Pleistocene, indicating differing precipitation patterns and/or moisture supply (Hawkins, 1985; Zielinski and McCoy, 1987).

Although climate in the western United States is believed to have been drier than present during the glacial episodes (Crowley and North, 1991), many researchers have found that precipitation patterns were largely unchanged during the full-glacial conditions, whereas temperatures were significantly lowered (Brackenridge, 1987; Leonard, 1984; Zwick, 1980; Locke, 1990). On the other hand, a number of studies suggests that precipitation indeed differed during the glacial episodes (Galloway, 1970; Wells, 1979; Gates, 1976; Spaulding and Graumlich, 1986; Zielinski and McCoy, 1987; Burbank, 1991; Jennings and Elliott-Fisk, 1993). The discrepancy between these two theories points to the need for further investigation of this problem.

The Uinta Mountains

The Uinta Mountains are part of the Rocky Mountain System (Figure 1) and are part of the Middle Rocky Mountain Physiographic Province (Hunt 1967). The Uinta Mountains have been the subject of a number of geoscience investigations and reconnaissances, beginning as early as 1869 with John Wesley Powell's expedition on the Green and Colorado Rivers (Stokes, 1969). The first systematic survey of the glacial geomorphology of the Uinta Mountains was carried out by Wallace Atwood (1909), who mapped and described the glacial deposits of the entire range. Atwood mapped and identified two stages of late-Pleistocene glaciation and speculated on the possibility of a third earlier stage.

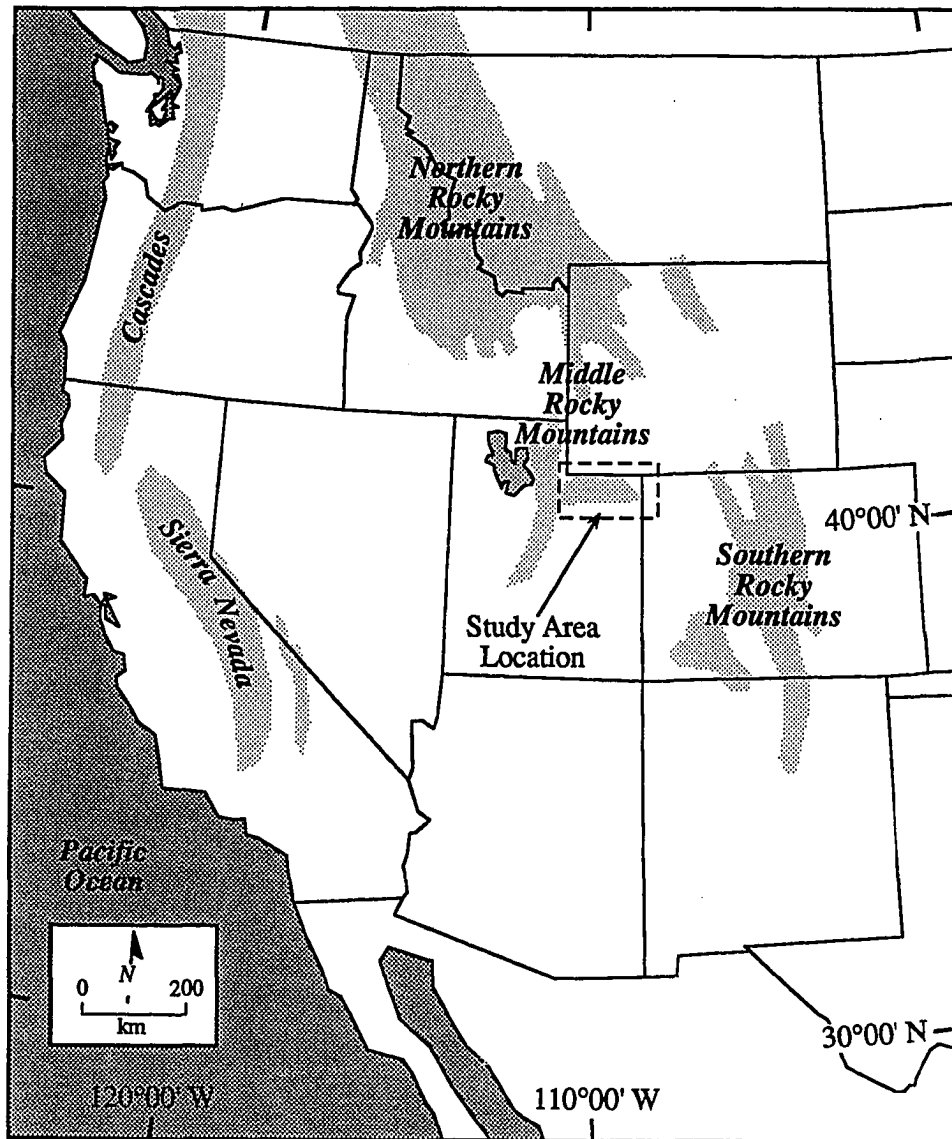


Figure 1. Study area location.

Wilmot Bradley (1936) investigated the geomorphology of the "North Flank" of the Uinta Mountains. Although Bradley's (1936) study focused on piedmont forms of the north slope, he also discussed and mapped Pleistocene glacial landforms in the area. Bradley verified Atwood's two stages of Pleistocene glaciation and confirmed the third earlier stage. Bradley (1936) named these three glacial stages after locations on the north slope of the range where prominent, distinguishing deposits of these stages are found. These stages are: the Little Dry, the Blacks Fork, and the Smiths Fork (oldest to youngest, Bradley 1936). Bradley (1936) also noted that the three stages showed morphogenetic correspondence to Blackwelder's (1915) Buffalo, Bull Lake, and Pinedale stages of glaciation in the Wind River Mountains. Blackwelder's (1915) Buffalo stage has since been revised by Richmond (1965), who has subdivided it into three glaciations, collectively referred to as pre-Bull Lake.

More recent investigations in the Uinta Mountains by Schoenfeld (1969), Barnhardt (1973), Grogger (1974), Gilmer (1986) and Schlenker (1988) have also demonstrated morphostratigraphic correlation with the Rocky Mountain glacial model. Schoenfeld (1969) mapped and described Pleistocene glacial deposits in the Burnt Fork area on the northeast side of the range. He recognized both sequential and morphological correlations of the Burnt Fork deposits with those of the Wind River area. Barnhardt (1973) investigated the late-Pleistocene and Holocene glacial and periglacial geomorphology of the Bald Mountain area on the west side of the range. Grogger (1974) identified and mapped late-Pleistocene and Holocene landforms throughout the High Uintas Primitive Area (i.e., now a designated wilderness area). Gilmer (1986) investigated landslide phenomenon in the Blacks Fork and Smiths Fork drainages. He also identified and mapped glacial moraine deposits and speculated on the relative ages of the glacial deposits. Schlenker (1988) investigated the late-Pleistocene glacial moraine sequence in the Blacks Fork Drainage on the north slope of the range. Relative-age, stratigraphic and morphostratigraphic

relationships observed in the Blacks Fork Drainage were found to verify the conclusions of the previous studies by Atwood (1909) and Bradley (1936). Prior to this present dissertation, no study has been undertaken to locally reconstruct the ELA of the Uinta Mountains.

Research Design

The design of this dissertation research was to reconstruct Pleistocene climate from models derived from present snow-climate relationships. This research was separated into three main steps: (1) spatial analysis of present snow accumulation patterns and the identification of the relationship between snow accumulation patterns and prevailing climatic conditions; (2) spatial analysis of late-Pleistocene ELAs to reconstruct glacial ice accumulation during the last two full-glacial episodes; and (3) reconstruction of late-Pleistocene climate for the two glacial episodes on the basis of variation of ELAs from present patterns of snow accumulation. Spatial analysis employed trend surface analysis. The estimation of the present ELAs was made from the present snow accumulation and climate data, and the estimation of snow accumulation and temperature during the Pleistocene glacial episodes was made from the Pleistocene ELAs and temperature estimates. These steps provided the data necessary so that the trend surfaces of the ELAs, snow accumulation and temperature of the present and the two glacial episodes could be compared.

Trend Surface Analysis And Methodology

Trend surface analysis is used to compare and evaluate change over space. Trend surfaces illustrate the pattern of change using predicted values calculated from observed variables. To estimate climate changes, trend surfaces from present snow accumulation patterns were compared to the trend surfaces from the ELAs of the two glacial episodes.

Additionally, the trend surfaces from the ELAs of the two glacial episodes were compared to produce estimates of climate differences between the episodes. The methodology used follows that of Unwin (1979) and Krumbein and Graybill (1965), and trend surfaces were constructed using Quick Basic[®] programming language and MYSTAT[®] statistical applications software. The trend surface modeling yields a three-dimensional map of snow accumulation or ELAs projected over the study area. The height, gradient and direction of the trend surface slopes were used to make comparisons between surfaces. The data from the trend surface analysis also provided variance statistics useful for the evaluation of the surface trends.

The equation used to calculate height or value (Z_t) on the trend surface is:

$$Z_t = a_0 + a_1 Lat + a_2 Lon \quad (1)$$

where Z_t is the predicted height or value on the surface as determined from northing and easting increments on the surface, Lat (latitude) and Lon (longitude) are northing and easting increments on the surface, a_0 is an origin where Lat and Lon are both equal to zero, and a_1 and a_2 are the rate of surface change along the respective directions (Unwin, 1979). Solving for a_0 , a_1 and a_2 is accomplished as:

$$\begin{aligned} a_0 N &+ a_1 \sum Lat &+ a_2 \sum Lon &= \sum Z_{obs} \\ a_0 \sum Lat &+ a_1 \sum Lat^2 &+ a_2 \sum Lat Lon &= \sum Z_{obs} Lat \\ a_0 \sum Lon &+ a_1 \sum Lat Lon &+ a_2 \sum Lon^2 &= \sum Z_{obs} Lon \end{aligned} \quad (2)$$

where Z_{obs} is the observed height or value, and N is the number of cases in the trend surface population (Unwin, 1979). When several cases are integrated into the calculation of the surface, the value predicted by the trend surface (Z_t) may differ significantly from the observed value (Z_{obs}). Because the differences between the predicted and observed

values can be large, or the population of observed values does not have a significant trend, the surfaces are evaluated using analysis of variance statistics. These statistics include, the trend correlation coefficient, the trend probability statistic, and the standard error of trend estimate. The correlation coefficient (R) is used to evaluate the strength of the surface trend. Surfaces with correlation coefficients ranging from 0.2 to 0.4 are considered to have low trends, from 0.4 to 0.7 are considered to have moderate trends, and from 0.7 to 0.9 are considered to have high trends (Unwin, 1979). The probability statistic (p) measures error probabilities from the surface calculation, and the standard error of estimate is the standard deviation of the surface residuals.

Data Resources

The data used to support this investigation fall into three categories: (1) snow accumulation data; (2) climate data; and (3) spatial analysis data.

Snow Accumulation Data

The snow and weather data define the relationship between present climate and snow accumulation patterns. Snow accumulation data for the Uinta Range are collected by the U.S. Department of Agriculture Soil Conservation Service, which publishes annual snow course reports on snow depths and water content for seasonal snow accumulation from gauges throughout the Uinta Mountains. As of 1990, there were 41 snow-course gauges in operation in the Uinta Mountain area. Although snow accumulation has been monitored in the Uinta Mountains since 1940, only since 1972 has the number of gauges been consistently sufficient to evaluate snow accumulation trends. Additionally, several SNOTEL (i.e., snow telemetry) remote-weather monitors have been in operation in the Uinta Range since 1984 providing local high altitude weather records (U.S. Dept. Agriculture, 1978; U.S. Dept. Agriculture, 1979-1990).

Climate Data

Monthly and annual climate data for Utah and Wyoming are monitored by the U.S. Department of Commerce, National Oceanic and Atmospheric Administration (NOAA) (U.S. Dept. Commerce-Utah, 1972-1990; U.S. Dept. Commerce-Wyoming, 1972-1990). These data are collected at specific stations, and tabulated by state divisions, providing a regional record of climate. High altitude weather data are also available for the region from rawinsonde weather balloon records. Balloons are released twice daily from surrounding National Weather Service stations including Salt Lake City, Utah, Lander, Wyoming, and Grand Junction, Colorado. Rawinsonde data from the aforementioned stations have been made available by the Utah Climate Center and from NOAA documents (U.S. Dept. Commerce National Summaries, 1972-1979).

Spatial Analysis Data

The spatial analysis data consist of thematic and topographic maps of the study area. The distribution of glacial landforms from the last two full-glacial episodes in the study area has been mapped by Atwood (1909). Revisions to Atwood's original mapping have been made by Bradley (1936) and Schlenker (1988). The spatial association of the glacial landforms is used to determine the past distribution of glacial ice. Planimetric and elevation data for the study area are available at a 1:250,000 and 1:24,000 scales from U.S. Geological Survey topographic maps. Using Geographic Information Systems technology, the spatial analysis data were integrated to construct a three-dimensional model of the study area to reconstruct the full-glacial ELAs.

Method Of Analysis

The structure of the research design is illustrated on Figure 2. The methodological sequence used for this research is summarized by six objectives: (1) evaluate the relationship of present snow accumulation and regional climate patterns; (2) estimate the present ELA from the snow accumulation and climate data; (3) reconstruct the ELAs for the last two Pleistocene glacial episodes from the Pleistocene geomorphology; (4) compare the height difference between the present and past ELAs to estimate temperature changes; (5) estimate the snow accumulation for the two glacial episodes from the Pleistocene temperature estimates; and (6) reconstruct the probable climate and paleoenvironmental conditions that occurred during the glacial episodes by comparing present and past ELAs and snow accumulation estimates, and literature research data from secondary resources for the region.

Model Synthesis

The results of this dissertation provide a model of paleoclimatic and paleoenvironmental change. Modeling parameters were based upon observations of rates and relationships observed from present climate, and assumed that the same rates and relationships observed for the present existed in the past. Thus, the results of this dissertation can be considered only estimations of past conditions, which can be used to test established hypotheses and to develop new hypotheses.

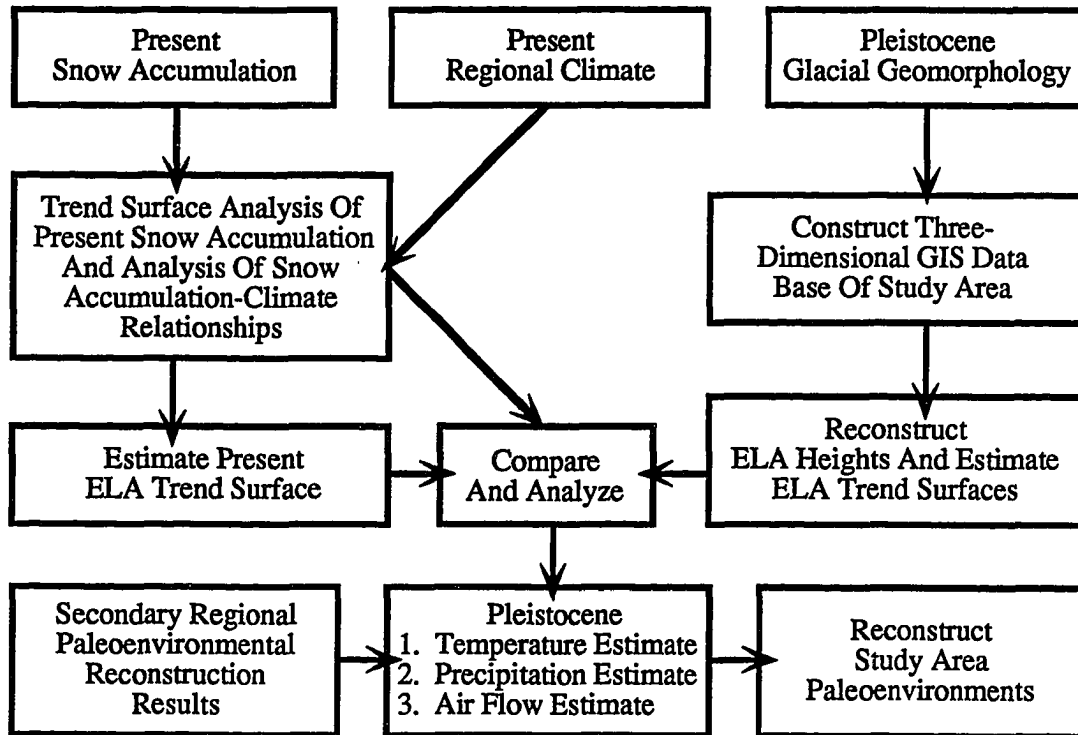


Figure 2. Research design.

CHAPTER II

STUDY AREA DESCRIPTION

Location And Physiography

The Uinta Mountains are an elongate east to west trending range, approximately 240 kilometers long and 60 kilometers wide. The range trends parallel to the Utah-Wyoming border in northeastern Utah. The location of the range and the general outline of the study area are shown on Figure 3. The Uinta Mountains are part of the Middle Rocky Mountain Physiographic Province, which Hunt (1967) describes as a heterogeneous assemblage of block-faulted, anticlinal and lava plateau ranges that trend in a diversity of directions. With the exception of the Uinta Mountains, which trend from east to west, most of the ranges in the Rocky Mountain System trend north to south. The nearest neighboring range is the Wasatch Mountains, which are located immediately to the west of the Uinta Mountains. The Wasatch Mountains have a general north to south structure and elevations exceeding 3,500 meters.

Structurally the Uinta Mountains are a thrust-faulted, anticlinal range with an arcuate east-west trending crest. The core of the range is comprised of pre-Cambrian quartzites and shales that collectively form the Uinta Mountain Group (Hansen, 1969). These rocks form a broad arc at the crest of the range and, for the most part, are horizontally to near-horizontally bedded (Ritzma, 1969). Steeply dipping Paleozoic limestones and sandstones bound the older rocks on the north and south, forming sharp hogback ridges where glacial or fluvial incision has occurred (Hansen, 1969). Outcrops of Mesozoic sandstones, limestones and shales flank the Paleozoic rocks on the eastern half of the range (Hansen, 1969). Tertiary age basin-fill shales and conglomerates are found in

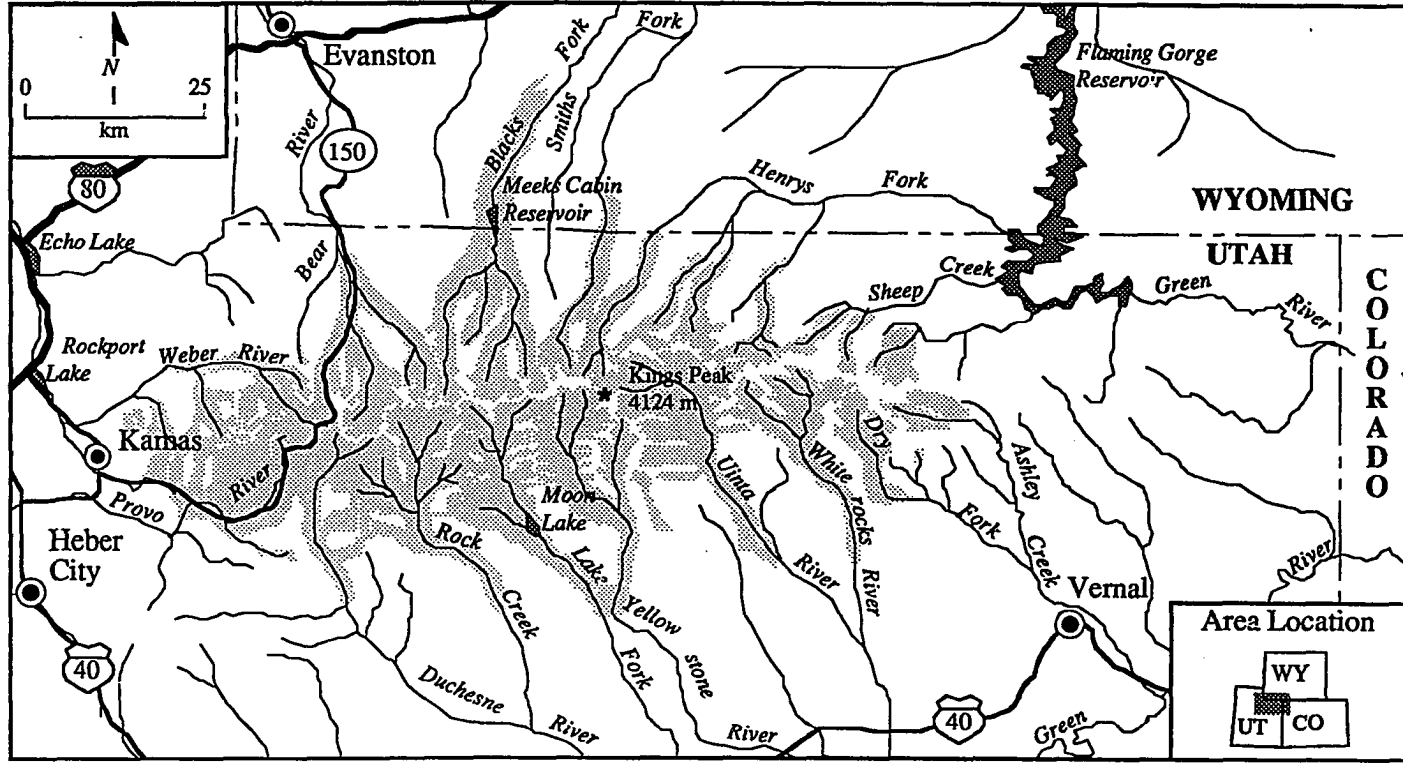


Figure 3. Detailed map of study area. Figure shows principle streams, cities, roadways, and state boundaries. Shaded areas indicate the extent of late-Pleistocene glaciation.

basins to the north and south of the range (Hunt, 1967). Tertiary volcanic ashes blanket older rocks on the west side of the range (Bryant, 1990). Elevations in the study area range from 2,000 meters to over 4,000 meters. Kings Peak, which stands at 4,124 meters, the highest point in Utah, is located near the center of the range. Generalized elevations of the study area are shown on Figure 4. Drainage from the Uinta Mountains is predominantly bi-directional--to the north and south into the Green River system and the Great Salt Lake Basin, respectively.

The uplift of the Uinta Mountains began in the late Cretaceous in the form of two east and west oriented structural domes (Hansen, 1969). The approximate boundary between the two domes is the present location of the Utah-Colorado border. By late Oligocene, uplift on the eastern dome faltered and was surpassed by uplift of the western dome. Presently, summits in the western dome, which comprise the present Uinta mountains, are 1,200 meters to 1,500 meters above those of the eastern dome (Hansen, 1986). During the Pleistocene, the High Uinta Mountains were subjected to extensive glaciation, whereas no evidence of Pleistocene glaciation has been documented on the eastern dome.

The existing terrain has been modified by Quaternary glacial and periglacial processes, and well preserved landforms resulting from these processes are abundant throughout the range (Atwood, 1907; Bradley, 1936; Hansen, 1969; Schoenfeld, 1969; Barnhardt, 1973; Grogger, 1974; Schlenker, 1988). During the late Pleistocene, it is estimated that most ranges in the western United States higher than 3,500 meters were subjected to glaciation (Blackwelder, 1915); and over fifty of the ranges in the western United States experienced glaciation (Porter et al., 1983). The reconstruction of Pleistocene glaciation for the Rocky Mountains has been studied for over eighty years, and through these studies sequences of glacial stratigraphy and morphostratigraphy have been found to be relatively consistent throughout the region. Subsequently, a regional standard

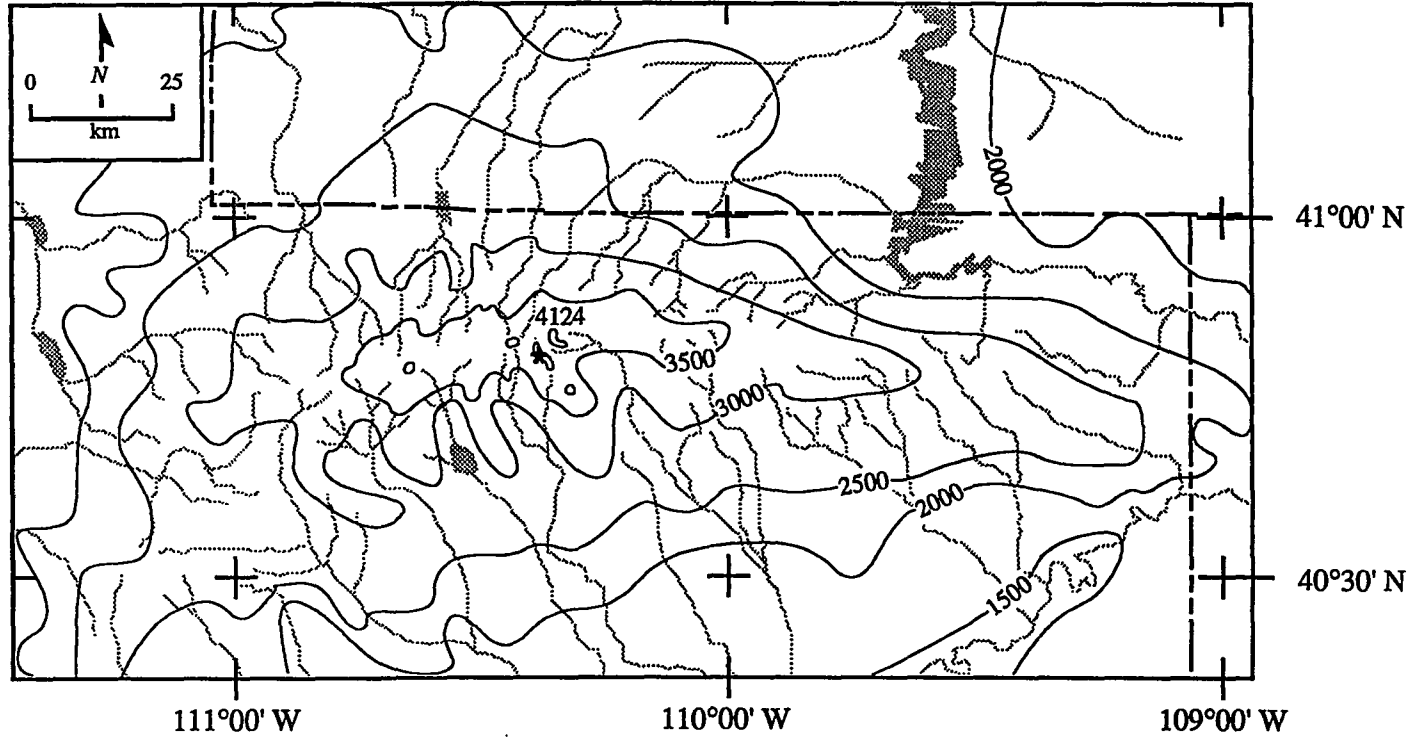


Figure 4. Generalized topographic map of study area. Contour interval is 500 Meters, and Kings Peak, the highest point in Utah at 4124 meters, is shown near the center of the range.

Rocky Mountain glacial model has evolved (Richmond, 1965; Mears, 1974; Pierce, 1979). The model is based largely on the type sequence of Pleistocene and Holocene glacial and glaciofluvial depositional features in the Wind River Range of Wyoming. The Wind River sequence has been extended to other ranges in the region via long-range correlations that are based either on morphostratigraphic or age-related phenomena (Pierce, 1979). Correlations have been extended further to link the Rocky Mountain sequence to the North American continental glacial sequence, as well as with the marine oxygen isotope record of deep sea cores (Pierce et al., 1976; Richmond and Fullerton, 1986).

Although local numeric age control has been sparse, morphostratigraphic and relative age criteria from a number of investigations have shown that the glacial episodes that occurred in the Uinta Mountains correlate to the regional standard Rocky Mountain glacial model (Bradley, 1936; Schoenfeld, 1969; Barnhardt, 1973; Grogger, 1974; Schlenker, 1988). The two most recent Pleistocene glaciations in the Uinta Mountains, the Blacks Fork age and the Smiths Fork age, have been correlated with the Bull Lake and Pinedale glacial episodes of the Rocky Mountain model, respectively. At other sites in the Rocky Mountains, the Bull Lake age has been estimated to have occurred between 155,000 BP and 130,000 BP (Pierce et al., 1976), equivalent to the oxygen isotope stage six. The Pinedale age is estimated to have occurred between 30,000 BP and 12,000 BP (Madole, 1986), equivalent to the oxygen isotope stage two (Shackleton and Opdyke, 1973).

Study Area Climate

The climate of the study area can be characterized as highly variable. A sampling of long-term weather records from the area provides for an understanding of the study area climate. The records of four local weather stations and three surrounding NOAA regional divisions are presented in Tables 1 and 2, respectively. Graphical representations of the climate records are shown in Figures 5 and 6, respectively. All of the records, except the

Table 1
Climate Data For Selected Local Weather Stations[†]

Echo Dam, Utah													
40°11' N; 111°26' W: 1,667 m													
	J	F	M	A	M	J	J	A	S	O	N	D	Annual
P	2.9	2.4	3.0	4.0	3.9	3.0	1.8	2.3	2.4	3.3	2.9	3.1	33.8 cm
T	-9.8	-8.3	4.1	9.1	11.8	15.4	21.7	18.9	14.9	8.6	2.2	-3.5	7.0 °C

Evanston, Wyoming													
41°16' N; 110°57' W: 2,076 m													
	J	F	M	A	M	J	J	A	S	O	N	D	Annual
P	1.9	1.6	2.2	3.0	3.0	2.5	1.9	2.3	2.3	2.6	2.0	1.9	27.1 cm
T	-7.3	-5.7	-2.8	2.8	8.5	13.2	17.4	16.2	11.6	5.9	-1.7	-6.0	4.3 °C

Roosevelt, Utah													
40°17' N; 109°58' W: 1,527 m													
	J	F	M	A	M	J	J	A	S	O	N	D	Annual
P	1.4	1.1	1.4	1.6	1.6	1.8	1.0	1.9	1.7	2.1	1.3	1.5	18.3 cm
T	-8.2	-4.1	2.7	8.6	14.2	19.0	23.0	21.4	16.4	9.8	1.3	-5.8	6.9 °C

Steel Creek Park, Utah													
40°55' N; 110°30' W: 3,078 m													
	J	F	M	A	M	J	J	A	S	O	N	D	Annual
P	2.5	3.0	3.9	4.9	5.9	6.5	7.0	7.8	8.3	0.4	1.1	1.9	53.1 cm
T	-10.3	-8.2	-7.6	0.4	3.2	7.6	9.9	9.6	4.9	-1.0	-5.5	-9.4	-0.6 °C

P= Precipitation

T= Temperature

[†]Station data for this table are from U.S. Department of Commerce-Utah 1972-1990 and U.S. Department of Commerce-Wyoming 1972-1990. Steel Creek Park data made available by Soil Conservation Service.

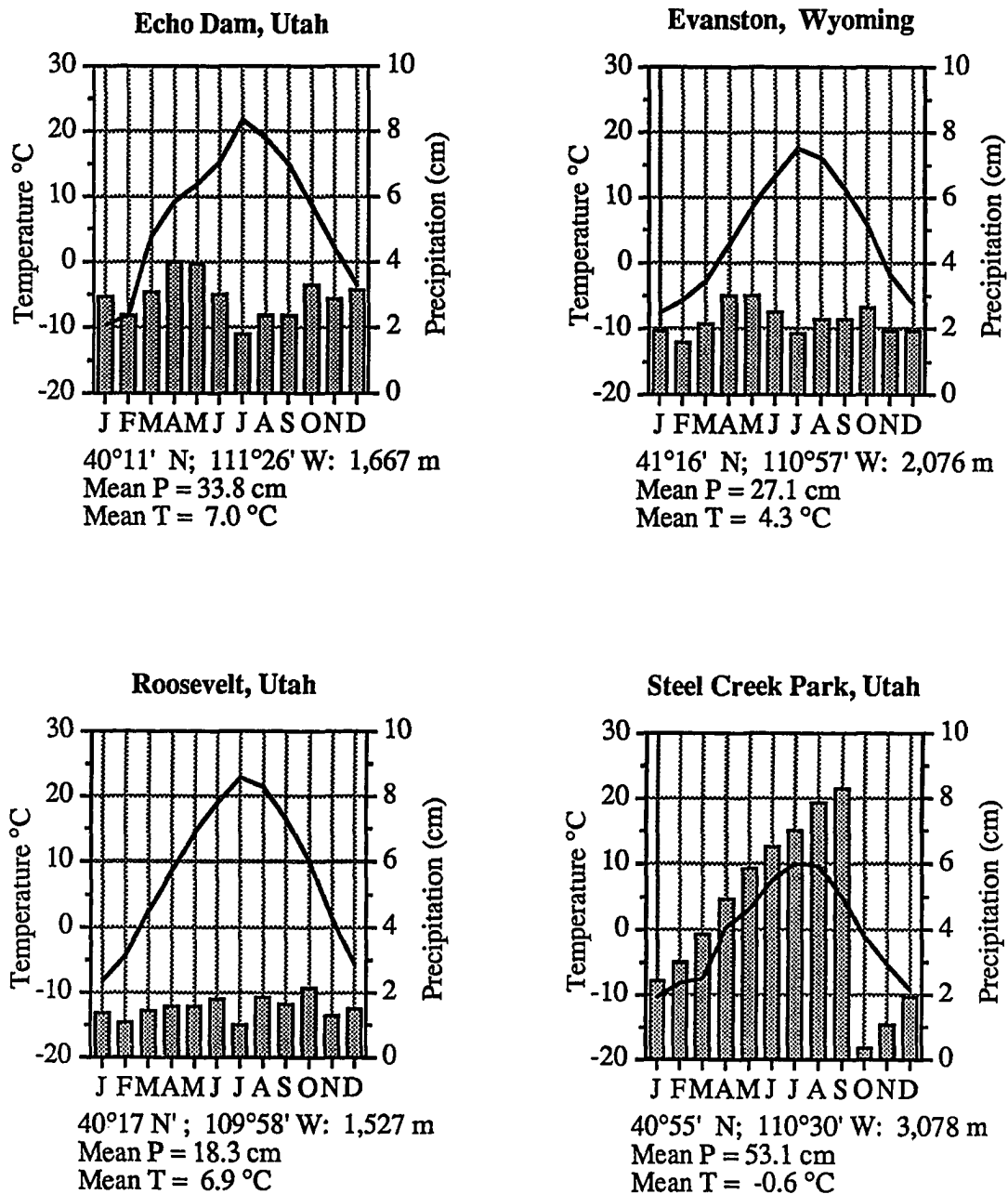


Figure 5. Climographs of selected local weather stations. Corresponding numerical data are shown in Table 1 (Station data are from U.S. Department of Commerce-Utah 1972-1990 and U.S. Department of Commerce-Wyoming 1972-1990. Steel Creek Park data made available by Soil Conservation Service).

Table 2
Climate Data For Selected NOAA Weather Divisions[†]

NOAA Division Five, Utah													
Northern Mountains													
	J	F	M	A	M	J	J	A	S	O	N	D	Annual
P	5.5	4.9	4.8	4.8	3.9	3.0	2.2	3.1	2.9	3.7	4.1	5.0	47.9 cm
T	-6.0	-4.1	-0.8	4.4	9.8	14.2	18.5	17.3	12.8	7.2	0.0	-4.7	5.7 °C

NOAA Division Six, Utah													
Uinta Basin													
	J	F	M	A	M	J	J	A	S	O	N	D	Annual
P	1.3	1.1	1.4	1.7	2.0	1.8	1.5	2.1	1.8	2.2	1.4	1.5	19.9 cm
T	-8.2	-4.4	1.9	7.9	13.4	18.3	22.3	20.7	15.7	9.2	0.8	-6.0	7.7 °C

NOAA Division Three, Wyoming													
Green and Bear River Drainage													
	J	F	M	A	M	J	J	A	S	O	N	D	Annual
P	1.8	1.3	1.5	2.2	3.0	2.8	1.9	2.2	2.1	2.0	1.5	1.6	23.9 cm
T	-8.7	-6.5	-3.1	3.2	8.9	13.6	17.7	16.3	11.4	5.7	-2.3	-7.2	4.1 °C

Composite of NOAA Division Five, Utah, Division Six, Utah, and Division Three, Wyoming													
	J	F	M	A	M	J	J	A	S	O	N	D	Annual
P	2.8	2.5	2.6	2.9	3.0	2.5	1.9	2.5	2.3	2.6	2.3	2.7	30.6 cm
T	-7.6	-5.0	-0.6	5.2	10.7	15.4	19.5	18.1	13.3	7.3	-0.5	-5.9	5.8 °C

P= Precipitation

T= Temperature

[†]Data for this table are from U.S. Department of Commerce-Utah 1972-1990 and U.S. Department of Commerce-Wyoming 1972-1990.

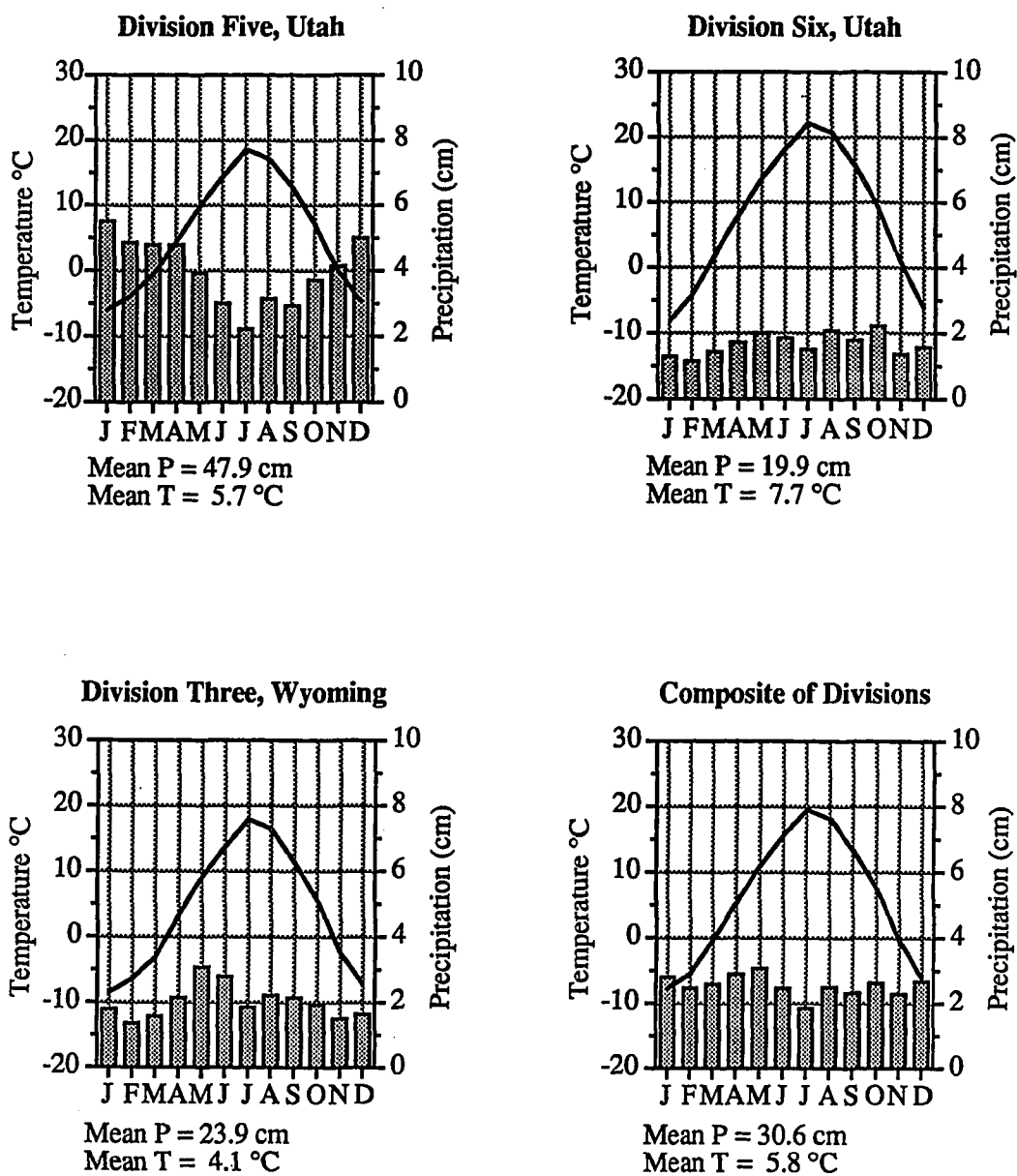


Figure 6. Climographs of selected NOAA weather divisions. Corresponding numerical data are shown in Table 2 (Data are from U.S. Department of Commerce-Utah 1972-1990 and U.S. Department of Commerce-Wyoming 1972-1990).

Steel Creek Park, Utah record, represent a thirty year or greater compilation of data. The Steel Creek Park station is a remote high-elevation SNOTEL station which has been in operation since 1983. The climographs shown in Figures 5 and 6 indicate that the micro-scale climates of the region range from cool arid steppes, Köppen BSk, to cool-moist microthermal, Köppen Dfc, categories (Trewartha, 1968). Assuming an average normal lapse rate of 0.65°C , a polar, Köppen E, climate regime is thought to prevail at elevations above 3,100 meters.

The locations of the climate stations and divisional boundaries with respect to the study area are presented on Figure 7. From the climate data in Table 1, three climatic continuums can be identified: (1) a general decrease in average annual temperature occurs from south to north across the study area; (2) a decrease in average annual precipitation from west to east across the study area; and (3) both a decrease in average annual temperature and an increase in average annual precipitation with increases in elevation in the study area.

Rawinsonde data from the surrounding National Weather Service (WSO) stations shown in Figure 7 provide free-air temperature data for the region. Free-air temperature and lapse rate data from the three stations are shown in Table 3. To project the free air structure of the study area, the data in Table 3 are interpolated from the National Weather Service stations for the study area location. The projected free-air structure for the study area is presented in Table 4. The data from Table 4 indicate that the annual lapse rate is $0.63^{\circ}\text{C } 100^{-1}$ meters. The rate of $0.63^{\circ}\text{C } 100^{-1}$ meters is only slightly lower than average normal lapse rates of $0.65^{\circ}\text{C } 100^{-1}$ meters and lapse rates of mountainous areas reported elsewhere in the western United States (Westbrook, 1980; Dohrenwend, 1984). Because the summer (June through August) temperature and lapse rate data and 0°C altitude are used for analyses in later chapters, the calculated summer lapse rates and 0°C altitude are shown in Tables 3 and 4. The summer lapse rate of $0.75^{\circ}\text{C } 100^{-1}$ meters is substantially

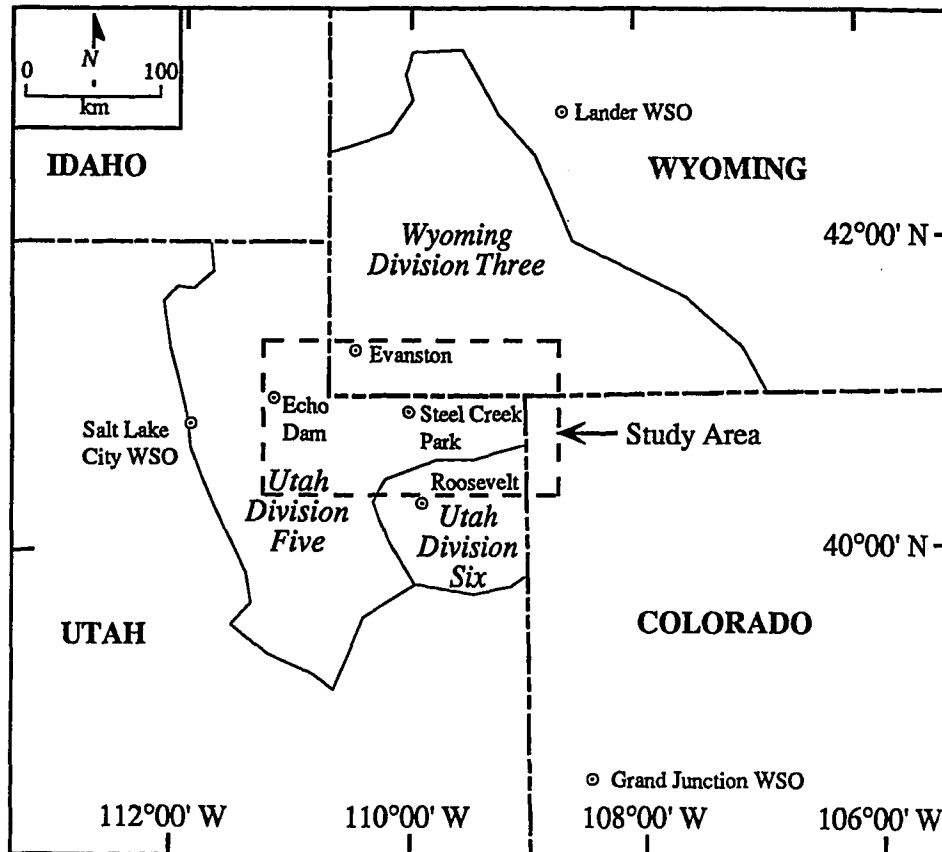


Figure 7. Location of selected local weather stations, NOAA divisional boundaries and National Weather Service Office (WSO) stations.

Table 3
Annual And Summer (June Through August) High
Altitude Temperature Data And Lapse Rate Means
For Selected National Weather Service Stations†

Standard Pressure	Annual Dynamic Height (m)	Annual Temperature (°C)	Summer Dynamic Height (m)	Summer Temperature (°C)
Grand Junction, Colorado				
Surface	1,472	11.9	1,472	21.4
800 mb	1,998	10.1	2,033	20.5
700 mb	3,239	1.3	3,256	11.1
600 mb	4,480	-7.4	4,528	0.9
500 mb	5,722	-15.7	5,865	-9.2

Annual 800 mb to 500 mb Lapse Rate: 0.69 °C 100 ⁻¹ m				
Summer 800 mb to 500 mb Lapse Rate: 0.78 °C 100 ⁻¹ m				
Summer 0° C Altitude: 4,668 m				
Lander, Wyoming				
Surface	1,695	7.9	1,695	17.7
800 mb	1,980	7.6	2,016	17.6
700 mb	3,212	-1.7	3,230	10.1
600 mb	4,445	-10.4	4,497	0.9
500 mb	5,677	-17.0	5,833	-10.3

Annual 800 mb to 500 mb Lapse Rate: 0.67 °C 100 ⁻¹ m				
Summer 800 mb to 500 mb Lapse Rate: 0.73 °C 100 ⁻¹ m				
Summer 0° C Altitude: 4,553 m				
Salt Lake City, Utah				
Surface	1,288	11.9	1,288	20.8
800 mb	2,003	8.6	2,022	19.0
700 mb	3,097	0.9	3,151	10.3
600 mb	4,323	-5.2	4,410	0.7
500 mb	5,722	-13.1	5,844	-9.8

Annual 800 mb to 500 mb Lapse Rate: 0.58 °C 100 ⁻¹ m				
Summer 800 mb to 500 mb Lapse Rate: 0.76 °C 100 ⁻¹ m				
Summer 0° C Altitude: 4,528 m				

†Compiled from Grand Junction, Colorado, Lander, Wyoming, and Salt Lake City, Utah National Weather Service Rawinsonde Data (1972 to 1979 data from U.S. Department of Commerce, National Weather Service National Summaries; 1980 to 1989 data provided by Utah Climate Center).

Table 4
Interpolated Annual And Summer (June Through August)
High Altitude Temperature Data And Lapse Rate Means
For Uinta Mountain Study Area[†]

Standard Pressure	Annual Dynamic Height (m)	Annual Temperature (°C)	Summer Dynamic Height (m)	Summer Temperature (°C)
800 mb	2,006	8.8	2,024	19.1
700 mb	3,209	0.5	3,640	10.4
600 mb	4,413	-6.8	4,456	0.7
500 mb	5,616	-11.4	5,847	-9.8

 Annual 800 mb to 500 mb Lapse Rate: 0.63 °C 100⁻¹ m

Summer 800 mb to 500 mb Lapse Rate: 0.75 °C 100⁻¹ m

Summer 0° C Altitude: 4,567 m

[†]Interpolated from Grand Junction, Colorado, Lander, Wyoming and Salt Lake City, Utah National Weather Service data listed in Table 3.

higher than the annual rate of $0.65\text{ }^{\circ}\text{C } 100^{-1}$ meters. The calculated summer 0°C altitude of 4,567 is on the order of 443 meters above Kings Peak.

An important regional climatic influence is a westerly air flow, which dominates during the winter months. The westerly flow brings moist frontal storms inland from the Pacific Ocean. When frontal storms encounter the Wasatch and Uinta mountains, the resultant orographic uplift causes a marked increase in precipitation. Precipitation decreases eastward as the frontal storms track across the Wasatch and Uinta mountains. During the summer months, moisture comes primarily in the form of convectional storms that are driven northward from the Pacific (Gifford et al., 1967). Mitchell (1976) has identified a regional winter air mass boundary immediately to the north of the Uinta Mountains. This air mass boundary is believed to separate a largely zonal westerly pattern of flow on the north, from anticyclonic circulation on the south (Mitchell, 1976). Cooler air masses from the north and warmer southerly air masses converge on this boundary resulting in frontal storm activity. Snow accumulation for the region generally occurs between November and March. However, because of higher elevations, snow cover in the Uinta Mountains generally lasts from October to late April (U.S. Department of Agriculture, 1978).

Study Area Vegetation

With elevations ranging from 2,000 meters to over 4,000 meters, the vegetation of the study area is variable. Responding to increases in precipitation and decreases in temperature, a sequence of vegetational associations occurs with increase in elevation. Below 2,800 meters, a sagebrush (Artemisia tridentata) and grass steppeland comprise the dominant plant assemblage. Interspersed within the sagebrush-grass association are patches of lodgepole pine (Pinus contorta) and aspen (Populus tremuloides) that occupy sheltered areas and north-facing slopes. Above 2,800 meters, the steppeland is succeeded

by a lodgepole pine and aspen woodland. Subalpine species consisting of subalpine fir (Abies lasiocarpa), Engelmann spruce (Picea engelmanni), and lodgepole pine become the woodland constituents above 3,200 meters. Above 3,500 meters, a non-woodland alpine association of grasses, forbs and sedges dominates. Isolated patches of stunted subalpine species are found in sheltered areas of the alpine zone. Riparian zones are dominated by narrowleaf cottonwood (Populus angustifolia) below 2,500 meters and pussy willow (Salix wolfii) and Bebb willow (Salix bebbiana) above 2,500 meters (Johnson, 1970).

Study Area Selection

The Uinta Mountains and the surrounding region provide an excellent setting for the objectives of this dissertation. Ample climatic data (U.S. Dept. Commerce-National summary, 1972-1980; U.S. Dept. Commerce-Utah, 1972-1990; U.S. Dept. Commerce-Wyoming, 1972-1990) and snow accumulation data (U.S. Dept. Agriculture, 1978; U.S. Dept. Agriculture, 1979-1990) are available for evaluating snow and climate relationships. Additionally, the extent of past glaciation for both of the last two full-glacial episodes, the Blacks Fork (stage six) and Smiths Fork (stage two) episodes, has been well documented and mapped by previous workers (Atwood, 1909; Bradley, 1936; Schoenfeld, 1969; Barnhardt, 1973; Grogger, 1974; Schlenker, 1988).

In contrast to the general north-south structural trend of the Rocky Mountain System, the Uinta Mountains trend east to west. The east-west trend has resulted from thrust faulting on the north and south of the range, which has caused broad anticlinal uplift to extend from east to west (Hansen, 1969). Because air mass movement in the western United States is predominantly driven by westerly air flow, ranges that are oriented on a north-south axis are not well-suited for the evaluation of northerly or southerly variations of snow accumulation. Subsequently, the measure of air-flow variability is not usually evaluated when ELA investigations are conducted. In contrast, the Uinta Range with an

east to west structure presents an opportunity to evaluate northerly or southerly variations in snow accumulation and interpretation of air flow directions. A schematic digital elevation model shown in Figure 8 illustrates the topographic structure of the study area.

The Uinta Mountains are also located in a region that has undergone substantial paleoenvironmental research. Enlarged Pleistocene paleolakes west of the range have undergone extensive paleoenvironmental reconstruction (Galloway, 1970; McCoy, 1981; Scott, et al., 1983; Currey and Oviatt, 1985; Oviatt et al., 1987; Currey, 1990). Currey speculates that the paleolakes influenced glaciation in the Uinta Mountains (Donald Currey, 1992, personal communication). Pleistocene glaciation in the Wasatch Mountains has also been the subject of a number of studies (Atwood, 1909; Richmond, 1964; Madsen and Currey, 1979; Mulvey, 1985), and periglacial phenomena in the intermontane basins of Wyoming have yielded hypotheses regarding late-Pleistocene temperature change (Mears, 1981; Péwé, 1983).

As with other ranges in the Rocky Mountain System, the Uinta Mountains have been subject to a sequence of late-Pleistocene glaciation that has been found to be consistent across the region (Bradley, 1936; Schoenfeld, 1969; Barnhardt, 1973; Grogger, 1974; Schlenker, 1988). Unlike the other ranges in the Rocky Mountain System, the Uinta Mountains have an east-west trending structure which presents an opportunity to evaluate northerly or southerly air flow variations. The present climate and free air structure data for the study area and surrounding region have been compiled to provide an understanding of the present climatic setting and to provide a basis for the reconstruction of paleoclimatic parameters. Because substantial paleoenvironmental research has taken place in the surrounding region, a more comprehensive paleoclimatic and paleoenvironmental synthesis for the study area can be made.

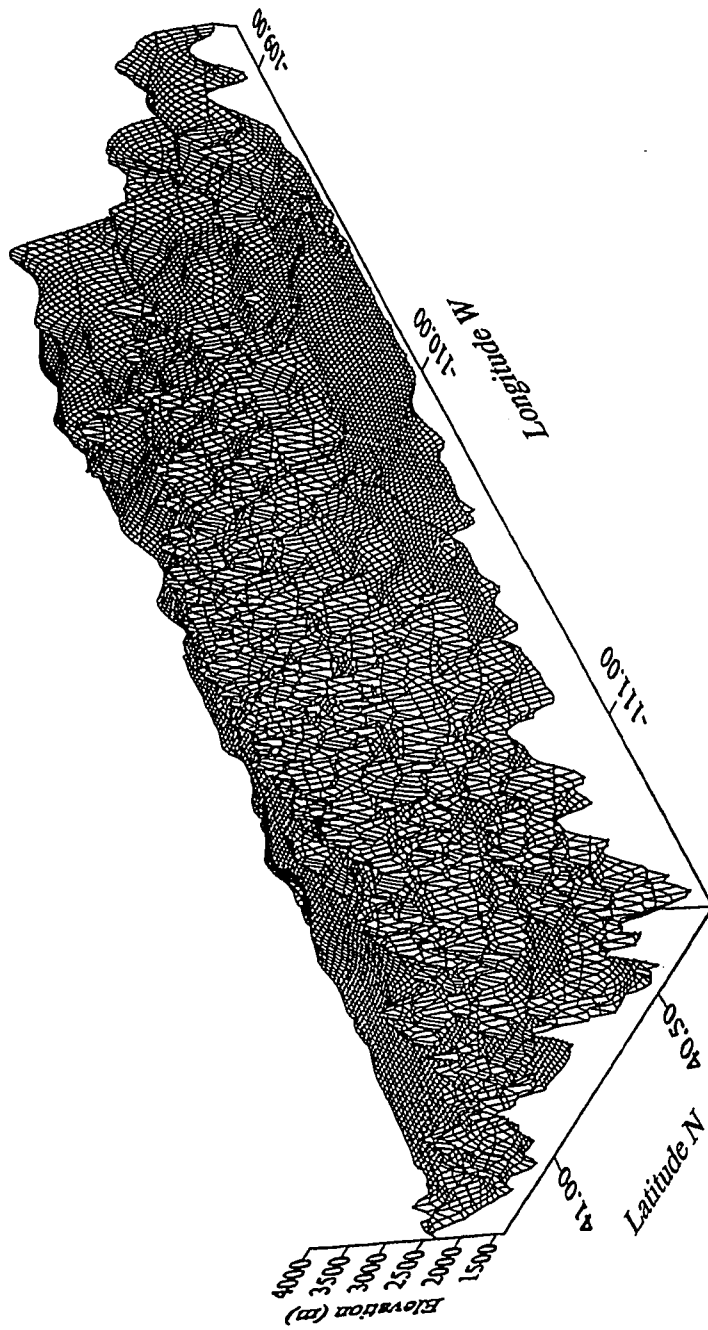


Figure 8. Schematic digital elevation model of the study area. Vertical exaggeration factor equals 24.

CHAPTER III

ANALYSIS OF SNOW ACCUMULATION AND CLIMATE VARIABILITY

Introduction

Snow accumulation records have been maintained for the Uinta Mountains for a number of years (U.S. Dept. Agriculture, 1978; U.S. Dept. Agriculture, 1979-1990). Data from these records provide a proxy for characterization of winter season climate. For the purposes of this dissertation, the snow accumulation data provide a useful means of understanding the winter season climate of the study area. The benefits of evaluating snow accumulation data are as follows: (1) snow accumulation data are analogous to glacial ice accumulation (Zwick, 1980; Zielinski and McCoy, 1987; Leonard, 1989) and can be analyzed using trend surface analysis (Mulvey, 1985; Locke, 1989; Locke 1990); (2) snow accumulation data can be correlated to surrounding regional climate records and can be used to interpret seasonal climate patterns; and (3) snow accumulation data can be used to estimate the present ELA (Leonard, 1989). Whereas the variability of snow accumulation in mountainous terrain is influenced by several factors, including but not limited to elevation, slope, aspect, and landforms (Cain, 1975; Graf, 1976; Barry, 1981; McKay, 1981), climate variance appears to be a significant factor affecting snow accumulation variability in the Uinta Mountains.

Regional winter season climate data and snow accumulation trend surface patterns are compared to identify relationships between snow accumulation and climate variability. These relationships will be used to interpret the climate of the late-Pleistocene glacial episodes. In addition, numerical models derived from present snow and temperature measurements taken at ELA sites world-wide (Loewe, 1971; Sutherland, 1984; Leonard,

1989) are used to estimate present study area glacial ELA from the 1972 to 1990 snow accumulation records.

Snow Accumulation Data Resources

Snow accumulation records have been maintained in the Uinta Mountains since 1940 (U.S. Dept. Agriculture, 1978; U.S. Dept. Agriculture, 1979-1990). The snow accumulation data are maintained to predict stream runoff from mountain watersheds. The Soil Conservation Service has compiled these records for the State of Utah since 1939. The data are recorded in inch-scale units as snow water equivalents (SWE). Because snow accumulation gauges or snow course stations are located in remote areas, data from these sites are collected, at best, on a monthly basis during the snow accumulation season, which extends from October 1 to April 1 or later. On or within a few days of April 1, when the winter snow accumulation is normally at the highest point for the season, measurements are taken at all of the snow accumulation sites. Since 1970, many SNOTEL (i.e., snow telemetry) radio transmitting data recorders have been installed both at new sites and at old sites upgrading the existing manually-monitored snow course gauges. The SNOTEL recorders provide instantaneous data transmission to personnel in regional offices (U.S. Dept. Agriculture, 1978; U.S. Dept. Agriculture, 1979-1990).

As of 1990, 41 snow survey sites were monitored in the Uinta Mountains. A listing of these sites is presented in Table 5. Of the 41 sites, 19 of the sites are snow course only sites, 2 are SNOTEL only sites, and the remaining 20 sites have both snow course and SNOTEL data collection systems. The coordinate locations, elevations, and the average 1972 to 1990 April 1 SWE for the sites are listed in Table 5 (U.S. Dept. Agriculture, 1990), and the locations of the sites are shown on Figure 9.

Table 5
Snow Survey Measurements Uinta Mountains 1972 To 1990†

Site	Name	Site Type ^a	N Latitude	W Longitude	Elevation (m)	Mean April 1 SWE (cm)
1.	Ashley-Twin Lakes	1	40°43'	109°48'	3,200	39.4
2.	Atwood Lake	2	40°44'	110°17'	3,200	35.2
3.	Beaver Creek Divide	3	40°37'	111°04'	2,524	35.4
4.	Blacks Fork Junction	1	40°58'	110°35'	2,722	29.0
5.	Brown Duck Ridge	3	40°35'	110°35'	3,231	48.1
6.	Buck Pasture	1	40°51'	110°40'	2,957	41.7
7.	Burts-Miller Ranch	1	41°00'	110°52'	2,408	21.1
8.	Chalk Creek #1	3	40°51'	111°04'	2,774	63.1
9.	Chalk Creek #2	3	40°54'	111°04'	2,499	41.9
10.	Chalk Creek #3	1	40°55'	111°06'	2,286	33.1
11.	Chepeta	3	40°46'	110°00'	3,139	36.3
12.	Chepeta-White R. Lake	1	40°46'	109°59'	3,155	40.4
13.	E. Fork Blacks Fork G.S.	1	40°53'	110°32'	2,847	30.3
14.	Five Points Lake	3	40°43'	110°28'	3,328	44.8
15.	Hayden Fork	3	40°47'	110°53'	2,774	48.4
16.	Henry's Fork	1	40°53'	110°22'	3,048	34.3
17.	Hewinta G.S.	3	40°57'	110°29'	2,896	31.9
18.	Hickerson Park	3	40°54'	109°58'	2,774	24.7
19.	Hole in the Rock	3	40°55'	110°12'	2,789	16.8
20.	Hole in the Rock G.S.	1	40°57'	110°09'	2,530	10.9
21.	Kings Cabin-Upper	3	40°43'	109°33'	2,661	29.7
22.	Lake Fork Basin	3	40°45'	110°37'	3,322	48.5
23.	Lake Fork Mountain	3	40°36'	110°26'	3,078	34.3
24.	Lake Fork Mountain #3	1	40°33'	110°21'	2,560	18.0
25.	Lightning Lake	3	40°43'	110°45'	3,200	63.2
26.	Lily Lake	3	40°52'	110°48'	2,758	39.3
27.	Middle Beaver Creek	1	40°57'	110°11'	2,637	11.4
28.	Mosby Mountain	3	40°37'	109°53'	2,896	33.9
29.	Paradise Park	1	40°41'	109°55'	3,078	39.1
30.	Redden Mine Lower	1	40°41'	111°13'	2,591	51.5
31.	Reynolds Park	1	40°45'	109°55'	3,170	43.4
32.	Rock Creek	3	40°33'	110°41'	2,408	27.4
33.	Sergeant Lakes	1	40°50'	111°17'	2,530	36.1
34.	Smith and Morehouse	1	40°48'	111°05'	2,316	42.4
35.	Smith and Morehouse	2	40°47'	111°06'	2,316	37.0
36.	Soapstone R.S.	1	40°34'	111°02'	2,377	39.3
37.	Spirit Lake	1	40°50'	110°00'	3,139	37.8
38.	Steel Creek Park	3	40°55'	110°30'	3,078	41.2
39.	Stillwater Camp	1	40°52'	110°50'	2,606	30.9
40.	Trial Lake	3	40°41'	110°57'	3,036	62.4
41.	Trout Creek	3	40°44'	109°40'	2,865	31.4

†Data for this table compiled from U.S. Dept. Agriculture, 1978 and U.S. Dept. Agriculture, 1979-1990.

^aType: 1= snow course survey site; Type 2 = SNOTEL survey site; Type 3 = snow course and SNOTEL survey.

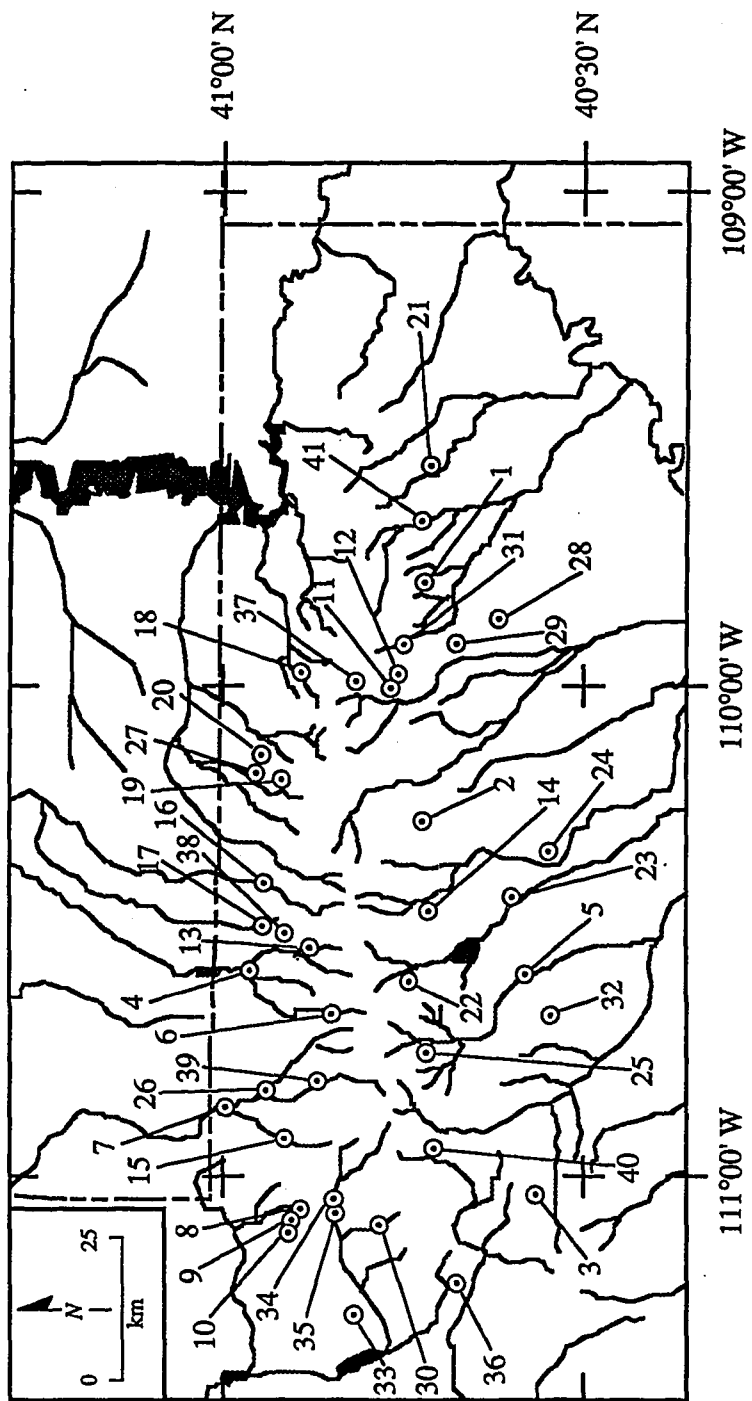


Figure 9. Location map of operating snow survey sites in the Uinta Mountains. Site numbers correspond to listing in Table 5.

Analysis Of Snow Accumulation Data

The record keeping of snow accumulation in the Uinta Mountains has been sporadic, but it has generally improved over time. Less than 20 sites were measured prior to 1972. Since 1972 numerous sites have been added. Because of the paucity of site records for the period prior to 1972, the analysis in this dissertation is based on the records of surveys for the 1972 to 1990 period. Trend surface models of the annual snow accumulation patterns and average snow seasonal accumulation data are used to evaluate yearly snow accumulation patterns and to make comparisons from year to year. The direction of surface trend indicates the direction that snow accumulation increases over the study area and is expressed as an azimuth. The gradient indicates the rate of snow accumulation change over the study area and is expressed as the rate of SWE-cm change kilometer⁻¹ of distance. The snow accumulation trend surface gradient, direction and average SWE or snow accumulation for each year are compared to the winter season climate records to evaluate the effect that climate variations have on snow accumulation patterns.

Because the elevations of the snow accumulation sites generally rise to the southeast (128° Az.), the elevations of the sites were calculated into the trend equation to eliminate errors that would be caused by this elevation trend. Shown below is the trend surface equation for the mean 1972 to 1990 snow accumulation:

$$A = -1240.72 + (-21.835Lat) + (18.898Lon) + (0.028Elev) \quad (3)$$

where A is the predicted accumulation, Lat and Lon are site northing and easting increments, respectively; $Elev$ is the elevation of the snow accumulation sites. By assuming the mean snow survey site elevation of 2,822 meters across the study area, equation 3 is simplified by equation 4:

$$A = -1161.702 + (-21.835Lat) + (18.898Lon) \quad (4)$$

From equation 3 snow accumulation trend surface statistics were calculated, and from equation 4 trend surface maps were constructed to evaluate the trend direction and gradient. A trend surface map of the mean 1972 to 1990 snow accumulation is shown in Figure 10. The contours of the snow accumulation surface slope in a northeasterly direction, indicating that the pattern of snow accumulation is highest in the southwestern portion of the study area and decreases to the northeast. Trend surface statistics for the 1972 through 1990 annual records and the 1972 to 1990 average record of snow accumulation are listed on Table 6. The data in Table 6 indicate that particular winters such as 1974, 1975 and 1986 have relatively strong surface trends with correlation coefficients (R) exceeding 0.80 and probability statistics (p) below 0.005. Other winters, such as 1977 and 1981, recorded relatively weaker trends with correlation coefficients (R) of less than 0.65 and suspect probability statistics (p) greater than 0.050 (Unwin, 1979).

Analysis Of Snow Accumulation Patterns And Climate Variability

To evaluate relationships between snow accumulation in the Uinta Mountains and climate variability for the surrounding region, comparisons of annual snow accumulation patterns and averaged winter season climate data were made. The winter season climate data consists of the combined winter (October to April) averages of precipitation and temperature for NOAA regional divisions Utah five and six, and Wyoming division three for the 1972 to 1990 period. Included with the precipitation and temperature data is the mean 800 millibar to 700 millibar resultant wind direction recorded from rawinsonde balloons released from the aforementioned surrounding National Weather Service Stations; these data have been interpolated for the study area. The 800 millibar to 700 millibar height

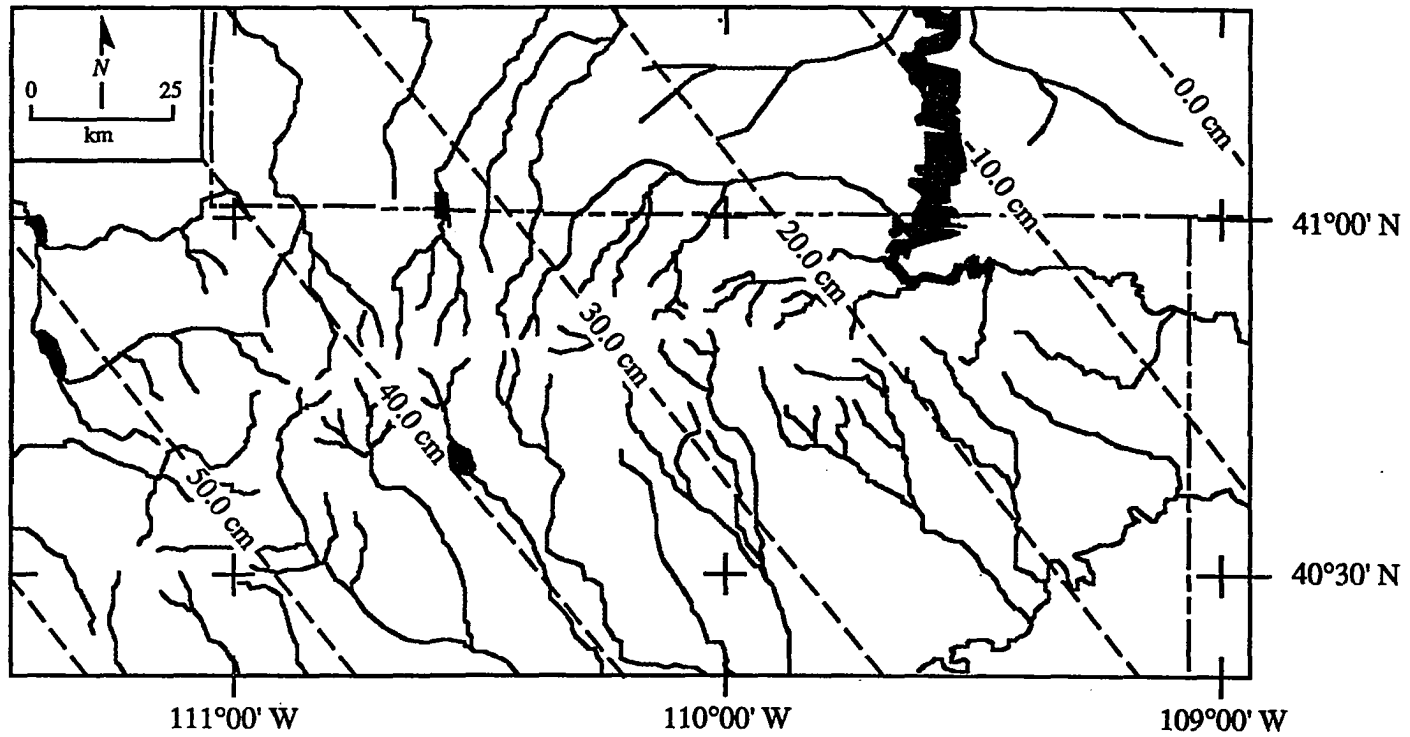


Figure 10. Mean 1972 to 1990 snow accumulation trend surface map. Corresponding trend surface statistics are listed in Table 6. Trend surface equation, $A = -1161.702 + -21.835Lat + 18.898Lon$.

Table 6.
Annual Snow Accumulation Trend Surface Statistics 1972 To 1990

Year	Mean SWE (cm) ^a	<i>r</i> ^b	<i>n</i> ^c	<i>p</i> ^d	Standard Error
1972	45.9	0.753	24	0.001	8.3
1973	47.7	0.706	18	0.019	8.3
1974	36.7	0.848	21	0.000	6.9
1975	40.7	0.882	19	0.000	7.1
1976	35.5	0.672	20	0.019	8.9
1977	21.6	0.606	17	0.104	4.3
1978	39.5	0.789	20	0.001	9.0
1979	41.8	0.847	11	0.025	9.0
1980	49.3	0.678	18	0.031	9.4
1981	30.8	0.577	21	0.084	5.7
1982	54.0	0.731	29	0.000	10.7
1983	45.2	0.704	29	0.001	9.2
1984	46.9	0.687	30	0.001	9.2
1985	38.9	0.787	28	0.000	7.9
1986	43.1	0.821	41	0.000	13.1
1987	27.8	0.634	41	0.000	6.4
1988	24.3	0.770	41	0.000	6.3
1989	29.2	0.675	39	0.000	8.3
1990	29.5	0.700	29	0.001	8.7
-----	-----	-----	-----	-----	-----
1972-1990	36.7	0.791	41	0.000	7.6

^aApril 1 mean of all reporting sites. Data compiled from U.S. Dept. Agriculture 1978, and U.S. Dept. Agriculture, 1979-1990.

^bCorrelation coefficient

^cNumber of cases (sites reported)

^dProbability statistic

interval was selected to evaluate wind direction because this interval corresponds to the 2,286 meter to 3,328 meter height range of the snow accumulation sites. The seasonal snow accumulation trend surface parameters and the corresponding regional winter season climate data are shown in Table 7. The data in Table 7 indicate that all snow accumulation trend surfaces except the 1977, 1987, 1988 and 1989 surfaces increased in a northwesterly direction. The 1977, 1987, 1988 and 1989 surfaces increased in a southwesterly direction. The gradients of the surfaces ranged from a relatively flat gradient decreasing at a rate of $0.09 \text{ cm kilometer}^{-1}$ in 1977 to $0.55 \text{ cm kilometer}^{-1}$ in 1986.

The possible relationships between snow accumulation patterns and regional climate were identified using Pearson's product-moment correlation analysis of the data from Table 7. The results of the correlation analysis are shown in Table 8. These results indicate that trend surface direction has a slightly inverse relationship to regional winter precipitation ($r = -0.662$). In contrast, trend surface gradient has a positive correlation to regional winter precipitation ($r = 0.686$). Mean annual SWE is strongly related to regional winter precipitation ($r = 0.936$), whereas regional winter temperature appears to have little to no relationship to snow accumulation ($r = -0.279$) or precipitation patterns ($r = -0.193$). Regional wind direction showed a positive relationship to trend surface direction ($r = 0.837$), and inverse relationships to mean annual SWE ($r = -0.733$) and regional winter precipitation ($r = -0.651$).

To evaluate multivariate relationships between regional climate and snow accumulation, a regression analysis was conducted on selected related variables identified from the correlation analysis. The results of the regression analysis are shown in Table 9. The results show that mean annual SWE is strongly correlated ($R = 0.944$) with the variables of regional winter precipitation and temperature. The regression equation indicates mean annual SWE increased with increases in regional winter precipitation and decreases in regional winter temperature. Mean annual SWE also correlates with trend

Table 7
Annual Snow Accumulation Trend Surface Parameters
And Mean Regional Winter Climate Data 1972 To 1990

Year	Surface Direction (°Az) ^a	Surface Gradient (cm per km) ^b	Mean SWE (cm) ^c	Regional Precip. (cm) ^d	Regional Temp. (°C) ^e	Regional Wind (°Az) ^f
1972	223	0.36	45.9	18.1	-2.3	241
1973	200	0.42	47.7	20.2	-4.7	229
1974	278	0.30	36.7	13.7	-2.5	237
1975	214	0.51	40.7	16.9	-1.8	237
1976	229	0.24	35.5	13.8	-2.4	242
1977	277	0.09	21.6	5.5	-1.3	264
1978	217	0.41	39.5	17.3	-0.1	244
1979	217	0.10	41.8	15.5	-4.5	237
1980	220	0.30	49.3	22.1	-2.0	233
1981	225	0.10	30.8	12.7	0.7	223
1982	219	0.44	54.0	23.8	-1.4	232
1983	202	0.38	45.2	18.7	-1.9	224
1984	234	0.27	46.9	20.7	-4.0	230
1985	212	0.41	38.9	16.3	-4.6	224
1986	216	0.55	43.1	19.0	-1.2	231
1987	276	0.11	27.8	13.0	-1.2	272
1988	322	0.25	24.3	13.4	-2.3	269
1989	290	0.19	29.2	9.4	-2.5	267
1990	219	0.16	29.5	10.7	-1.0	N/A
-----	-----	-----	-----	-----	-----	-----
1972-1990	230	0.29	36.7	15.8	-2.1	241

^aDirection of snow accumulation decreases across study area

^bRate of change in cm per km in direction of trend surface decrease

^cApril 1 mean of all reporting sites, data compiled from U.S. Dept. Agriculture, 1978 and U.S. Dept. Agriculture, 1979-1990.

^dMean winter precipitation for NOAA divisions Utah five and six and Wyoming division three. Data compiled from U.S. Department of Commerce-Utah 1972-1990 and U.S. Department of Commerce-Wyoming 1972-1990.

^eMean winter temperature for NOAA divisions Utah five and six and Wyoming division three. Data compiled from U.S. Department of Commerce-Utah 1972-1990 and U.S. Department of Commerce-Wyoming 1972-1990.

^fMean winter 800 to 700 millibar wind direction interpolated from Grand Junction, Colorado, Lander, Wyoming, and Salt Lake City, Utah, National Weather Service rawinsonde data, 1972 to 1979 data from U.S. Department of Commerce, National Weather Service National Summaries; 1980 to 1989 Data provided by Utah Climate Center.

Table 8
Correlation Matrix Of 1972 To 1990 Annual Snow Accumulation
Trend Surface Parameters And Mean Regional Winter Climate Data

	Surface Direction	Surface Gradient	Mean SWE	Regional Precip.	Regional Temp.	Regional Wind
Surface Direction	1.000					
Surface Gradient	-0.519	1.000				
Mean SWE	-0.768	0.633	1.000			
Regional Precip.	-0.662	0.686	0.936	1.000		
Regional Temp.	0.115	-0.060	-0.279	-0.193	1.000	
Regional Wind	0.837	-0.493	-0.733	-0.651	0.165	1.000

Table 9
Regression Analysis Of Annual Snow Accumulation Trend Surface
Parameters And Mean Regional Winter Climate Data 1972 To 1990

Dependent Variable (X ₁)	Independent Variable (X ₂)	Independent Variable (X ₃)	R	n	p	Standard Error	Equation
Mean SWE	Regional Precip.	Regional Temp.	0.944	19	0.000	3.2	$X_1 = 8.414 + 1.809X_2 + -0.598X_3$
Mean SWE	Surface Direction	Surface Gradient	0.797	19	0.000	5.8	$X_1 = 63.319 + -0.138X_2 + 25.695X_3$
Surface Direction	Regional Precip.	Regional Temp.	0.602	19	0.027	29.0	$X_1 = 305.668 + -4.559X_2 + -1.315X_3$
Surface Gradient	Regional Precip.		0.686	19	0.001	0.11	$X_1 = -0.045 + 0.021X_2$
Surface Direction	Regional Wind		0.837	18 ^a	0.000	19.8	$X_1 = -196.535 + 1.801X_2$

^an = 18 because 1990 rawinsonde data are not available.

surface direction and trend surface gradient variables ($R = 0.797$). Increases in mean annual SWE corresponds to decreases in trend surface direction, indicating a more northerly direction, and increases in trend surface gradient. Trend surface direction correlates ($R = 0.602$) with the variables of regional winter precipitation and temperature. The regression equation indicates that the trend surface direction will increase, having a more southerly trend direction, with decreases in both regional winter precipitation and temperature. The trend surface gradients correlate ($R = 0.686$) to regional winter precipitation. The regression equation indicates that trend surface gradients increase with increases in regional winter precipitation. The regression of regional winter wind direction to snow accumulation trend surface direction and gradient has a strong correlation ($R = 0.837$) indicating that regional wind patterns can be estimated with relative certainty from the snow accumulation patterns. It should be noted that from the correlation analysis, regional winter temperature variability appears to have little relationship to the snow accumulation patterns. However, when integrated with the precipitation variable, temperature variability improves the correlations.

The findings of this analysis can be summarized: (1) mean snow accumulation increases with increases in winter precipitation and decreases in winter temperature; (2) snow accumulation trend surface direction decreases, taking a more southerly oriented trend, with decreases in regional winter precipitation and temperature; (3) snow accumulation trend surface gradients steepen with increase in regional winter precipitation; and (4) regional wind direction is related to the resultant snow accumulation trend surface direction. These findings suggest that wet and cold winters result in higher accumulations of snow, that snow accumulation will diminish towards a southerly direction during dry and cold winters, and that snow accumulation gradients will be steeper during wet winters. The findings also suggest that precipitation is the primary climatic influence on snow accumulation, whereas temperature has a more secondary influence on snow accumulation.

Long-term interpretations can be made from the averaged 1972 to 1990 snow accumulation and trend surface data. Because the Uinta Mountains are subjected to a predominantly westerly air-flow, a west to east decline in snow accumulation and trend direction would be expected. However, the average trend direction for the 1972 to 1990 period of 230° indicates that a northeasterly decline occurs. The northeasterly diminishment of snow accumulation indicates that the air-flow has a significant southerly component. The 1972 to 1989 wind direction data in Table 7, indicate the wind direction at the 800 millibar to 700 millibar height on average maintained a slightly more zonal heading of 241° . The difference between the rawinsonde direction and the snow accumulation trend surface direction suggests that a more southerly flow is present when storms pass through the region, and westerly air-flow dominates during stable periods. This air-flow pattern is presumably influenced by the anticyclonic flow, which originates to the southwest of the study area, as described by Mitchell (1976).

Synthesis Of Present ELA

Presently no glaciers exist in the Uinta Mountains. Thus, the present ELA for the Uinta Mountains has not been established. Because glacial mass balance is controlled primarily by the combined effects of precipitation (accumulation) and temperature (ablation), the height of the present ELA can be thought to occur at an undetermined altitude above the Uinta Mountains where temperatures are sufficiently cold to sustain permanent ice.

Studies of present glaciers have shown that the ELA will occur where specific precipitation and temperature criteria are satisfied (Loewe, 1971; Sutherland, 1984; Leonard, 1989). Leonard (1989), after other researchers (Loewe, 1971; Sutherland, 1984), has developed a refined model for the prediction of winter accumulation and summer temperature, in other words net accumulation over net ablation at ELA. Equations

5 and 6 describe the relationship of winter accumulation and summer temperature at the ELA: Thus,

$$A = 1.33 (T_{vi-viii} + 6.66)^{2.85} \quad (5)$$

$$A = 1.33 (T_{vi-viii} + 9.66)^{2.85} \quad (6)$$

Equation 5 defines the higher margin of the ELA, and Equation 6 defines the lower margin (Leonard, 1989). Where A = winter accumulation in millimeters; and $T_{vi-viii}$ = the mean June through August temperature. A graph illustrating curves computed from equations 5 and 6 is shown in Figure 11. Rearranging equations 5 and 6 $T_{vi-viii}$ can be solved:

$$T_{vi-viii} = ((A/1.33)\sqrt[2.85]{}) - 6.66 \quad (7)$$

$$T_{vi-viii} = ((A/1.33)\sqrt[2.85]{}) - 9.66 \quad (8)$$

Because snow accumulation, temperature and lapse rate data are available for the study area, solving for $T_{vi-viii}$ enables the calculation of the altitude at which glacial equilibrium would occur under present conditions. By determining the height difference between the temperature at ELA ($T_{vi-viii}$) and the 0°C isotherm using the summer lapse rate ($L_{vi-viii}$), and adding the height difference to the summer 0°C isotherm altitude ($ZT0^{\circ}_{vi-viii}$), the present ELA ($ZELA$) is estimated. Thus,

$$ZELA = (((0^{\circ} - T_{vi-viii})/L_{vi-viii})100) + ZT0^{\circ}_{vi-viii} \quad (9)$$

Employing equations 5 through 9, high and low estimates of the present ELA can be

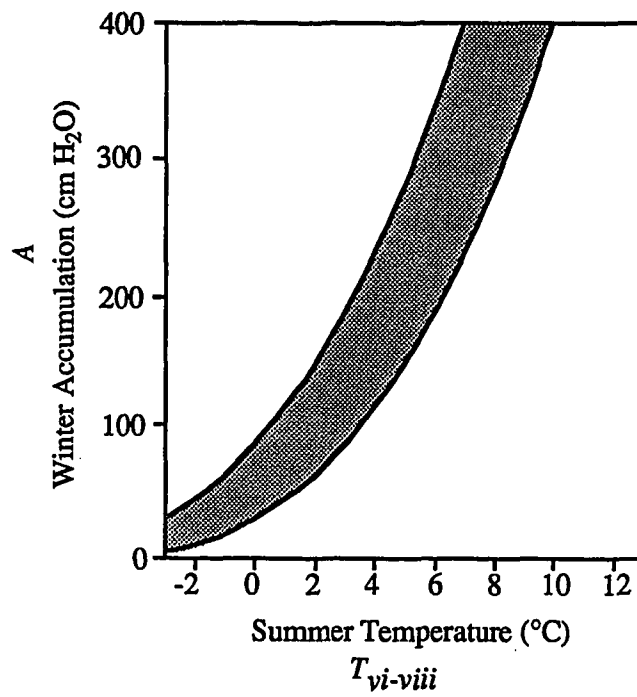


Figure 11. Relationship of winter accumulation (A) and summer temperature ($T_{vi-viii}$) at ELA sites world wide (after Leonard, 1989).

derived from snow accumulation measurements. These estimates are shown in Table 10, and trend surface maps of the high and low estimates are shown in Figure 12.

The direction of the two estimated trend surfaces shown in Figure 12 is 230° for both surfaces, the same direction as the 1972 to 1990 snow accumulation trend surface. The gradients of the two surfaces are 2.7 meters kilometer⁻¹. The mean altitude of the low ELA estimate is 4,507 meters, and the high ELA estimate is 4,907 meters, ~ a 400 meter difference in altitude. The average estimated ELAs are located 383 to 783 meters above the 4,124 meter elevation of Kings Peak. Based on these estimates, a 383 to 783 meter lowering of the estimated ELA would be necessary for glaciation to occur on the higher reaches of the Uinta Mountains.

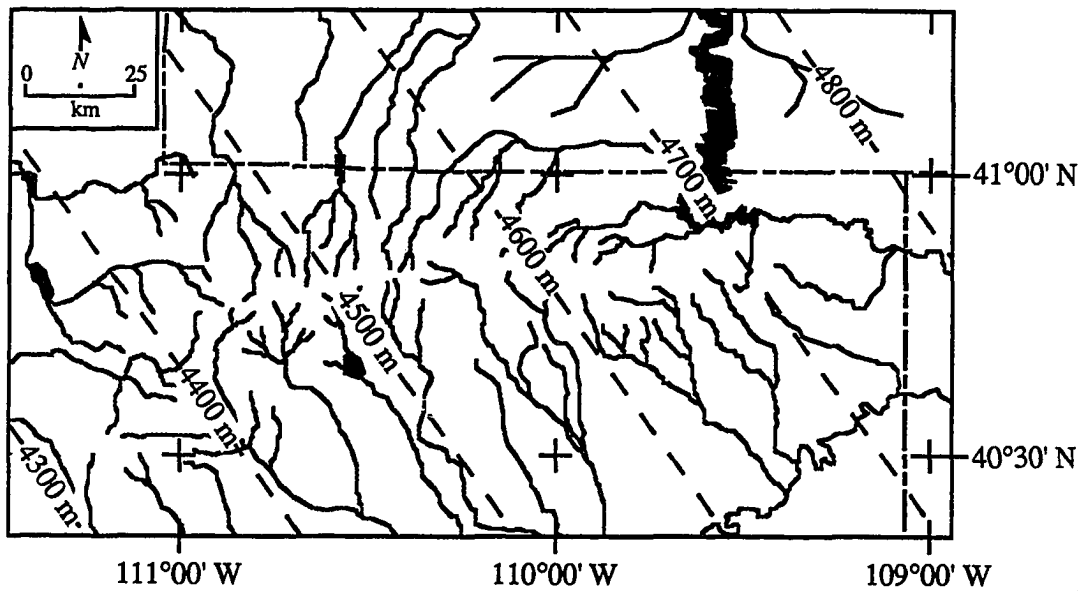
Assuming a lapse rate of 0.75 °C 100 meters⁻¹ and unchanged snow accumulation, a 2.9°C to 5.9°C lowering of the mean summer temperature would be required to lower the estimated ELA to the height of Kings Peak. However, if the mean summer temperature remained unchanged, the present average winter accumulation of 36.7 cm must be increased from ~ 93 cm to 197 cm; these increases are on the order of 250% to 540%. These estimations demonstrate that a relatively small decrease in temperature coupled with minimal to no increase in precipitation would reinitiate glaciation of Kings Peak.

Table 10
Estimated Present ELA From
1972 To 1990 Snow Accumulation Values

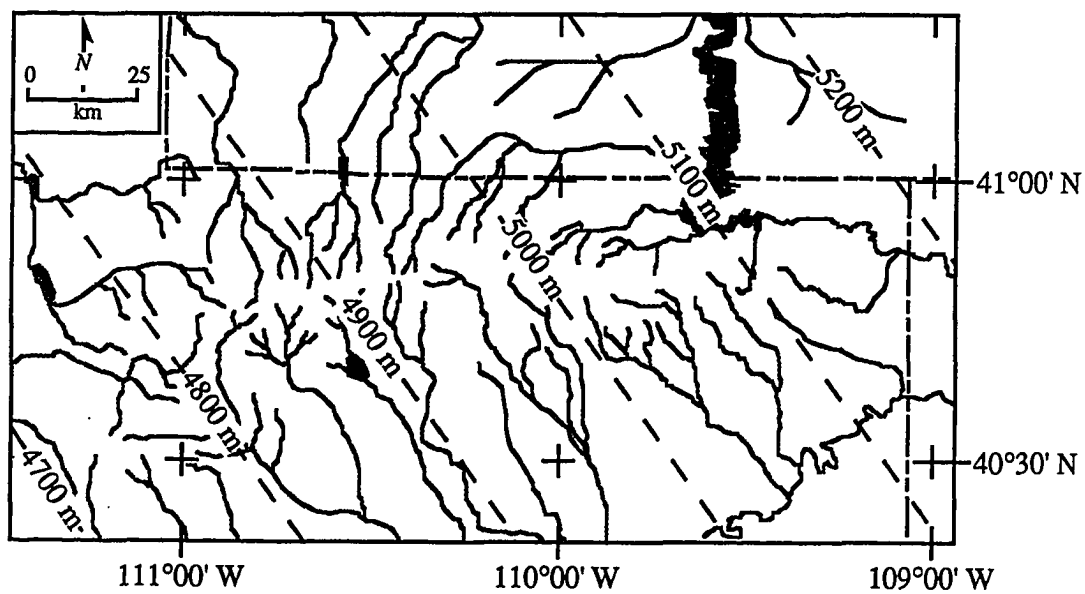
Site Name	N Latitude	W Longitude	Low Estimate (m) ^a	High Estimate (m) ^b
1. Ashley-Twin Lakes	40°43'	109°48'	4,624	5,024
2. Atwood Lake	40°44'	110°17'	4,530	4,930
3. Beaver Creek Divide	40°37'	111°04'	4,383	4,783
4. Blacks Fork Junction	40°58'	110°35'	4,525	4,925
5. Brown Duck Ridge	40°35'	110°35'	4,449	4,849
6. Buck Pasture	40°51'	110°40'	4,486	4,886
7. Burts-Miller Ranch	41°00'	110°52'	4,482	4,882
8. Chalk Creek #1	40°51'	111°04'	4,423	4,823
9. Chalk Creek #2	40°54'	111°04'	4,431	4,831
10. Chalk Creek #3	40°55'	111°06'	4,428	4,828
11. Chepeta	40°46'	110°00'	4,594	4,994
12. Chepeta-White R. Lake	40°46'	109°59'	4,598	4,998
13. E. Fork Blacks Fork G.S.	40°53'	110°32'	4,516	4,916
14. Five Points Lake	40°43'	110°28'	4,495	4,895
15. Hayden Fork	40°47'	110°53'	4,438	4,838
16. Henry's Fork	40°53'	110°22'	4,547	4,947
17. Hewinta G.S.	40°57'	110°29'	4,540	4,940
18. Hickerson Park	40°54'	109°58'	4,634	5,034
19. Hole in the Rock	40°55'	110°12'	4,589	4,989
20. Hole in the Rock G.S.	40°57'	110°09'	4,607	5,007
21. Kings Cabin-Upper	40°43'	109°33'	4,686	5,086
22. Lake Fork Basin	40°45'	110°37'	4,475	4,875
23. Lake Fork Mountain	40°36'	110°26'	4,477	4,877
24. Lake Fork Mountain #3	40°33'	110°21'	4,481	4,881
25. Lightning Lake	40°43'	110°45'	4,448	4,848
26. Lily Lake	40°52'	110°48'	4,468	4,868
27. Middle Beaver Creek	40°57'	110°11'	4,600	5,000
28. Mosby Mountain	40°37'	109°53'	4,582	4,982
29. Paradise Park	40°41'	109°55'	4,590	4,990
30. Redden Mine Lower	40°41'	111°13'	4,372	4,772
31. Reynolds Park	40°45'	109°55'	4,607	5,007
32. Rock Creek	40°33'	110°41'	4,428	4,828
33. Sergeant Lakes	40°50'	111°17'	4,388	4,788
34. Smith and Morehouse (1)	40°48'	111°05'	4,412	4,812
35. Smith and Morehouse (2)	40°47'	111°06'	4,406	4,806
36. Soapstone R.S.	40°34'	111°02'	4,380	4,780
37. Spirit Lake	40°50'	110°00'	4,609	5,009
38. Steel Creek Park	40°55'	110°30'	4,530	4,930
39. Stillwater Camp	40°52'	110°50'	4,463	4,863
40. Trial Lake	40°41'	110°57'	4,410	4,810
41. Trout Creek	40°44'	109°40'	4,660	5,060

^aLow estimate calculated using equations 7 and 9

^bHigh estimate calculated using equations 8 and 9



A. Low ELA estimate.



B. High ELA estimate

Figure 12. Low (A) and high (B) present estimated ELA trend surfaces. Estimated from mean 1972 to 1990 snow accumulation. Mean height is 4,507 meters for low surface and 4,907 meters for high surface. For both surfaces direction is 230° and gradient is 2.8 meters per kilometer $^{-1}$. Trend surface equation, low $ELA = 16408.707 + 193.296Lat + -179.033Lon$, high $ELA = 16808.707 + 193.296Lat + -179.033Lon$.

CHAPTER IV

RECONSTRUCTION OF LATE-PLEISTOCENE EQUILIBRIUM-LINE ALTITUDES: METHODS AND ANALYSIS

Introduction

A number of methods have been used to reconstruct paleoELAs (Meierding, 1982). These methods are discussed in the following sections. Following this discussion is a rationale for the selection of the most appropriate reconstruction method for this dissertation. The reconstructions of the Pleistocene glaciations are based on the interpretations and mapping by previous workers in the study area (Atwood, 1909; Bradley, 1936; and Schlenker, 1988). A Geographic Information System (GIS) was used to reconstruct heights and extents of the glaciers. The GIS data base integrated the mapping and interpretations of previous workers and was used to query areal and vertical data for the estimation of the ELAs.

The sequence of steps taken to reconstruct and evaluate the paleoELA was: (1) evaluation and selection of paleoELA estimation methods; (2) construction of a study area GIS data base to measure areal and vertical data to estimate ELAs; (3) construction of ELA trend surfaces using differing paleoELA estimation methods (i.e., toe-to-headwall altitude ratio [THAR], and accumulation-area ratio [AAR] methods); (4) selection of the most appropriate paleoELA estimation method through analysis of trend surface statistics. Using the selected reconstruction method, trend surfaces for the two episodes were analyzed to evaluate differences between the two glacial episodes and between present and the glacial episodes.

Estimation Of Late-Pleistocene ELA

Numerous methods have been developed to estimate paleoELAs (Meierding, 1982). The methods initially considered for this dissertation included: cirque floor elevation, glaciation threshold elevation, maximum lateral moraine elevation, toe-to-headwall altitude ratio (THAR), and accumulation-area ratio (AAR). Meierding's (1982) evaluation of these methods served as a basis for the selection of the methods used in this dissertation.

Commonly, the mean elevation of cirque floors has been used to index the ELA (Peterson and Robinson, 1969; Trenhaile, 1975; Flint, 1977; Zielinski and McCoy, 1987; Burbank, 1991). This index assumes glacial erosion of cirque basins is a function of glaciation height and, therefore, a reasonable approach for measuring past climate change. However, cirque-floor elevations can represent a composite ELA from multiple glacial episodes (Flint, 1957). Thus, when multiple glacial episodes are to be evaluated this method is inappropriate.

The glaciation threshold method is a measure of the mean elevation of the lowest glaciated summits and the highest unglaciated peaks in an area of study (Flint, 1971; Porter, 1977). Thus, this method is most effective for regional-scale analyses and is not appropriate for the analysis of a specific mountain range. As with the cirque-floor elevation method, the glaciation threshold method does not allow for discrimination between the heights of multiple glacial episodes.

Maximum lateral moraine elevations have also been used to index the ELA of past glaciations (Meierding, 1982; Hawkins, 1985). This method assumes the maximum elevation of lateral moraines approximates the height of the ELA. Unfortunately, this approach can be subject to errors. The interpretation of lateral moraines from aerial and topographic data resources can be subjective and time consuming, and post-glacial modification of moraines (i.e., erosion and mass-wasting) is likely to introduce height

measurement errors (Meierding, 1982). Because of the subjectivity and the potential for measurement error, this method was considered inappropriate for this dissertation.

Toe-to-headwall altitude ratio (THAR), and accumulation-area ratio (AAR) measurements are two methods that utilize glacier height and extent dimensions to estimate ELAs (Porter, 1975; Pierce, 1979; Meierding, 1982; Hawkins, 1985; Leonard, 1984; Leonard, 1989; Locke, 1990). Both the THAR and AAR indices are based on observations of present glaciers (Meierding, 1982). These methods have also been used to estimate the ELAs of reconstructed Pleistocene glaciers. The THAR is a bottom to top height ratio of vertical altitude of a glacier and is measured from the lowermost terminal moraine to the uppermost-headwall trim line. Thus, a THAR of 0.40 is 40 % of the vertical height from the toe to the headwall of a glacier (Meierding, 1982).

The AAR measurement is calculated from the hypsometric area ratio of a glacier. AAR is determined from trim lines and end moraines that indicate the areal extent of glaciation and from elevations on the glacier surface. The AAR is expressed as an elevation on the glacier surface that represents a ratio of accumulation area verses ablation area. For example, an AAR of 0.65 means that the ELA is located at an elevation on the glacier surface immediately below the upper 65 % of the glaciated area.

Meierding's (1982) evaluation of the methods that have been discussed here, demonstrated that the applicability of a particular method can depend upon the size and type of a glacier. In his analysis of reconstructed glaciers for the Front Range of Colorado, Meierding (1982) found that the THAR and AAR methods yielded lower error values than cirque elevation, glaciation threshold or maximum lateral moraine height methods.

Following Meierding's (1982) evaluation of the methods, and because the scope of this dissertation is to reconstruct the ELAs of the two glacial episodes, cirque floor elevation, glaciation threshold and lateral moraine elevation methods appeared to be

inappropriate for this dissertation. Thus, AAR and THAR methods were used for the ELA reconstruction.

GIS Data Resources And Data Base Construction

Maps of the last two Pleistocene glacial episodes in the study area (Atwood, 1909; Bradley, 1936; and Schlenker, 1988) provided the basis for the reconstruction of the extent of Pleistocene glaciers. Because the previous mapping has been conducted at differing scales and needed to be integrated, and because AAR and THAR methods require both height and area measurements, a GIS data base of the study area was constructed to query the ELA heights.

The topographical and topological base data of the study area were constructed from portions of four adjoining U.S. Geological Survey 1:250,000 scale topographic map sheets. These sheets are: Salt Lake City, Utah and Wyoming; Vernal, Utah and Colorado; Ogden, Utah and Wyoming; and Rock Springs, Wyoming and Colorado. The distribution of the reconstructed extent of late-Pleistocene glaciers of oxygen isotope stage six and stage two ages was derived from maps of varying scales: Atwood's (1909) 1:125,000 reconnaissance of the entire range; Bradley's (1936) 1:36,000 analysis of the north slope of the range; and Schlenker's (1988) 1:24,000 analysis of the Blacks Fork Drainage on the north slope of the range. These maps were combined at a common nominal scale in the GIS.

The combining of the map data bases enabled an interpolation of areal and topographic parameters for determination of AAR and THAR elevations for the two glacial episodes. The GIS also facilitates the conversion of map units from English units to metric units. The output resolution of the GIS data base was 10 meters for vertical measurements, and 18.5 meters and 14.2 meters, respectively, for latitude and longitude measurements. The data base was constructed from maps having 200 foot contour intervals; consequently,

vertical measurement errors as large as 30 meters might have been tabulated. Horizontal errors ranging from 0.4 km for longitude measurements to 0.5 km for latitude measurements might have resulted from the resolution of the coordinate system. Although the Universal Transverse Mercator (UTM) grid coordinate system may have provided better spatial resolution than Latitude-Longitude coordinates, the older maps (Atwood, 1909; Bradley, 1936) used to construct the data base were drawn prior to the development of the UTM system, necessitating the use of latitude-longitude coordinates for this analysis.

The map data bases were assembled and analyzed using INTERA TYDAC® SPANS GIS. Topographical and topological data from the four adjoining U.S. Geological Survey topographic maps were joined to form an integrated topographical and topological study area data base. The former extent of glacial ice was determined from the maximum limits of glacial erosional and depositional landforms delimited by previously cited map sources. The outermost moraines and trim lines for the two glaciations were used to plot the extent of ice during full-glacial time. Complexes of smaller cirque glaciers that joined in the main valleys were grouped into single reconstructed glaciers. A separate topological overlay was constructed for each of the two glacial episodes, and these were overlain onto the study area data base. From GIS data base height, area and coordinate location parameters of the reconstructed glacier overlays were rapidly computed. From the height, area and coordinate location parameters, the AAR and THAR (height and coordinates) for each of the glacial basins was measured for both of the glacial episodes. The spatial extents of the glacial margins for the two episodes are shown in Figures 13 and 14. Tabulation of height and area parameters for the reconstructed extent of the glaciers are shown in Tables 11 and 12.

Examination of the maps in Figures 12 and 13 reveals a significant variation between the two episodes. This variation exists in the extent of glaciation from west to east across the range. From Figures 12 and 13, the stage six glaciers are larger than the stage

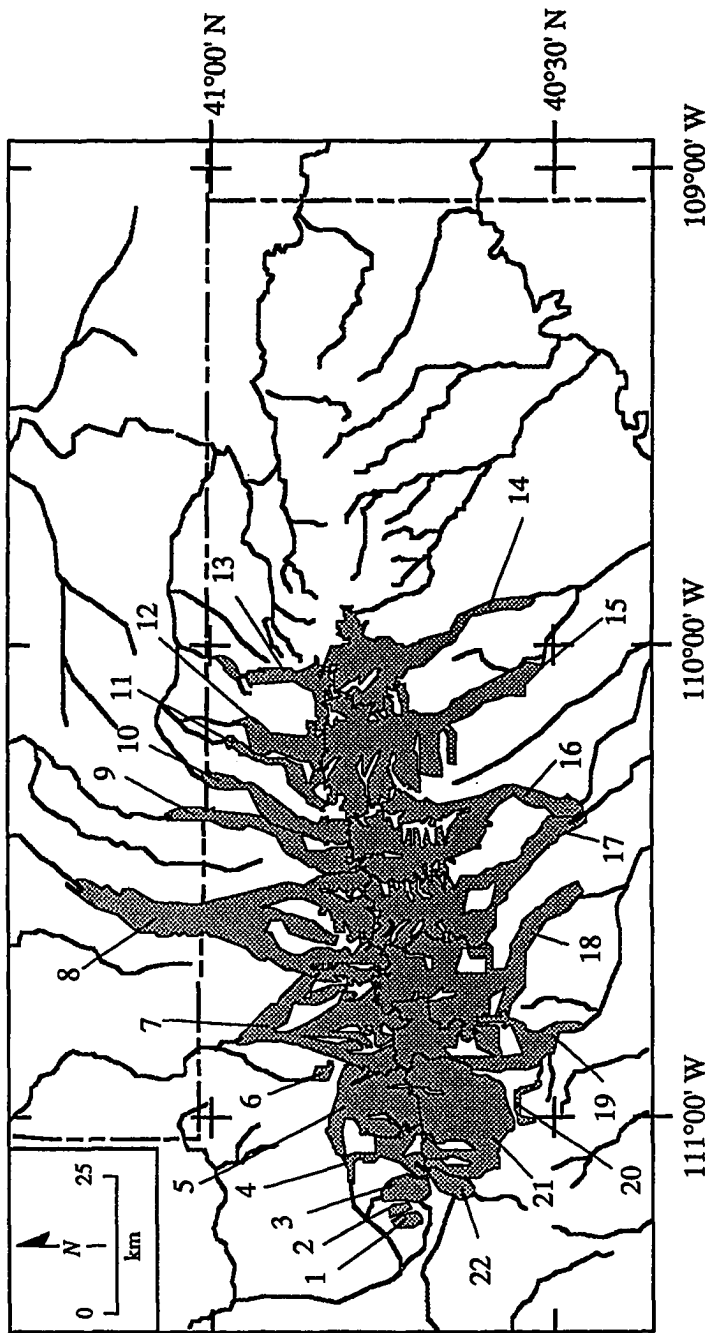


Figure 13. Reconstructed oxygen isotope stage six glaciers. Index numbers of reconstructed glaciers correspond to listings in Table 12.

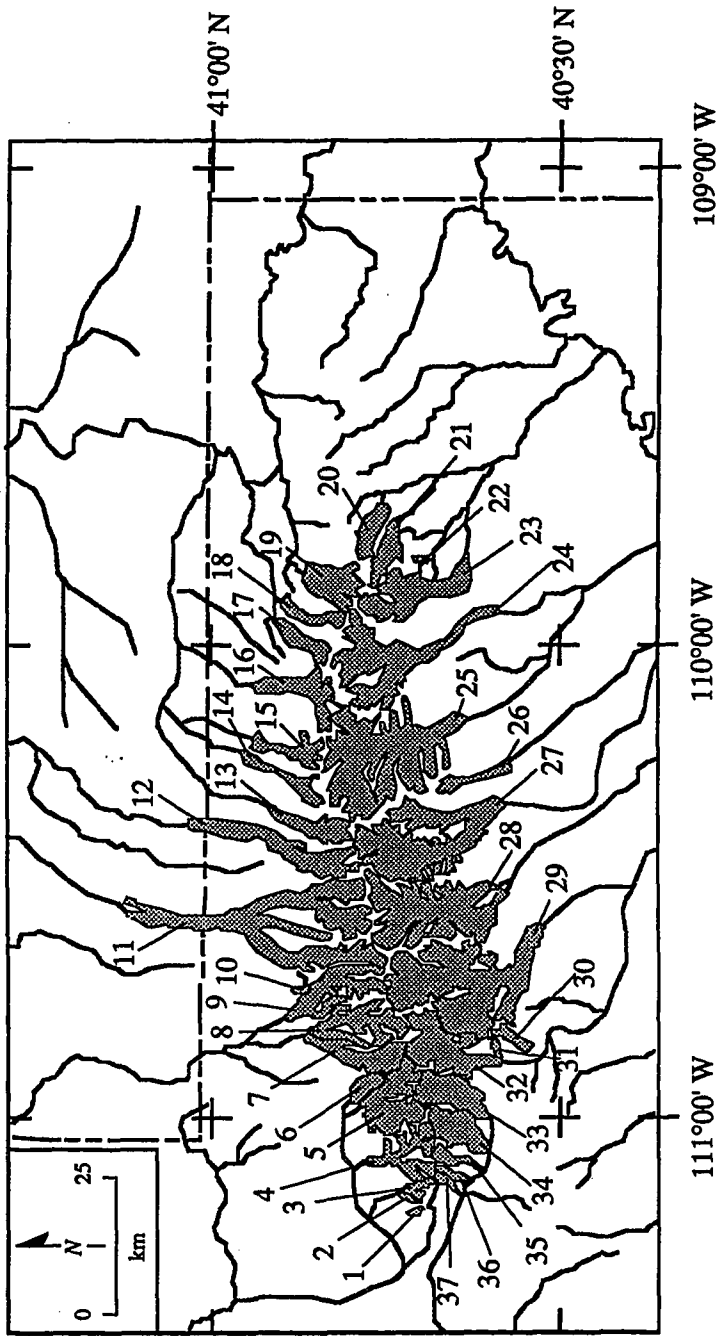


Figure 14. Reconstructed oxygen isotope stage two glaciers. Index numbers of reconstructed glaciers correspond to listings in Table 13.

Table 11
Oxygen Isotope Stage Six Reconstructed Extent of Glaciers

Basin	N Latitude	W Longitude	Terminal Elevation (m)	Headwall Elevation (m)	Area (km)
1. Swifts Canyon	40°41'	111°12'	2,360	3,100	3.7
2. Shingle Mill Creek	40°43'	111°12'	2,400	2,840	1.6
3. Ledge Fork Canyon	40°42'	111°10'	2,390	3,060	12.5
4. Smith and Morehouse	40°42'	111°04'	2,270	3,360	56.8
5. Weber River	40°43'	110°59'	2,330	3,480	112.6
6. Whitney	40°47'	110°55'	3,040	3,060	2.8
7. Bear River	40°45'	110°48'	2,510	3,680	211.8
8. Blacks Fork	40°55'	110°35'	2,410	3,810	320.5
9. Smiths Fork	40°52'	110°25'	2,730	3,960	92.3
10. Henrys Fork	40°52'	110°21'	2,720	3,810	62.5
11. West Fork Beaver Creek	40°53'	110°15'	2,610	3,670	30.4
12. Middle Fork Beaver Creek	40°53'	110°12'	2,670	3,640	36.8
13. Burnt Fork	40°52'	110°52'	2,420	3,710	54.8
14. White Rocks	40°45'	110°00'	1,660	3,690	150.7
15. Uinta River	40°45'	110°13'	2,100	3,980	295.2
16. Yellowstone River	40°42'	110°42'	2,170	4,040	222.6
17. Lake Fork	40°42'	110°34'	2,160	3,910	245.1
18. Rock Creek	40°38'	110°46'	2,220	3,790	286.3
19. Duchesne River	40°41'	110°51'	2,150	3,670	151.4
20. Soapstone	40°32'	110°59'	2,730	2,860	5.4
21. Provo River	40°39'	111°03'	2,350	3,460	188.6
22. Left Fork Beaver Creek	40°40'	111°12'	2,280	3,080	15.6

Table 12
Oxygen Isotope Stage Two Reconstructed Extent of Glaciers

Basin	N Latitude	W Longitude	Terminal Elevation (m)	Headwall Elevation (m)	Area (km)
1. Swifts Canyon	40°41'	111°12'	2,880	3,100	2.1
2. Red Pine Creek	40°43'	111°10'	2,390	2,980	3.1
3. Ledge Fork Canyon	40°41'	111°90'	2,390	3,060	8.1
4. Smith and Morehouse	40°42'	111°03'	2,370	3,360	49.1
5. Weber River	40°42'	111°00'	2,300	3,410	75.8
6. Gold Hill	40°46'	110°55'	2,640	3,390	14.8
7. Hayden Fork Bear River	40°44'	110°52'	2,690	3,560	48.8
8. Stillwater Fork Bear River	40°44'	110°48'	2,680	3,680	65.7
9. East Fork Bear River	40°46'	110°43'	2,660	3,680	66.2
10. Mill Creek	40°52'	110°43'	3,030	3,380	3.0
11. Blacks Fork	40°52'	110°36'	2,450	3,800	253.2
12. Smiths Fork	40°52'	110°26'	2,730	3,960	86.8
13. Henrys Fork	40°50'	110°23'	3,000	3,810	43.6
14. West Fork Beaver Creek	40°52'	110°16'	2,710	3,670	27.6
15. Middle Fork Beaver Creek	40°52'	110°13'	2,730	3,640	32.3
16. Burnt Fork	40°51'	110°05'	2,730	3,710	48.2
17. West Fork Sheep Creek	40°51'	110°01'	2,760	3,440	31.2
18. East Fork Sheep Creek	40°51'	109°55'	2,730	3,400	19.9
19. Carter Creek	40°49'	109°52'	2,620	3,390	51.0
20. Leidy Peak	40°46'	109°46'	2,650	3,380	27.0
21. Ashley Fork	40°44'	109°49'	2,910	3,500	30.6
22. Marsh Peak	40°41'	109°48'	3,030	3,350	2.4
23. Dry Fork	40°42'	109°54'	2,300	3,660	86.5
24. White Rocks	40°45'	110°00'	2,350	3,680	141.7
25. Uinta River	40°45'	110°14'	2,360	3,980	250.4
26. Crow Canyon	40°36'	110°16'	2,650	3,650	23.2
27. Yellowstone River	40°45'	110°24'	2,440	4,040	186.4
28. Lake Fork	40°43'	110°36'	2,700	3,890	186.2
29. Rock Creek	40°39'	110°48'	2,370	3,760	256.8
30. Hades Canyon	40°34'	110°50'	2,490	3,360	13.7
31. Granddaddy Mountain	40°36'	110°51'	2,890	3,370	4.4
32. Duchesne River	40°42'	110°52'	2,540	3,670	100.2
33. Provo River	40°40'	110°57'	2,460	3,460	64.4
34. North Fork Provo River	40°39'	111°00'	2,360	3,380	52.2
35. Shingle Creek	40°39'	111°05'	2,400	3,060	14.8
36. Slate Creek	40°40'	111°10'	2,420	3,060	10.7
37. Left Fork Beaver Creek	40°39'	111°11'	2,370	3,080	5.2

two glaciers on the western and central portion of the range. The size of the stage six glaciers becomes increasingly smaller eastward across the range. On the very eastern portion of the range, the stage two glaciers appear to have over-run the deposits of the stage six glaciers. This indicates that ice accumulation differed substantially between the two glacial episodes and suggests that considerable climatic differences, specifically moisture supply occurred between the two episodes.

Analysis Of Late-Pleistocene ELA Trend Surfaces

Differing AAR and THAR ratios were evaluated to determine the method and ratio that best approximate the heights of the Pleistocene ELAs. AAR ratios of 0.65, 0.60 and 0.55 and THAR ratios of 0.45, 0.40 and 0.35 calculated via the GIS were used to determine the ELAs for both ages. Table 13 shows the trend surface variance statistics for the differing ELA measurements and height ratios. By comparing the surface trend (R), probability statistics (p), and standard error statistics in Table 13, the most appropriate method and ratio for evaluating the ELAs of both episodes can be selected. For this comparison, the strongest trends and lowest overall errors for the two episodes were obtained using the AAR method with a ratio of 0.55. It is assumed that the method and ratio that produces the strongest trends and lowest overall errors best approximates the actual ELA surface heights during the glacial episodes.

Using the AAR method with a ratio of 0.55, the ELA was calculated for the reconstructed extent of glaciers listed in Tables 11 and 12; the ELA trend surfaces were reconstructed for both episodes. The observed and estimated ELA elevations and residual values for the basins presented in Tables 14 and 15, and ELA trend surface maps are shown on Figures 15 and 16.

The extent of stage six glaciation appears to have a lower mean ELA and a steeper gradient than the stage two glaciation. The mean stage six ELA is ~2,950 meters and has a

Table 13
Full-Glacial ELA Trend Surface Statistics^a

Isotope Stage	Method-Ratio	Mean ELA (m)	<i>R</i>	<i>n</i>	<i>p</i>	Standard Error (m)
Stage Six	AAR-0.65	2,885	0.77	22	0.000	123.8
	AAR-0.60	2,920	0.77	22	0.000	127.3
	AAR-0.55	2,949	0.76	22	0.000	132.4
	THAR-0.45	2,905	0.61	22	0.012	162.5
	THAR-0.40	2,849	0.64	22	0.006	156.0
	THAR-0.35	2,791	0.67	22	0.003	152.1
Stage Two	AAR-0.65	2,980	0.53	37	0.004	136.5
	AAR-0.60	3,006	0.59	37	0.001	128.4
	AAR-0.55	3,037	0.62	37	0.000	127.1
	THAR-0.45	3,008	0.62	37	0.000	145.2
	THAR-0.40	2,962	0.61	37	0.000	144.6
	THAR-0.35	2,917	0.60	37	0.001	145.9

^aTrend surface statistics to regression with northing (*Lat*) and easting (*Lon*) variables

Table 14
Oxygen Isotope Stage Six ELA Parameters At 0.55 AAR

Basin	N Latitude	W Longitude	Observed Elevation (m)	Estimated Elevation (m)	Residual (m)
1. Swifts Canyon	40°41'	111°12'	2,940	2,759	181
2. Shingle Mill Creek	40°43'	111°12'	2,700	2,756	-56
3. Ledge Fork Canyon	40°42'	111°10'	2,730	2,770	-40
4. Smith and Morehouse	40°42'	111°04'	2,750	2,808	-58
5. Weber River	40°43'	110°59'	2,960	2,838	122
6. Whitney	40°47'	110°55'	3,040	2,859	181
7. Bear River	40°45'	110°48'	3,010	2,910	100
8. Blacks Fork	40°55'	110°35'	2,960	2,974	-14
9. Smiths Fork	40°52'	110°25'	3,030	3,041	-11
10. Henrys Fork	40°52'	110°21'	3,070	3,069	1
11. West Fork Beaver Creek	40°53'	110°15'	3,030	3,107	-77
12. Middle Fork Beaver Creek	40°53'	110°12'	3,060	3,127	-67
13. Burnt Fork	40°52'	110°52'	3,040	3,176	-136
14. White Rocks	40°45'	110°00'	3,150	3,222	-72
15. Uinta River	40°45'	110°13'	3,260	3,137	123
16. Yellowstone River	40°42'	110°42'	3,170	3,064	106
17. Lake Fork	40°42'	110°34'	3,060	3,000	60
18. Rock Creek	40°38'	110°46'	3,030	2,929	101
19. Duchesne River	40°41'	110°51'	2,980	2,892	88
20. Soapstone	40°32'	110°59'	2,740	2,857	-117
21. Provo River	40°39'	111°03'	2,790	2,838	-48
22. Left Fork Beaver Creek	40°40'	111°12'	2,390	2,759	-369

Table 15
Oxygen Isotope Stage Two ELA Parameters At 0.55 AAR

Basin	N Latitude	W Longitude	Observed Elevation (m)	Estimated Elevation (m)	Residual (m)
1. Swifts Canyon	40°41'	111°12'	3,020	2,909	111
2. Red Pine Creek	40°43'	111°10'	2,620	2,911	-291
3. Ledge Fork Canyon	40°41'	111°90'	2,720	2,919	-199
4. Smith and Morehouse	40°42'	111°03'	2,810	2,937	-127
5. Weber River	40°42'	111°00'	3,020	2,950	70
6. Gold Hill	40°46'	110°55'	3,000	2,961	39
7. Hayden Fork Bear River	40°44'	110°52'	3,020	2,975	45
8. Stillwater Fork Bear River	40°44'	110°48'	3,050	2,989	61
9. East Fork Bear River	40°46'	110°43'	3,070	3,001	69
10. Mill Creek	40°52'	110°43'	3,050	2,995	55
11. Blacks Fork	40°52'	110°36'	3,020	3,022	-2
12. Smiths Fork	40°52'	110°26'	3,040	3,055	-15
13. Henrys Fork	40°50'	110°23'	3,210	3,069	141
14. West Fork Beaver Creek	40°52'	110°16'	3,090	3,091	-1
15. Middle Fork Beaver Creek	40°52'	110°13'	3,200	3,102	98
16. Burnt Fork	40°51'	110°05'	3,160	3,131	29
17. West Fork Sheep Creek	40°51'	110°01'	3,030	3,145	-115
18. East Fork Sheep Creek	40°51'	109°55'	3,030	3,164	-134
19. Carter Creek	40°49'	109°52'	2,990	3,178	-188
20. Leidy Peak	40°46'	109°46'	3,030	3,204	-174
21. Ashley Fork	40°44'	109°49'	3,180	3,196	-16
22. Marsh Peak	40°41'	109°48'	3,280	3,202	78
23. Dry Fork	40°42'	109°54'	3,070	3,182	-112
24. White Rocks	40°45'	110°00'	3,190	3,154	36
25. Uinta River	40°45'	110°14'	3,310	3,107	203
26. Crow Canyon	40°36'	110°16'	3,030	3,108	-78
27. Yellowstone River	40°45'	110°24'	3,290	3,071	219
28. Lake Fork	40°43'	110°36'	3,210	3,032	178
29. Rock Creek	40°39'	110°48'	3,040	2,996	44
30. Hades Canyon	40°34'	110°50'	2,990	2,993	-3
31. Granddaddy Mountain	40°36'	110°51'	3,230	2,989	241
32. Duchesne River	40°42'	110°52'	3,030	2,975	55
33. Provo River	40°40'	110°57'	3,010	2,963	47
34. North Fork Provo River	40°39'	111°00'	2,850	2,951	-101
35. Shingle Creek	40°39'	111°05'	2,860	2,934	-74
36. Slate Creek	40°40'	111°10'	2,780	2,914	-134
37. Left Fork Beaver Creek	40°39'	111°11'	2,860	2,913	-53

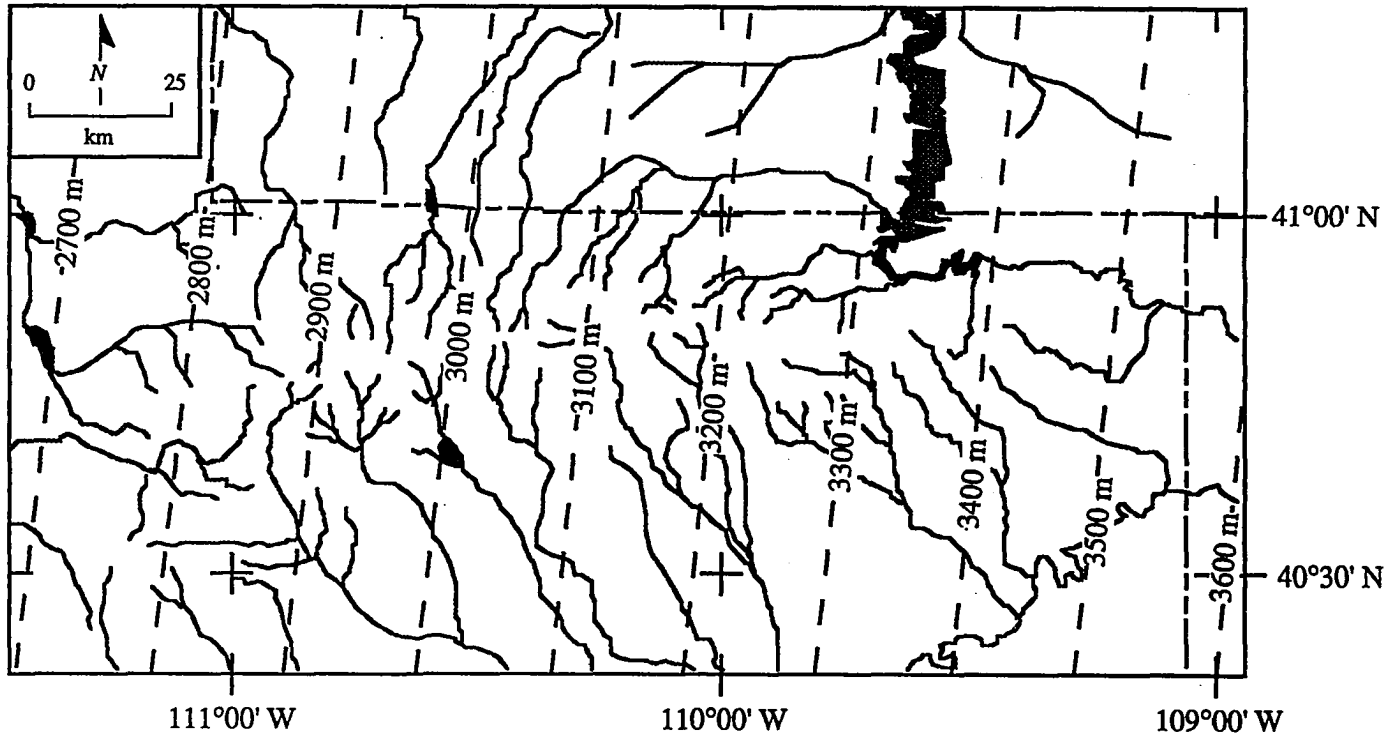


Figure 15. Oxygen isotope stage six 0.55 AAR ELA trend surface. Corresponding trend surface statistics are listed in Table 14. Trend surface direction is 276° and gradient is $4.8 \text{ meters km}^{-1}$. Trend surface equation is $\text{ELA} = 50445.936 + -101.774\text{Lat} + -391.597\text{Lon}$.

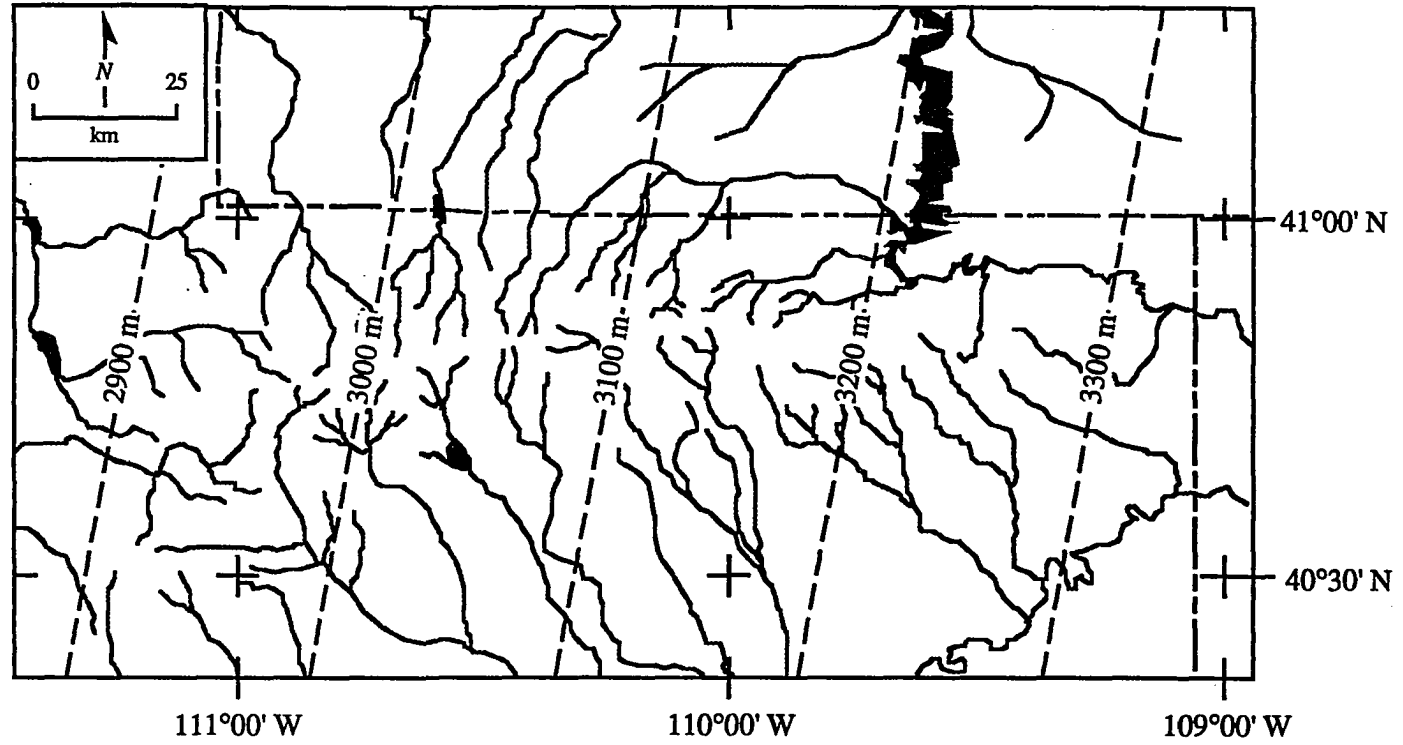


Figure 16. Oxygen isotope stage two 0.55 AAR ELA trend surface. Corresponding trend surface statistics are listed in Table 14. Trend surface direction is 279° and gradient is $2.4 \text{ meters km}^{-1}$. Trend surface equation is $ELA = 29233.82 + -71.138Lat + -210.706Lon$.

trend surface gradient that rises at a rate of 4.8 meters km^{-1} . The mean stage two ELA is ~ 3,040 meters and has a trend surface gradient that rises at a rate of 2.4 meters km^{-1} . From the snow accumulation pattern and climate variability relationships summarized in Chapter 3, it is implied that the gradient differences indicate that the stage six glaciation was more moist than the stage two glaciation. Another difference between the two episodes is the direction of the ELA trend surface slopes. The stage six glaciation has a slope that rises on an almost zonal axis of 276° , whereas the stage two surface rises from a slightly more northerly axis of 279° . Although slight, the difference in slope directions suggests that airflow during stage two might have been slightly more zonal than airflow during stage six glaciation. The more northerly oriented slope of the stage two glaciation also suggests that the stage two glaciation was not as moist and possibly cooler than the stage six glaciation.

In comparison to present ELA estimates and trend surfaces, the reconstructed Pleistocene ELAs and trend surfaces are substantially different. The differences between the ELA trend surfaces include: (1) the height of the present surfaces above the Pleistocene surfaces; (2) the more zonal direction of the Pleistocene surfaces compared to the direction of the present surfaces; and (3) the difference in trend surface gradients of the present and stage six surfaces compared to the stage two surface.

Average height differences indicate that the reconstructed ELA surfaces are from 1,288 meters to 1,868 meters lower than the present estimates. The height difference suggests that substantial temperature and/or precipitation change has occurred between the present and the late Pleistocene, whereas a rather slight difference occurred between the two glacial episodes. However, the mean stage six ELA surface height estimate of 2,949 meters may be too low. Because stage six glacial deposits on the eastern third of the range were overridden by subsequent stage two glaciers (Stage two basins 17 to 23), stage six glaciers that are believed to have occupied the eastern basins could not be calculated into the mean stage six ELA surface height estimate. It is suspected that several higher unmeasured

basins on the eastern third of the range would have significantly raised the mean stage six ELA height estimate.

The present ELA trend surface direction rises from the direction of 230° , and the stage six surface rises from 276° , and the stage two surface rises from 279° . The more-zonal trend surface directions of the glacial episodes suggest that air-mass movement or moisture supply has changed substantially since late Pleistocene. This change might have been influenced by a more zonal Pleistocene circulation pattern (CLIMAP, 1976; Gates, 1976; Barry 1983; COHMAP, 1988; Crowley and North, 1991) or the proximity of the Uinta Mountains to enlarged paleolakes (Scott, et al., 1983; Mulvey, 1985; Currey, 1990). The relationship of the ELA trend surfaces and Pleistocene climate models are discussed in Chapter 5.

The present ELA trend surface gradient rises at ~ 2.8 meters km^{-1} . The stage six ELA gradient has a rate of 4.8 meters km^{-1} (higher than present ELA gradient) and the stage two rate is substantially lower at 2.4 meters km^{-1} (lower than present ELA gradient). Because the surface gradients of the present and stage two ELA surfaces are similar and both rise at a lower rate than the stage six ELA surface, the stage six episode can be inferred to have been more moist than present, and the stage two episode can be inferred to have had snow accumulation conditions similar to, or perhaps, lower than present.

Both standard error measurements of 132 meters for the stage six ELA and 127 meters (Table 13) for the stage 2 ELA seem high. However, several factors might contribute to produce trend surface errors. For example, glaciation elevation can be influenced by variables, which are not related to elevation or climate. As Graf (1976) points out, most glaciers that exist in the present-day Rocky Mountains are found at geomorphically optimal locations for the accumulation and preservation of year-round snowpack. Thus, non-climatic and climatic variables might have differing contributions for different glaciers. It is important to understand that the AAR value of 0.55 might be the

best ELA approximation for the population of the study area reconstructed glaciers only. Individual basins might be better represented by AAR values higher or lower than 0.55. Leonard (1984) believes that AAR values are influenced by the morphology of glaciers, where the highest ratios will occur on icecap glaciers, and valley and piedmont glaciers will have lower AAR values. The glacial morphology of the study area population consisted of cirque and valley glaciers, with many interconnected basins on the west side of the range. Thus, the variety of glacier morphology might have contributed trend surface error.

The height of the glacial ELA can be predicted with relative certainty (i.e., stage six AAR 0.55 $r = 0.763$, stage two AAR 0.55 $r = 0.615$) using northing (latitude) and easting (longitude) increments. To further understand the nature of the ELA height errors, an analysis of the ELA residuals was conducted. Factors that are believed to contribute to estimation errors include: areal parameters of the reconstructed glaciers and measurement errors. The areal parameters include: the lower limit or terminal moraine elevation; the upper limit or headwall trimline elevation; the elevation range from lower limit to upper limit; the area of the reconstructed glacier; the length of the reconstructed glacial extent; the overall gradient of the reconstructed glacial extent; and the distance of the glacier from the center of the range (40°45' N, 110°30' W).

A listing of the stage six and stage two 0.55 AAR residuals and corresponding areal parameters are presented in Tables 16 and 17, respectively. In Table 18, correlation statistics between the residuals and areal parameters are tabulated. The correlation coefficients for the stage six residuals suggest no significant pattern of error associated with the areal parameters; however, the stage two residuals do show a possible relationship ($r = 0.570$) with the upper limit elevations of reconstructed glacial extent. The possible relationship indicates that residuals were generally positive for glaciers with upper limits of glaciation occurring at higher elevations, and negative for glaciers with upper limits of glaciation occurring at lower elevations. Additionally, stage two residuals show an inverse

Table 16
 Oxygen Isotope Stage Six 0.55 AAR ELA Trend Surface
 Residuals And Areal Parameters Of Reconstructed Glacial Extent

Basin Number	Residual (m)	Lower Limit (m)	Upper Limit (m)	Elevation Range (m)	Glacier Area (km)	Glacier Length (km)	Glacier Gradient (%)	Distance From Center [†] (km)
1.	181	2,360	3,100	740	3.7	4.2	18	58.1
2.	-56	2,400	2,840	440	1.6	2.5	18	56.9
3.	-40	2,390	3,060	670	12.5	7.0	10	55.3
4.	-58	2,270	3,360	1,090	56.8	17.1	6	47.0
5.	122	2,330	3,480	1,150	112.6	19.9	6	40.2
6.	181	3,040	3,060	20	2.8	2.5	1	35.1
7.	100	2,510	3,680	1,170	211.8	26.7	4	23.8
8.	-14	2,410	3,810	1,400	320.5	49.1	3	14.8
9.	-11	2,730	3,960	1,230	92.3	32.3	4	11.1
10.	1	2,720	3,810	1,090	62.5	24.8	4	16.7
11.	-77	2,610	3,670	1,060	30.4	18.5	6	25.0
12.	-67	2,670	3,640	970	36.8	15.4	6	29.0
13.	-136	2,420	3,710	1,290	54.8	22.9	6	37.7
14.	-72	1,660	3,690	2,030	150.7	35.4	6	40.1
15.	123	2,100	3,980	1,880	295.2	43.1	4	22.2
16.	106	2,170	4,040	1,870	222.6	39.9	5	8.5
17.	60	2,160	3,910	1,750	245.1	40.6	4	8.1
18.	101	2,220	3,790	1,570	286.3	39.2	4	26.9
19.	88	2,150	3,670	1,520	151.4	28.3	5	31.1
20.	-117	2,730	2,860	130	5.4	6.1	2	47.9
21.	-48	2,350	3,460	1,110	188.6	30.5	4	44.8
22.	-369	2,280	3,080	800	15.6	7.3	11	60.6

[†]Distance from center of range

Table 17
Oxygen Isotope Stage Two 0.55 AAR ELA Trend Surface
Residuals And Areal Parameters Of Reconstructed Glacial Extent

Basin Number	Residual (m)	Lower Limit (m)	Upper Limit (m)	Elevation Range (m)	Glacier Area (km)	Glacier Length (km)	Glacier Gradient (%)	Distance From Center [†] (km)
1.	111	2,880	3,100	220	2.1	2.6	8	58.1
2.	-291	2,390	2,980	590	3.1	4.3	14	55.3
3.	-199	2,390	3,060	670	8.1	5.4	12	54.2
4.	-127	2,370	3,360	990	49.1	12.1	8	46.6
5.	70	2,300	3,410	1,110	75.8	11.4	10	41.8
6.	39	2,640	3,390	750	14.8	6.5	12	34.6
7.	45	2,690	3,560	870	48.8	15.2	6	29.8
8.	61	2,680	3,680	1,000	65.7	16.5	6	24.2
9.	69	2,660	3,680	1,020	66.2	18.7	5	19.5
10.	55	3,030	3,380	350	3.0	3.8	9	23.4
11.	-2	2,450	3,800	1,350	253.2	41.0	3	13.1
12.	-15	2,730	3,960	1,230	86.8	29.5	4	10.3
13.	141	3,000	3,810	810	43.6	15.2	5	12.6
14.	-1	2,710	3,670	960	27.6	16.5	6	23.8
15.	98	2,730	3,640	910	32.3	12.7	7	27.4
16.	29	2,730	3,710	980	48.2	13.7	7	36.8
17.	-115	2,760	3,440	680	31.2	11.4	6	42.8
18.	-134	2,730	3,400	670	19.9	11.1	6	49.9
19.	-188	2,620	3,390	770	51.0	10.2	8	52.2
20.	-174	2,650	3,380	730	27.0	10.5	7	58.8
21.	-16	2,910	3,500	590	30.6	12.7	5	54.4
22.	78	3,030	3,350	320	2.4	2.5	13	57.3
23.	-112	2,300	3,660	1,360	86.5	22.1	6	49.8
24.	36	2,350	3,680	1,330	141.7	29.5	4	39.3
25.	203	2,360	3,980	1,620	250.4	29.8	5	20.6
26.	-78	2,650	3,650	1,000	23.2	13.3	8	23.4
27.	219	2,440	4,040	1,600	186.4	27.0	6	7.1
28.	178	2,700	3,890	1,190	186.2	23.5	5	8.8
29.	44	2,370	3,760	1,390	256.8	31.1	4	28.1
30.	-3	2,490	3,360	870	13.7	7.9	11	34.7
31.	241	2,890	3,370	480	4.4	4.8	10	34.2
32.	55	2,540	3,670	1,130	100.2	16.1	7	32.3
33.	47	2,460	3,460	1,000	64.4	10.2	10	39.1
34.	-101	2,360	3,380	1,020	52.2	13.0	8	44.3
35.	-74	2,400	3,060	660	14.8	8.3	8	50.7
36.	-134	2,420	3,060	640	10.7	5.5	12	57.4
37.	-53	2,370	3,080	710	5.2	4.8	15	58.6

[†]Distance from center of range

Table 18
Correlation Table^a Of Oxygen Isotope Stage Six And Stage Two 0.55 AAR
ELA Trend Surface Residuals And Areal Parameters Of Reconstructed Glacial Extent

	Lower Limit	Upper Limit	Elevation Range	Glacier Area	Glacier Length	Glacier Gradient	Distance From Center
Stage Six Residuals	0.032	0.273	0.174	0.370	0.245	-0.148	-0.381
Stage Two Residuals	0.325	0.570	0.261	0.392	0.291	-0.289	-0.620

^aPearson product-moment correlation

relationship ($r = -0.632$) with the distance from the center of the range. The inverse relationship indicates that the further a glacier was from the center of the range, where surrounding elevations are highest, the residuals were generally more negative. This relationship indicates that the height of the surrounding terrain is a likely cause for the high standard error values.

The highest elevations in the Uinta Mountains are located near the center of the range in the vicinity of Kings Peak ($40^{\circ}45' N 110^{\circ}30' W$). East and west of Kings Peak, elevations gradually decline, and north and south of Kings Peak the elevations sharply decline. With a decline in peak elevation, a general decline in the upper limit of glaciation can be expected. The relationship between the residual values and the distance from the center of the range suggests that much of the error can be attributed to upper limit variance, which is to some extent controlled by the height of the surrounding terrain.

CHAPTER V

RECONSTRUCTION OF LATE-PLEISTOCENE CLIMATES

Temperature, Snow Accumulation, And Wind Direction Estimates

Glacial mass balance and ELA heights are controlled by a range of temperature and precipitation conditions. Thus, the temperature and precipitation that prevailed during the Pleistocene glacial episodes cannot be determined precisely from the reconstructed ELAs (Leonard, 1989; Locke, 1990). However, the ranges of temperature and precipitation conditions required to lower the ELAs from their present heights provide an index for the change that has occurred. By comparing present climate conditions to the range of conditions that are estimated to have prevailed during the glacial episodes, temperature and precipitation ranges can be calculated. Through the comparison of present and late-Pleistocene ELA trend surfaces, climatic factors such as temperature change, snow accumulation and wind direction can be inferred for the late-Pleistocene glacial episodes. Temperature change estimates are based on the depression of the mean Pleistocene ELA heights and assumes that the depression of temperature was uniform across the study area. Snow accumulation change estimates are made on the basis of temperature depression. Wind direction during the glacial episodes is calculated from the direction of the reconstructed snow accumulation trend surfaces.

Temperature Change Estimates

Temperature change is estimated by determining the vertical height difference between the estimated present and reconstructed Pleistocene ELAs and converting the

vertical height difference to temperature difference using a normal lapse rate (i.e., $0.65^{\circ}\text{C } 100\text{ m}^{-1}$). Thus, the temperature change estimate (T_c) is given by:

$$T_c = ((ELA_m - ELA_p)/100) L_n \quad (10)$$

where ELA_m is the present mean ELA height; ELA_p is the Pleistocene mean ELA height; L_n is an assumed lapse rate of $0.65^{\circ}\text{C } 100\text{ m}^{-1}$.

As discussed earlier, the mean height estimate of the stage six ELA is likely to be low because several of the stage six basins on the eastern third of the range were overridden by stage two glaciers and could not be measured. Presuming that smaller stage six glaciers occupied the stage two basins on the eastern third of the range, which includes stage two Basins 17 to 23, the ELAs of the unmeasured basins can be estimated using the stage two coordinates listed in Table 12, and the stage six ELA trend surface equation from Table 13 (i.e., AAR 0.55). The calculated heights of the unmeasured basins are shown in Table 19. Comparison of Table 19 with Table 12, indicates that the estimated ELA heights of the unmeasured basins fall within the upper and lower limits of the stage two glaciers and were probably occupied by smaller stage six glaciers. With the ELA heights of the unmeasured basins included, the mean stage six ELA height estimate becomes 3,027 meters, rather than 2,949 meters as initially estimated.

Using equation 10, temperature change estimates can be made from the height differences of the glacial and present estimated ELAs. The results shown in Table 20 indicate that the ELA was lowered from 1,480 meters to 1,880 meters during stage six, and from 1,470 meters to 1,870 meters during stage two. From the height differences, a 9.6°C to 12.2°C decrease in temperature is estimated to have occurred during both of the glacial episodes. Assuming an equivalent lowering of the 0°C isotherm occurred during the glaciations, the present 0°C summer isotherm height of 4,567 meters would have been

Table 19
Oxygen Isotope Stage Six ELA Estimates Including Unmeasured Basins

Basin ^a	N Latitude	W Longitude	Observed Elevation (m)	Estimated Elevation (m)
1. Swifts Canyon	40°41'	111°12'	2,940	2,759
2. Shingle Mill Creek	40°43'	111°12'	2,700	2,756
3. Ledge Fork Canyon	40°42'	111°10'	2,730	2,770
4. Smith and Morehouse	40°42'	111°04'	2,750	2,808
5. Weber River	40°43'	110°59'	2,960	2,838
6. Whitney	40°47'	110°55'	3,040	2,859
7. Bear River	40°45'	110°48'	3,010	2,910
8. Blacks Fork	40°55'	110°35'	2,960	2,974
9. Smiths Fork	40°52'	110°25'	3,030	3,041
10. Henrys Fork	40°52'	110°21'	3,070	3,069
11. West Fork Beaver Creek	40°53'	110°15'	3,030	3,107
12. Middle Fork Beaver Creek	40°53'	110°12'	3,060	3,126
13. Burnt Fork	40°52'	110°52'	3,040	3,176
A. West Fork Sheep Creek	40°51'	110°01'	--	3,204
B. East Fork Sheep Creek	40°51'	109°55'	--	3,239
C. Carter Creek	40°49'	109°52'	--	3,263
D. Leidy Peak	40°46'	109°46'	--	3,311
E. Ashley Fork	40°44'	109°49'	--	3,294
F. Marsh Peak	40°41'	109°48'	--	3,303
G. Dry Fork	40°42'	109°54'	--	3,267
14. White Rocks	40°45'	110°00'	3,150	3,222
15. Uinta River	40°45'	110°13'	3,260	3,137
16. Yellowstone River	40°42'	110°42'	3,170	3,064
17. Lake Fork	40°42'	110°34'	3,060	3,000
18. Rock Creek	40°38'	110°46'	3,030	2,929
19. Duchesne River	40°41'	110°51'	2,980	2,892
20. Soapstone	40°32'	110°59'	2,740	2,857
21. Provo River	40°39'	111°03'	2,790	2,838
22. Left Fork Beaver Creek	40°40'	111°12'	2,390	2,759
-----			-----	-----
Average of all basins			2,949 [†]	3,027 ^{††}

^a Basins A to G are unmeasured basins estimated using stage two coordinate locations

[†] n = 22

^{††} n = 29

Table 20
Full-Glacial Temperature Change Estimates

ELA ^a (m)	Present High ELA Estimate ^a (m)	Present Low ELA Estimate ^a (m)	Difference High Estimate (m)	Difference Low Estimate (m)	High Temp. Change Estimate ^b (°C)	Low Temp. Change Estimate ^b (°C)
Stage Six						
3,027	4,907	4,507	-1,880	-1,480	-12.2	-9.6
-----	-----	-----	-----	-----	-----	-----
Stage Two						
3,037	4,907	4,507	-1,870	-1,470	-12.2	-9.6

^aMean of all ELA sites

^bEstimate assumes a 0.65 °C 100 m⁻¹ lapse rate

lowered from 2,687 meters to 3,087 meters during stage six, and from 2,697 meters to 3,097 meters during stage two.

Using the 0°C height estimates, the summer temperature of the glacial ELAs can be calculated by determining the height difference from the estimated 0°C altitude and converting the height difference to temperature difference using the normal lapse rate. Equation 11 is used to make this conversion:

$$ELA_t = ((0^{\circ}C_h - ELA)/100) L_n \quad (11)$$

where $0^{\circ}C_h$ is the estimated glacial summer 0°C height; ELA is the estimated ELA height of the glacial basins; and ELA_t is the estimated ELA temperature of the basins. The estimate ELA temperatures are presented in Tables 21 and 22.

Snow Accumulation Estimates

From the calculated ELA temperatures, full-glacial ELA snow accumulation can be estimated using equations 5 and 6. Because the glacial low temperature change estimate was ultimately calculated from the present low ELA elevation estimate, equation 5 is used to estimate snow accumulation for the low temperature change estimates. Equation 6 is used to estimate snow accumulation for the high temperature change estimates.

A comparison of present snow accumulation to the estimated full-glacial snow accumulation, present snow accumulation (1972 to 1990 mean) at the stage six and stage two ELA coordinates is estimated using the present snow accumulation trend surface equation as:

Table 21
Oxygen Isotope Stage Six ELA Temperature Estimates

Basin ^a	Estimated ELA Elevation (m)	2687 m 0°C Difference (m)	3087 m 0°C Difference (m)	2687 m Temp. Estimate (°C) ^b	3087 m Temp. Estimate (°C) ^c
1. Swifts Canyon	2,759	72	-328	-0.5	2.1
2. Shingle Mill Creek	2,756	69	-331	-0.4	2.2
3. Ledge Fork Canyon	2,770	83	-317	-0.5	2.1
4. Smith and Morehouse	2,808	121	-279	-0.8	1.8
5. Weber River	2,838	151	-249	-1.0	1.6
6. Whitney	2,859	172	-228	-1.1	1.5
7. Bear River	2,910	223	-177	-1.4	1.2
8. Blacks Fork	2,974	287	-113	-1.9	0.7
9. Smiths Fork	3,041	354	-46	-2.3	0.3
10. Henrys Fork	3,069	382	-18	-2.5	0.1
11. West Fork Beaver Creek	3,107	420	20	-2.7	-0.1
12. Middle Fork Beaver Creek	3,126	439	39	-2.9	-0.3
13. Burnt Fork	3,176	489	89	-3.2	-0.6
A. West Fork Sheep Creek	3,204	517	117	-3.4	-0.8
B. East Fork Sheep Creek	3,239	552	152	-3.6	-1.0
C. Carter Creek	3,263	576	176	-3.7	-1.1
D. Leidy Peak	3,311	624	224	-4.1	-1.5
E. Ashley Fork	3,294	607	207	-3.9	-1.3
F. Marsh Peak	3,303	616	216	-4.0	-1.4
G. Dry Fork	3,267	580	180	-3.8	-1.2
14. White Rocks	3,222	535	135	-3.5	-0.9
15. Uinta River	3,137	450	50	-2.9	-0.3
16. Yellowstone River	3,064	377	-23	-2.4	0.2
17. Lake Fork	3,000	313	-87	-2.0	0.6
18. Rock Creek	2,929	242	-158	-1.6	1.0
19. Duchesne River	2,892	205	-195	-1.3	1.3
20. Soapstone	2,857	170	-230	-1.1	1.5
21. Provo River	2,838	151	-249	-1.0	1.6
22. Left Fork Beaver Creek	2,759	72	-328	-0.5	2.1
-----	-----	-----	-----	-----	-----
Average of all basins	3,027	340	-60	-2.2	0.4

^a Basins A to G are unmeasured basins

^b Estimated ELA temperature assuming a 2,687 meter 0° C isotherm altitude

^c Estimated ELA temperature assuming a 3,087 meter 0° C isotherm altitude

Table 22
Oxygen Isotope Stage Two ELA Temperature Estimates

Basin	Estimated ELA Elevation (m)	2697 m 0°C Difference (m)	3097 m 0°C Difference (m)	2697 m Temp. Estimate (°C) ^a	3097 m Temp. Estimate (°C) ^b
1. Swifts Canyon	2,909	212	-188	-1.4	1.2
2. Red Pine Creek	2,911	214	-186	-1.4	1.2
3. Ledge Fork Canyon	2,919	222	-178	-1.4	1.2
4. Smith and Morehouse	2,937	240	-160	-1.6	1.0
5. Weber River	2,950	253	-147	-1.6	1.0
6. Gold Hill	2,961	264	-136	-1.7	0.9
7. Hayden Fork Bear River	2,975	278	-122	-1.8	0.8
8. Stillwater Fork Bear River	2,989	292	-108	-1.9	0.7
9. East Fork Bear River	3,001	304	-96	-2.0	0.6
10. Mill Creek	2,995	298	-102	-1.9	0.7
11. Blacks Fork	3,022	325	-75	-2.1	0.5
12. Smiths Fork	3,055	358	-42	-2.3	0.3
13. Henrys Fork	3,069	372	-28	-2.4	0.2
14. West Fork Beaver Creek	3,091	394	-6	-2.6	0.0
15. Middle Fork Beaver Creek	3,102	405	5	-2.6	-0.0
16. Burnt Fork	3,131	434	34	-2.8	-0.2
17. West Fork Sheep Creek	3,145	448	48	-2.9	-0.3
18. East Fork Sheep Creek	3,164	467	67	-3.0	-0.4
19. Carter Creek	3,178	481	81	-3.1	-0.5
20. Leidy Peak	3,204	507	107	-3.3	-0.7
21. Ashley Fork	3,196	499	99	-3.2	-0.6
22. Marsh Peak	3,202	505	105	-3.3	-0.7
23. Dry Fork	3,182	485	85	-3.2	-0.6
24. White Rocks	3,154	457	57	-3.0	-0.4
25. Uinta River	3,107	410	10	-2.7	-0.1
26. Crow Canyon	3,108	411	11	-2.7	-0.1
27. Yellowstone River	3,071	374	-26	-2.4	0.2
28. Lake Fork	3,032	335	-65	-2.2	0.4
29. Rock Creek	2,996	299	-101	-1.9	0.7
30. Hades Canyon	2,993	296	-104	-1.9	0.7
31. Granddaddy Mountain	2,989	292	-108	-1.9	0.7
32. Duchesne River	2,975	278	-122	-1.8	0.8
33. Provo River	2,963	266	-134	-1.7	0.9
34. North Fork Provo River	2,951	254	-146	-1.6	0.9
35. Shingle Creek	2,934	237	-163	-1.5	1.1
36. Slate Creek	2,914	217	-183	-1.4	1.2
37. Left Fork Beaver Creek	2,913	216	-184	-1.4	1.2
-----	-----	-----	-----	-----	-----
Average of all basins	3,037	341	-59	-2.2	0.4

^a Estimated ELA temperature assuming a 2,697 meter 0° C isotherm altitude

^b Estimated ELA temperature assuming a 3,097 meter 0° C isotherm altitude

$$A = 151.204 + -31.176Lat + 10.473Lon \quad (12)$$

Present snow accumulation (A) (equation 12), can be predicted by the latitude (Lat) and longitude (Lon) increments of the glacial ELA positions and constant functions.

Full-glacial and present snow accumulation estimates, and the differences of the estimates, are shown in Table 23 and Table 24. To characterize the estimates and differences, the means of the estimated ranges are also shown in the tables. The mean snow accumulation estimates are 40.6 cm for the stage six episode and 38.4 cm for the stage two episode. Comparison of the values indicates that snow accumulation during stage six averaged 1.9 cm lower than present and during stage two averaged 6.1 cm lower than present. Trend surfaces of the mean snow accumulation estimates (Tables 23 and 24) are shown in Figure 17 and Figure 18. The stage six surface has a nearly zonal direction of 268° , whereas the stage two surface direction trends 275° . The gradients of the two surfaces differ substantially. The stage six surface decreases at a rate of 0.45 cm km^{-1} , and the stage two surface decreases at a rate of 0.23 cm km^{-1} . The stage six snow accumulation surface direction differs slightly from the corresponding ELA surface presented in Figure 15 because of the inclusion of unmeasured basins in this analysis.

As discussed earlier, mean seasonal snow accumulation trend surfaces with lower surface directions (i.e., more southerly oriented) and steeper surface gradients correlate to higher seasonal snow accumulations (i.e., Table 9). The predicted mean snow accumulation is given by:

$$SWE = 63.319 + -0.138Dir + 25.695Gra \quad (13)$$

Table 23
 Estimated Oxygen Isotope Stage Six ELA Snow Accumulation
 And Difference From Present Snow Accumulation Estimates

Basin ^a	2687 m Estimate (cm) ^b	3087 m Estimate (cm) ^c	Mean of Estimates (cm)	Present Estimate (cm) ^d	Difference of Estimates (cm)
1. Swifts Canyon	74.0	65.2	69.6	49.7	19.9
2. Shingle Mill Creek	74.5	65.6	70.1	48.9	21.1
3. Ledge Fork Canyon	72.4	63.8	68.1	49.2	18.9
4. Smith and Morehouse	67.0	58.7	62.8	48.2	14.7
5. Weber River	62.8	54.9	58.9	47.3	11.6
6. Whitney	60.1	52.5	56.3	45.0	11.3
7. Bear River	53.7	46.6	50.2	45.0	5.1
8. Blacks Fork	46.3	39.9	43.1	38.9	4.2
9. Smiths Fork	39.3	33.5	36.4	38.9	-2.5
10. Henrys Fork	36.6	31.1	33.8	38.3	-4.5
11. West Fork Beaver Creek	33.1	28.0	30.5	37.3	-6.8
12. Middle Fork Beaver Creek	31.4	26.4	28.9	36.9	-8.0
13. Burnt Fork	27.4	22.9	25.1	36.4	-11.3
A. West Fork Sheep Creek	25.2	20.9	23.1	36.1	-13.1
B. East Fork Sheep Creek	22.7	18.7	20.7	35.4	-14.7
C. Carter Creek	21.1	17.3	19.2	36.0	-16.8
D. Leidy Peak	18.1	14.6	16.4	36.4	-20.0
E. Ashley Fork	19.1	15.5	17.3	37.5	-20.2
F. Marsh Peak	18.5	15.0	16.8	38.7	-21.9
G. Dry Fork	20.8	17.0	18.9	39.1	-20.2
14. White Rocks	23.9	19.8	21.8	38.5	-16.6
15. Uinta River	30.5	25.6	28.1	40.4	-12.4
16. Yellowstone River	37.1	31.5	34.3	43.3	-9.0
17. Lake Fork	43.5	37.3	40.4	44.3	-3.9
18. Rock Creek	51.4	44.5	48.0	47.6	0.4
19. Duchesne River	55.8	48.5	52.2	47.0	5.2
20. Soapstone	60.4	52.7	56.5	51.8	4.8
21. Provo River	62.9	55.0	59.0	49.2	9.8
22. Left Fork Beaver Creek	74.0	65.2	69.6	50.8	18.8
-----	-----	-----	-----	-----	-----
Average of all basins	43.6	37.5	40.6	42.5	-1.9

^a Basins A to G are unmeasured basins

^b Estimated snow accumulation assuming a 2,687 meter 0° C isotherm altitude

^c Estimated snow accumulation assuming a 3,087 meter 0° C isotherm altitude

^d Estimated present snow accumulation at oxygen isotope stage six ELA

Table 24
 Estimated Oxygen Isotope Stage Two ELA Snow Accumulation
 And Difference From Present Snow Accumulation Estimates

Basin	2697 m Estimate (cm) ^a	3097 m Estimate (cm) ^b	Mean of Estimates (cm)	Present Estimate (cm) ^c	Difference of Estimates (cm)
1. Swifts Canyon	55.1	47.8	51.4	53.9	-2.4
2. Red Pine Creek	54.8	47.6	51.2	52.9	-1.7
3. Ledge Fork Canyon	53.8	46.6	50.2	53.2	-3.0
4. Smith and Morehouse	51.6	44.7	48.1	51.8	-3.7
5. Weber River	50.1	43.3	46.7	51.0	-4.3
6. Gold Hill	48.8	42.1	45.5	48.1	-2.6
7. Hayden Fork Bear River	47.3	40.8	44.0	48.4	-4.4
8. Stillwater Fork Bear River	45.7	39.3	42.5	47.5	-5.0
9. East Fork Bear River	44.4	38.1	41.3	45.6	-4.4
10. Mill Creek	45.1	38.8	41.9	43.5	-1.5
11. Blacks Fork	42.2	36.1	39.2	41.8	-2.6
12. Smiths Fork	38.9	33.1	36.0	39.5	-3.5
13. Henrys Fork	37.6	32.0	34.8	39.8	-5.0
14. West Fork Beaver Creek	35.5	30.0	32.8	37.3	-4.5
15. Middle Fork Beaver Creek	34.4	29.1	31.8	36.8	-5.1
16. Burnt Fork	31.9	26.8	29.4	35.6	-6.3
17. West Fork Sheep Creek	30.7	25.8	28.2	34.5	-6.3
18. East Fork Sheep Creek	29.1	24.4	26.7	33.3	-6.6
19. Carter Creek	28.0	23.4	25.7	33.6	-7.9
20. Leidy Peak	26.0	21.6	23.8	33.4	-9.6
21. Ashley Fork	26.6	22.1	24.4	34.8	-10.4
22. Marsh Peak	26.2	21.8	24.0	35.8	-11.9
23. Dry Fork	27.7	23.1	25.4	36.8	-11.4
24. White Rocks	29.9	25.1	27.5	36.8	-9.3
25. Uinta River	34.0	28.8	31.4	40.0	-8.6
26. Crow Canyon	33.9	28.6	31.3	43.8	-12.6
27. Yellowstone River	37.4	31.8	34.6	42.2	-7.6
28. Lake Fork	41.2	35.2	38.2	45.1	-6.9
29. Rock Creek	45.0	38.7	41.8	49.6	-7.8
30. Hades Canyon	45.3	38.9	42.1	52.1	-10.0
31. Granddaddy Mountain	45.8	39.4	42.6	51.5	-8.9
32. Duchesne River	47.2	40.7	44.0	49.5	-5.5
33. Provo River	48.7	42.0	45.3	51.1	-5.8
34. North Fork Provo River	50.0	43.2	46.6	52.1	-5.5
35. Shingle Creek	52.0	45.0	48.5	53.2	-4.7
36. Slate Creek	54.4	47.2	50.8	54.1	-3.3
37. Left Fork Beaver Creek	54.5	47.3	50.9	54.5	-3.5
-----	-----	-----	-----	-----	-----
Average of all basins	41.4	35.4	38.4	44.4	-6.1

^a Estimated snow accumulation assuming a 2,697 meter 0° C isotherm altitude

^b Estimated snow accumulation assuming a 3,097 meter 0° C isotherm altitude

^c Estimated present snow accumulation at oxygen isotope stage two ELA

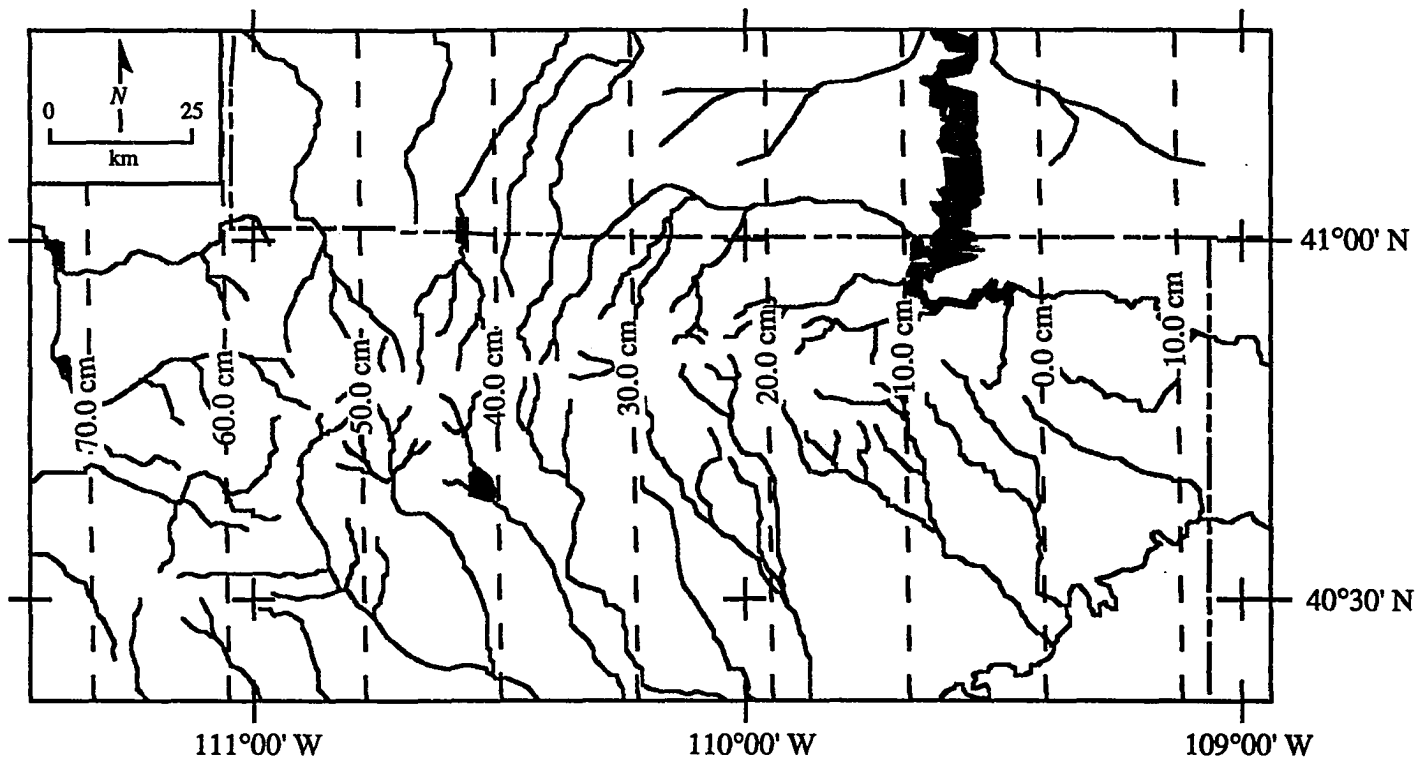


Figure 17. Estimated oxygen isotope stage six mean snow accumulation trend surface. Mean accumulation is 40.6 cm, surface direction is 268° and gradient is 0.45 cm km⁻¹. Trend surface equation is $A = -4030.46 + -0.703Lat + 37.101Lon$.

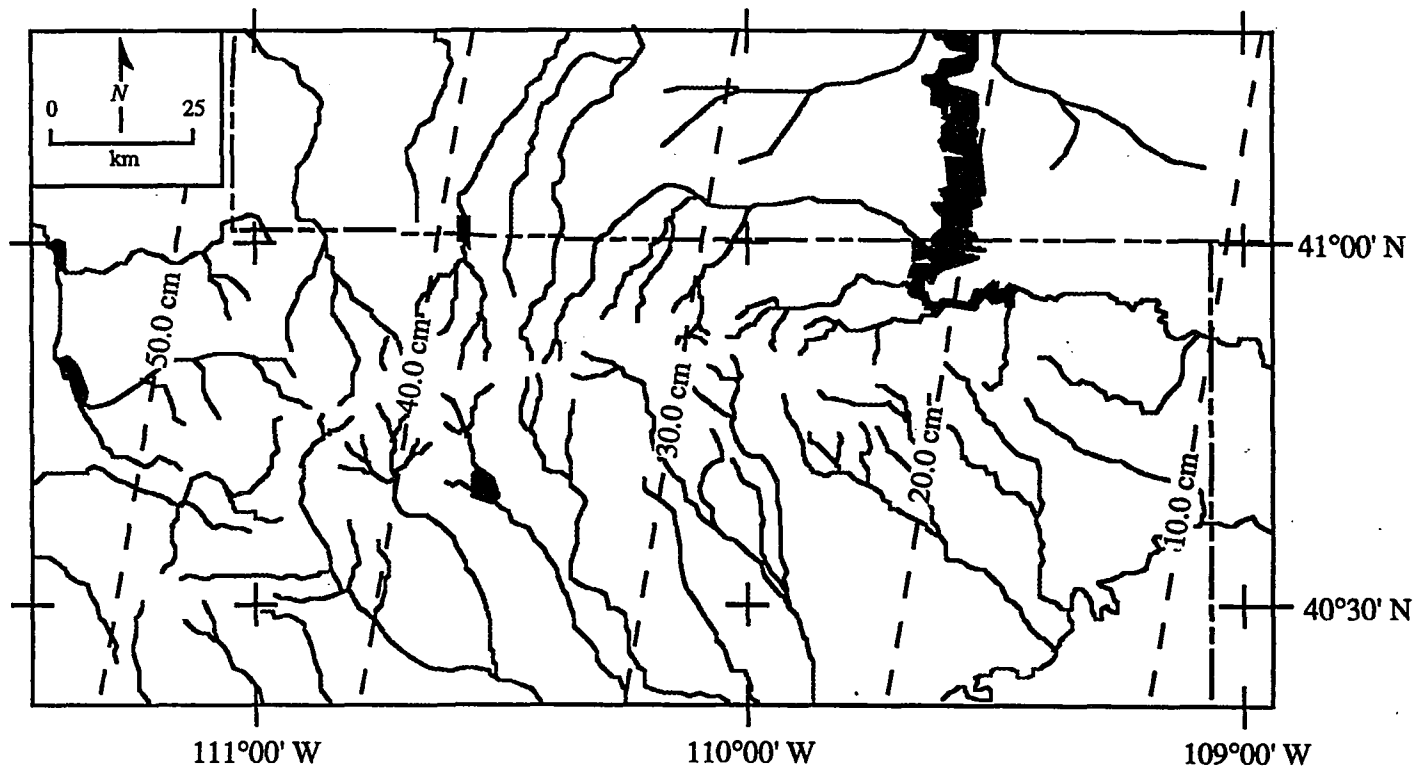


Figure 18. Estimated oxygen isotope stage two mean snow accumulation trend surface. Mean accumulation is 38.4 cm, surface direction is 275° and gradient is 0.23 cm km⁻¹. Trend surface equation is $A = -2301.183 + 4.22Lat + 19.604Lon$.

where *Dir* is the snow accumulation trend surface direction and *Gra* is the trend surface gradient. With significant confidence ($R = 0.797$; $p = 0.000$; standard error = 5.8 cm), equation 13 predicted the mean seasonal snow accumulation for the 1972 to 1990 seasons. Applying uniformitarianism principles, that is the present is the key to the past, it can be assumed that the glacial snow accumulation trend surface directions and gradients respond similarly. Thus, equation 13 can be used to predict the average snow accumulation during the glacial episodes.

Shown in Table 25 are the snow accumulation estimates. These estimates are similar to the estimates in Tables 23 and 24 that were made from the ELA height differences. A notable difference between the estimates made from trend surface direction and gradient variables and the estimates made from the ELA temperature estimates is the range between the stage six and stage two estimates. The range is 6.6 cm for the estimates using trend surface direction and gradient variables, as opposed to 2.2 cm for the estimates using the ELA temperature estimates. The results further demonstrate that the stage six episode was probably more moist than the stage two episode. With an ELA height difference of only 10 meters between the two glacial episodes, the difference in snow accumulation is expected to be small. However, the snow accumulation estimates made from both trend surface direction and gradient variables suggest that the stage six episode was substantially warmer and more moist than the stage two episode.

Wind Direction Estimates

In Chapter 3 the Present mean annual 800 millibar to 700 millibar wind direction (i.e., Table 9) was correlated ($R = 0.837$) with a certainty of $p = 0.000$ to snow accumulation trend surface direction. The regression equation for this relationship is:

$$Dir = -196.535 + (1.801Wnd) \quad (14)$$

Table 25
Comparison Of Full-Glacial Snow Accumulation Estimates

	Mean Snow Accumulation Estimates From Tables 21 and 22 (cm) ^a	Mean Snow Accumulation Estimates From Equation 13 (cm) ^b	Difference of Estimates (cm)
Stage Six -----	40.6 -----	37.9 ±5.8 -----	2.7 -----
Stage Two -----	38.4 -----	31.3 ±5.8 -----	7.1 -----
Range of Estimates	2.2	6.6	-4.4

^aMean snow accumulation estimated from ELA temperature estimates

^bMean snow accumulation estimated from trend surface direction and gradient variables

where trend surface direction (*Dir*) is estimated from wind direction (*Wnd*). Rearranging the equation variables to solve for wind direction, the equation becomes:

$$Wnd = 148.613 + (0.386Dir) \quad (15)$$

From equation 15, full-glacial wind directions are predicted as $R = 0.837$ ($p = 0.000$; standard error = 9.2). The estimated wind directions are $253^\circ \pm 9.2$ for the stage six episode and $256^\circ \pm 9.2$ for the stage two episode. These estimates range from 12° to 15° more northerly than the 1972 to 1989 mean wind direction of 241° . For both episodes, full-glacial air-flow appears to have been more zonal than present.

Summary of Estimates

A summary of the reconstructed full-glacial temperature, snow accumulation and wind direction estimates is given in Table 26. For comparison, corresponding estimates of the present conditions are also shown in Table 26. These estimates suggest: (1) full-glacial temperatures were substantially reduced from present; (2) full-glacial snow accumulation was about the same as present, and (3) full-glacial wind directions were more zonal than present.

Because the mean ELA trend surface heights for the two glacial episodes are only 10 meters apart vertically, the temperature reduction estimates are the same. Both episodes are estimated to have had temperature reductions between 9.6°C to 12.2°C . However, these estimates are based upon the assumption that the depression of the 0°C height was equivalent to the depression of the estimated ELA heights. The present 0°C altitude is

Table 26
 Summary Data Of Full-Glacial Temperature,
 Snow Accumulation, And Wind Direction Estimates

Age	Temperature Change Estimates (°C)	0° C Altitude (m)	Mean Snow Accumulation Estimates:		Wind Direction Estimates (°Az)
			From Tables 21 and 22 (cm)	From Equation 13 (cm)	
Stage Six	-9.6 to -12.2	2,687 to 3,087	40.6	37.9 ±5.8	253 ±9.2
Stage Two	-9.6 to -12.2	2,697 to 3,097	38.4	31.3 ±5.8	256 ±9.2
Present ^a	0	4,567	37.6	37.6	241

^aMean 1972 to 1990 estimates

4,567 meters. During the glacial episodes, the 0° C altitude was depressed 2,697 meters to 3,097 meters during the stage six episode, and 2,687 meters to 3,087 meters during the stage two episode.

Snow accumulation estimates derived from ELA temperature estimates were similar to the present 1972 to 1990 mean accumulation of 36.7 cm. The stage six estimate of 40.6 cm and the stage two estimate of 38.4 cm are both slightly higher than the present mean. On the other hand, the estimates made from trend surface direction and gradient variables have a higher range that extends from 37.9 ± 5.8 cm for the stage six episode to 31.3 ± 5.8 cm for the stage two episode. The stage six estimate is slightly higher (i.e., 0.3 cm) than the present mean, whereas the stage two estimate (i.e., 6.3 cm) is substantially lower. These results suggest that the stage six episode experienced higher snow accumulation than stage two, and that the mean stage six snow accumulation was similar to the present mean.

The wind direction estimates of 253° for the stage six episode and 256° for the stage two episode indicate that the air-flow during the glacial episodes was more zonal than present. These estimates range from 12° more northerly than present during the stage six episode and from 15° more northerly than present during the stage two episode.

CHAPTER VI

LATE-PLEISTOCENE PALEOENVIRONMENTS

Discussion Of Full-glacial Climate Estimates

In this chapter the full-glacial climate estimates derived in the preceding chapters are compared to estimates made from other studies for the region. The comparison provides verification of and/or speculation on the likelihood of these estimates, and ultimately suggests potential explanations as to paleoenvironmental setting of the study area. The following section is a discussion of the results from this dissertation and the findings made by others for the region. From the comparison of these results and the results of other studies, a model of the full-glacial paleoenvironmental conditions is proposed.

Full-Glacial Temperature

Full-glacial summer temperatures decreased from 9.6°C to 12.2° C for both glacial episodes. These temperature reductions are based on a 1,480 meter to 1,880 meter lowering of the mean stage six ELA, and a 1,470 meter to 1,870 meter lowering of the mean stage two ELA. Both temperature estimates are based on the assumption that the depression of the 0° C isotherm height is uniform with the depression of the ELA heights. The temperature reduction estimates for both episodes are the same because the mean ELA heights differ by ~ 10 meters. Inasmuch as the mean ELA heights are nearly equal, the two episodes are assumed to have had similar temperatures. However, without precise knowledge of the precipitation differences between the two episodes, a difference in temperature between the two episodes is difficult to detect.

Whereas the mean full-glacial temperatures are thought to have been within estimated ranges, substantial temperature differences between the two episodes might have existed. In fact, the results of this analysis, specifically in the context of snow accumulation estimates, suggest that the stage six episode was more moist and consequently warmer than the stage two episode.

Temperature reduction estimates from other studies for the region have not been made for the stage six episode; nevertheless, a number of estimates have been made for the stage two episode. The stage two temperature reduction estimates from this study are in relative agreement with those made for the region by other researchers (Galloway, 1970; Gates, 1976; McCoy, 1977; McCoy, 1981; Mears, 1981; Meierding 1982; Péwé, 1983; Mulvey, 1985).

From the CLIMAP (CLIMAP Project Members, 1976) computer simulation of global paleoclimatic data for 18,000 B.P., Gates (1976) presents large scale temperature reduction estimates for the region. The CLIMAP simulation estimates are considered a first-order approximation and are tabulated on 4° latitude by 5° longitude grids. The grids that overlie the study area have a 10° C to 13° C reduction of temperature (Gates, 1976).

Galloway (1970), assuming that reduced evaporation rates were the primary cause for the expansion of Lake Bonneville, estimates that full-glacial July temperatures for the Bonneville Basin would have to have been at least 10° C lower than present for the lake to have transgressed to the Bonneville level high stand. Furthermore, Galloway (1970) projects that precipitation was likely to have been 80% to 90% of present. Similarly, on the basis of amino acid racemization rates for Lake Bonneville mollusk shells, McCoy (1981) calculated that between 16,000 B.P. to 15,000 B.P. the temperature of the Bonneville Basin was reduced by at least 7° C and possibly as much as 16° C.

From the depression of the median altitude of reconstructed glaciers in the Bonneville Basin, Mulvey (1985) estimated that stage two full-glacial July temperatures

were reduced 14° C. On the basis of the reconstructed mass balance of the Little Cottonwood Canyon glacier in the Wasatch Mountains, McCoy (1977) estimated a 12° C temperature reduction for 21,000 B.P. It is important to understand that McCoy's 12° C estimate is contingent on precipitation levels increased on the order of 150% of present levels.

To the northeast of the study area, in the intermontane basins of Wyoming, relict periglacial frost and ice-soil involutions attributed to the stage two episode have been interpreted to indicate periglacial environmental conditions (Mears, 1981). Mears (1981) suggested the conditions necessary to produce the involutions indicate temperature reductions on the order of 10° C to 13° C. In another study, Péwé (1983) estimated temperature reductions of 8.9° C to 10.8° C for the same phenomenon.

In the Front Range of Colorado, Meierding (1982) estimated from stage two age ELAs that a 1,550 meter depression of the summer freezing level occurred. Meierding's depression estimate falls within the 1,470 meter to 1,870 meter depression calculated in this dissertation. Using 0.65° C 100 meter⁻¹ lapse rate, Meierding's 1,550 meter depression equates to a 10° C temperature reduction.

In the San Juan Mountains in southwestern Colorado, Leonard (1984) estimated stage two ELAs to range from 2,957 meters to 3,749 meters. Where the height range observed by Leonard overlaps with the 2,860 meter to 3,280 meter range estimated in this dissertation, Leonard's range extends almost 500 meters higher than the range estimated for the Uinta Mountains. The seemingly higher elevations observed by Leonard can be explained by the more southerly location of the San Juan Mountains which are located at latitudes roughly 2.5° to 3.5° south of the Uinta Mountains.

The results of the other studies for the region are either in agreement with or are within the 9.6° C to 12° C range of temperature reduction estimated from this dissertation. However, as previously stated, without an understanding of precipitation changes,

temperature estimates alone cannot be used to explain climate changes or paleoenvironmental conditions of the study area.

Full-Glacial Precipitation

Mean winter snow accumulation estimates are 40.6 cm for the stage six episode, and 38.4 cm the stage two episode. The snow accumulation for both episodes appears to have been slightly higher than the present mean of 37.6 cm. However, a more prolonged winter accumulation season is thought to have occurred during the glacial episodes. Today the snow accumulation season extends from October to April, essentially half of the year. Under a reduced full-glacial temperature regime, the snow accumulation season may have been lengthened as much as from September to June, or three-quarters of the year. The present 1972 to 1990 mean monthly snow accumulation rate during the six month accumulation season is 6.3 cm month⁻¹. With a nine month season, the full-glacial snow accumulation rates range from 4.5 cm during stage six to 4.3 cm during stage two. This difference in full-glacial snow accumulation rates is on the order of 71% to 68%, respectively, of present rates. The estimated net seasonal snow accumulation estimates might not have differed greatly from the present, but under a prolonged snow accumulation season the average monthly snow accumulation during the glacial episodes would have been substantially lower than present. Therefore, precipitation during the glacial episodes, at least during the snow accumulation seasons, was substantially lower than present.

Perhaps the most significant difference between the two episodes are the ELA and snow accumulation trend surface gradients and, to a lesser scale, the trend surface directions. The stage six trend surface has a steeper trend surface gradient and a more southerly orientation than the stage two surface. Because of these differences in the surface patterns, it is suggested that the stage six episode might have been warmer and substantially more moist than the stage two episode. The reasoning behind this suggestion is three fold:

(1) the stage six trend surface gradient rises at a much steeper rate than the stage two surface; (2) the stage six trend surface has a slightly more southerly trend direction; and (3) from studies elsewhere in the Rocky Mountains, the stage six glaciation was more extensive than the stage two glaciation (Blackwelder, 1915; Richmond, 1965; Madole, 1969; Mears, 1974; Pierce et al., 1976; Pierce 1979; Madsen and Currey, 1979).

As previously discussed, steeper ELA gradients correspond to more moist situations (Miller et al., 1975; Trenhaile, 1975; Porter, 1977). Furthermore, as demonstrated in Chapter 3, steeper trend surface gradients and more zonal trend directions are indicative of warmer winters and winters receiving higher snow accumulations. For other locations in the Rocky Mountains, a number of studies have shown, except where substantial landscape changes such as lava flows have occurred (Pierce, 1979), that the stage six episode glaciers were more extensive than the stage two episode glaciers (Blackwelder, 1915; Richmond, 1965; Madole, 1969; Mears, 1974; Pierce et al., 1976; Madsen and Currey, 1979). In the Uinta Mountains, the stage six glaciers are more extensive than the stage two glaciers on the western two-thirds of the range. However, on the eastern third of the range, the stage two glaciers completely overran the stage six glaciers. This pattern indicates that the stage six episode had higher accumulations, but a stronger eastward decrease of snow accumulation than the stage two episode. The difference between the two ELA trend surface gradients characterizes accumulation patterns herein described as accumulation limited (stage six), and ablation limited (stage two). The ELA of the accumulation limited stage six episode is thought to be controlled more by the amount of snow accumulation than by the height of temperature depression. In response to this condition, higher accumulations and lower ELAs occurred on the west side of the range, whereas substantially lower accumulations and higher ELAs occurred on the east side of the range. In contrast, the ELA of the ablation limited stage two episode appears to

have been controlled more by the height of temperature depression than accumulation variations. Consequently the stage two ELA has a comparatively flat trend surface.

Thus, the stage six glaciation appears to have been more moist than the stage two glaciation and regionally experienced more extensive glaciation (Blackwelder, 1915; Richmond, 1965; Madole, 1969; Mears, 1974; Pierce et al., 1976; Pierce, 1979; Madsen and Currey, 1979). The exception to this pattern occurs in the eastern third of the Uinta Mountains where snow accumulation was locally reduced because of lee orographic moisture reduction of westerly air masses. This unique condition is thought to be influenced by the elongate west to east structure of the Uinta Mountains.

Whereas Galloway (1970) hypothesized the precipitation in the Bonneville Basin may have been 80% to 90% of present, Mears (1981) believed that the periglacial phenomena in the Wyoming basins indicated not only colder, but much dryer conditions than present. Although it has been suggested that precipitation during the glacial episodes differed little from the present (Galloway, 1970; Brackenridge, 1987; Leonard, 1984; Zwick, 1980; Locke, 1990), the results from these analyses suggest otherwise. Intuitively, reduced specific humidity would be expected under cooler atmospheric conditions. However, because the study area is in proximity to the Bonneville Basin, the question arises as to whether or not enlarged paleolakes in the basin influenced precipitation in the Uinta Mountains.

Working at a global scale, Gates (1976) estimated that precipitable water in the Northern Hemisphere was 63% of present for the July climate of 18,000 B.P. On a similar line of reasoning, Leonard (1989) believes that a 44% reduction of present precipitation, coupled with a 5% reduction of present snow accumulation and a 10° C temperature reduction would have sustained stage two ELAs in the Colorado Rocky Mountains. In contrast, McCoy's (1981) estimation for the Pleistocene mass balance of the Little Cottonwood glacier requires a 150% increase in the present precipitation amounts.

However, the full-glacial ELA of the Little Cottonwood glacier is substantially lower at $2,400 \pm 20$ meters (Madsen and Currey, 1979) than any of the ELAs observed in the Uinta Mountains 50 km to the east of Little Cottonwood Canyon. The mass balance of the Little Cottonwood glacier is likely to have been greatly influenced by an enlarged Lake Bonneville directly west of Little Cottonwood Canyon.

On a regional context, the consensus as to full-glacial precipitation changes, whether reduced or similar to present, has been strongly debated. Brackenridge (1978) used paleobotanical and morphogenetic evidence to infer that full-glacial precipitation in the southwestern United States was little changed from present, and climate changes were primary responses to reduced temperatures. On the other hand, Wells (1979) refutes Brackenridge's conclusion pointing to *Neotoma* macrofossil evidence which suggests an increase in precipitation occurred in the full-glacial southwestern United States. Spaulding and Graumlich (1989) interpret a more moist southwestern United States south of the Sierra Nevada and dryer conditions in areas east of the Sierra Nevada. It would seem conceivable that under a reduced temperature regime and a predominantly zonal-westerly air flow (Gates, 1976; COHMAP Members, 1988; Spaulding and Graumlich, 1989; Jennings and Elliott-Fisk, 1993), areas east of the Sierra Nevada would experience less precipitation than present, except where locally affected by enlarged paleolakes. East of the Sierra Nevada, the Wasatch and other ranges immediately adjacent to paleolake basins were influenced by the size and duration of paleolakes.

Paleolakes and the Uinta Mountains

During both glacial episodes, the Bonneville Basin, 50 km west of the study area, was occupied by enlarged paleolakes (Currey, 1990). The stage six equivalent, Little Valley lake cycle, occurred between 150,000 B.P. and 130,000 B.P. The Little Valley cycle rose to a level of 1,493.5 meters (Scott et al., 1983) with a surface area of 44,000

km² (Oviatt et al., 1987). The stage two Bonneville cycle occurred between 32,000 B.P. and 12,000 B.P. Because of increased discharge attributed to the diversion of the Bear River into the Basin (Oviatt et al., 1987), the Bonneville cycle peaked and overflowed at a level of 1,585 meters. At peak level (i.e., the Bonneville level), Lake Bonneville covered an area of 51,000 km² (Currey and Oviatt, 1985). However, the peak level of the Bonneville cycle was not synchronous with glacial maxima in Little Cottonwood Canyon in the Wasatch Mountains (Madsen and Currey, 1977) or sites elsewhere in the region (Pierce, 1979; Madole, 1986). The stage two glacial maxima is believed to have occurred between 20,000 B.P. and 19,000 B.P. (Madsen and Currey, 1977; Pierce, 1979; Madole, 1986), whereas the Bonneville level high stand occurred a few thousand years later (i.e., 17,000 B.P. and 15,000 B.P.)

At the time of the stage two glacial maxima the lake level was 214 meters lower than the Bonneville level high stand, at a level attributable to the 1,371 meter Stansbury shoreline. Covering only 24,000 km², the Stansbury level was substantially contracted from the Bonneville level (Currey and Oviatt, 1985). The various late-Pleistocene lake levels are shown in Figure 19.

Although evidence is insufficient, it is speculated that the stage six glaciation might have been more strongly influenced by a Little Valley cycle lake level higher than the Stansbury level. The results of this dissertation strongly suggest that the stage six glaciation was both more moist and warmer than the stage two glaciation, indicating that a larger water body to the west might have increased precipitation and moderated temperatures during the stage six episode. However, because the stage six glaciation has been found to be more extensive than the stage two glaciation region-wide, it is possible that the differences between the two episodes in the Uinta Mountains are in response to regional climate differences, rather than to either the size and/or duration of paleolakes in the Bonneville Basin.

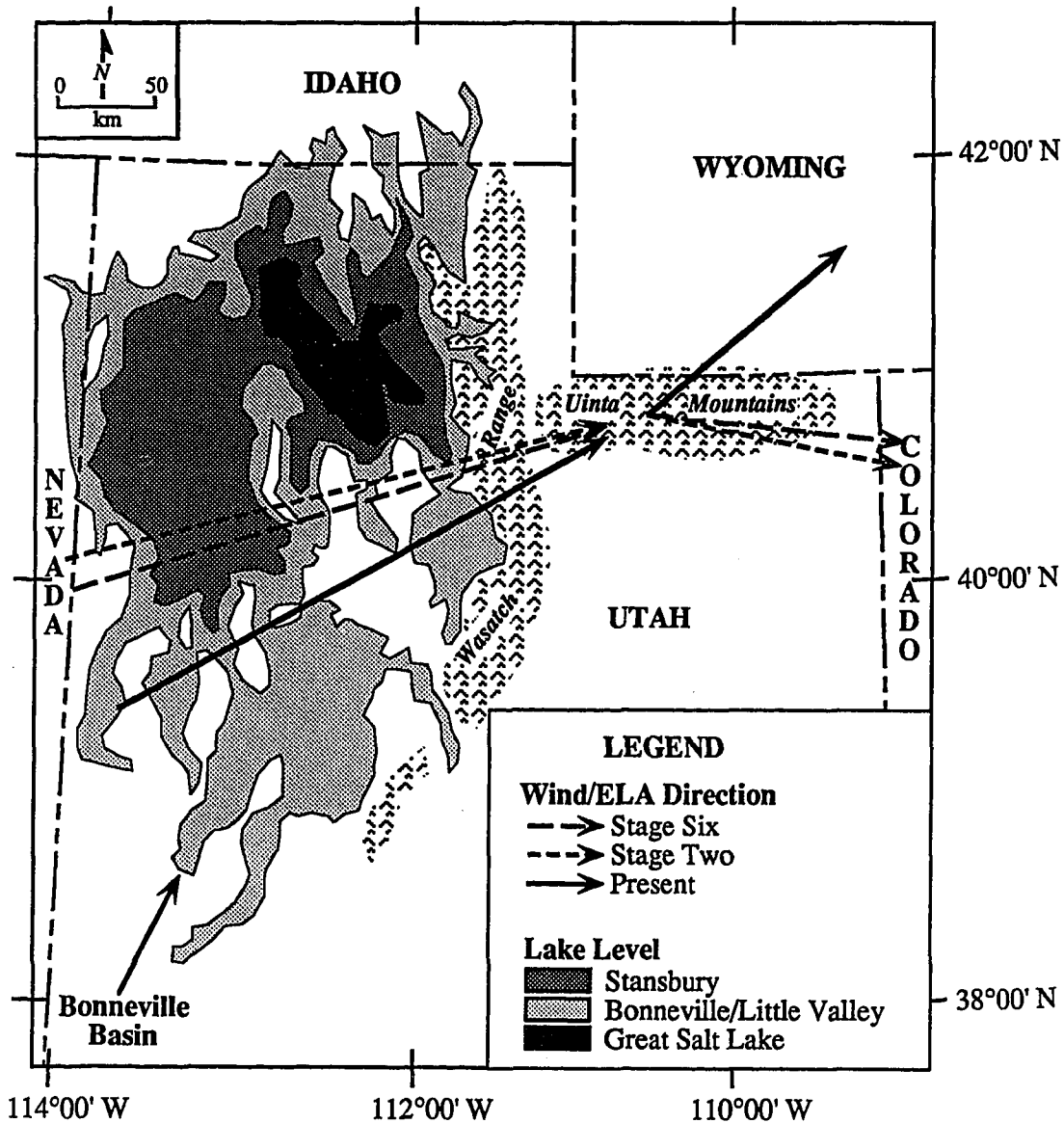


Figure 19. Study area and adjacent Bonneville Basin. Present and paleolake levels, present and estimated full-glacial wind directions, and present full-glacial ELA trend surface directions are shown. The Little Valley and Bonneville cycles experienced similar levels and are shown as a single level. Long arrows pointing toward the Uinta Mountains show estimated wind directions relative to lake levels. Short arrows pointing from the Uinta Mountains show the reconstructed and present estimated ELA surface directions (Lake levels after Currey and Oviatt, 1985; and Mulvey, 1985).

A west to east transect of reported stage two ELA heights from selected sources is given in Table 28. The transect extends from the Pacific Ocean east across the Uinta Mountains to the Colorado Rocky Mountains. The locations listed are all within a half of a degree north or south of $40^{\circ}30'$ N latitude. Although the selected sources have used different methods for estimating the ELA heights, this listing provides a relative comparison across the transect. The ELAs listed in Table 27 are plotted on Figure 20. The general trend across the transect, shown by the solid regression line, increases inland at a rate of 54.9 meters degree longitude⁻¹, whereas across the Uinta Mountains, as shown by the dashed regression line, the ELA height increases at a rate of 215.2 meters degree longitude⁻¹. The general inland increase in ELA heights shown on Figure 20 agrees with a similar transect drawn by Porter et al. (1983) along a $44^{\circ} 30'$ N latitude from the Pacific Northwest to the Yellowstone, Wyoming area.

Three significant characteristics revealed by Figure 20 are: (1) the Uinta Mountain ELA is steeper and higher than the general trend; (2) a significant depression of ELA heights occurs in the Wasatch Range immediately east of the Bonneville Basin, whereas the ELA heights of the Uinta Mountains are substantially higher than the Wasatch ELA heights; and (3) the height and gradient of the Uinta Mountain ELA surface appear to be comparable to that of the Colorado Rocky Mountains. Because the height and gradient of the Uinta Mountains ELA is steeper than that of the general west to east trend, it is speculated that the Uinta Mountains were comparatively dryer than the other ranges to the west. The depression of ELA heights in the Wasatch Range indicates that ELA heights immediately east of the Bonneville Basin were probably enhanced by paleolake moisture. In contrast to the Wasatch Range, the height and gradient of the Uinta ELA surface are similar to the height and gradient of the ELA surface in the Colorado Rocky Mountains. Furthermore it should be noted that the Colorado Rocky Mountains were not located in the proximity of any major Pleistocene paleolakes. Therefore, these patterns suggest that influence on the

Table 27

ELA Of Selected Locations On A 40°30' North Latitude Transect
From the Pacific Ocean To The Colorado Rocky Mountains

Location	N Latitude	W Longitude	ELA (m)	Source; Method
Lassen Peak, California	40°30'	121°32'	2,100	Porter et al. (1983); Cirque floor elevation
Western Great Basin, Nevada	40°30'	117°00'	2,679	Dohrenwend (1984); Cirque floor elevation
Shoshone Range, Nevada	40°26'	116°52'	2,650	Dohrenwend (1984); Cirque floor elevation
Ruby-East Humboldt Range, Nevada	40°30'	115°22'	2,628	Mulvey (1985); Median altitude of reconstructed glaciers
Stansbury Mountains, Utah	40°25'	112°37'	2,686	Mulvey (1985); Median altitude of reconstructed glaciers
Oquirrh Mountains, Utah	40°25'	112°15'	2,720	Mulvey (1985); Median altitude of reconstructed glaciers
Central Wasatch Range, Utah	40°37'	111°33'	2,647	Mulvey (1985); Median altitude of reconstructed glaciers
Western Uinta Mountains, Utah	40°30'	111°00'	2,938	This Dissertation; 0.55 AAR
Eastern Uinta Mountains, Utah	40°30'	109°45'	3,207	This Dissertation; 0.55 AAR
Park Range, Colorado	40°50'	106°34'	2,895	Leonard (1989); 0.65 AAR
Western Front Range, Colorado	40°32'	105°52'	3,068	Leonard (1989); 0.65 AAR
Medicine Bow Mountains, Colorado	40°51'	105°39'	3,049	Leonard (1989); 0.65 AAR
Eastern Front Range, Colorado	40°01'	105°35'	3,313	Leonard (1989); 0.65 AAR
Eastern Front Range, Colorado	40°28'	105°31'	3,170	Leonard (1989); 0.65 AAR

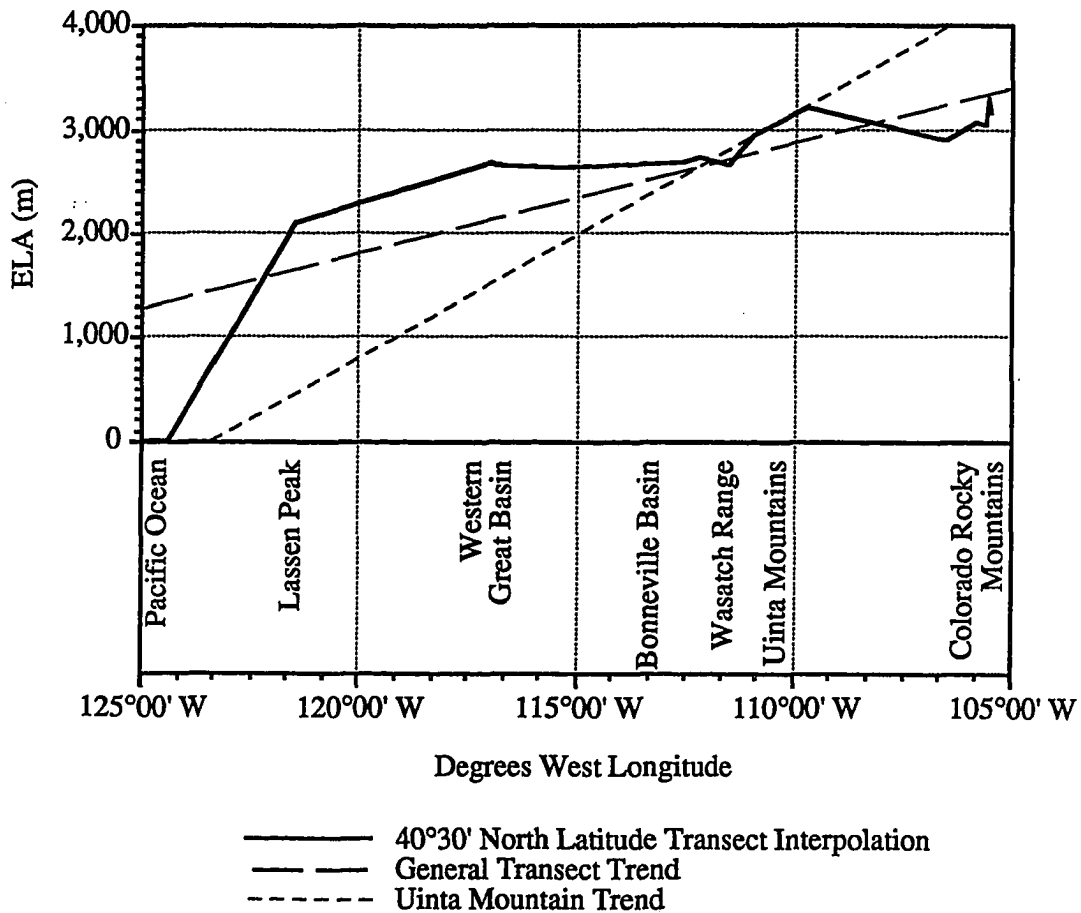


Figure 20. ELA height transect from the Pacific Ocean east to the Colorado Rocky Mountains along 40°30' N latitude. General transect trend shown by the long dashed line, increases at a rate of 54.9 meters degree longitude⁻¹. The Uinta Mountain trend, shown by the short dashed line, increases at a rate of 215.2 meters degree longitude⁻¹.

Uinta Mountains from the paleolakes was substantially reduced by orographic shielding from the Wasatch Mountains, and that the height and gradient of the Unita Mountain ELA surface was comparable to that of the Colorado Rocky Mountains, which were located in an entirely continental environment, far removed from any significant moisture sources.

Full-Glacial Air-Flow

The prevailing wind direction for the two glacial episodes was projected from the estimated snow accumulation trend surfaces. The wind direction estimates are $253 \pm 9.2^\circ$ for the stage six episode and $256 \pm 9.2^\circ$ for the stage two episode. Both of these estimates have a more zonal orientation than the present winter wind direction of 241° . These estimates differ significantly, therefore, it is assumed that the full-glacial air-flow directions differed substantially from the present. However, because the full-glacial wind directions were ultimately estimated from the glacial ELA trend surface directions, the question arises as to whether the ELA trend surface directions were controlled more by air flow, or by moisture source, which for the Uinta Mountains would be paleolakes occupying the Bonneville Basin.

The present wind direction was found to be related inversely to annual snow accumulation ($R = -0.733$) and regional winter precipitation ($R = -0.651$). The seasons experiencing more zonal-oriented wind directions tended to be dryer. The full-glacial wind directions are both estimated to have had more zonal-oriented directions than present, reaffirming the idea that the glacial episodes were dryer than present.

Leonard's (1984) observations from the San Juan Mountains of Colorado suggest that moisture supply and general circulation during the late Pleistocene differed little from the present. Leonard found that both the present snow accumulation and the late-Pleistocene ELA possessed similar west to east gradients which wrapped around the San Juan Mountains. From these observations, Leonard concluded that the similarity between

the present and late-Pleistocene patterns suggested that general accumulation-season circulation patterns and moisture differed little between the late-Pleistocene and present (Leonard, 1984). Meierding (1982), did not project circulation patterns or speculate upon moisture sources for the Front Range of Colorado. Nevertheless, Meierding did find that the late-Pleistocene ELA surfaces declined northward across the range along gradients similar to the present temperature gradient. Likewise, both Dohrenwend (1984) and Zielinski and McCoy (1987) found that ELA surfaces in the Great Basin sloped to the north along gradients similar to the present temperature gradient. However, Zielinski and McCoy (1987) found that the late-Pleistocene ELA heights in the northwestern Great Basin were anomalously low in comparison to present winter snow accumulation, which they suggested was controlled by differing accumulation and/or temperature conditions.

For western Montana, Locke (1990) found the regional trend of paleoELAs parallels the present glacial ELAs, except on the eastern side of the Montana Rocky Mountains, where Locke believed that katabatic air flow from continental ice sheets formed a local zone of convergence. Mulvey (1985) likewise did not detect significant differences between present snow accumulation and the stage two ELA. Porter et al. (1983) compared winter snow accumulation and late-Pleistocene glaciation threshold elevations across a transect from the Pacific Ocean to the Great Plains. The transect followed 44°30' N latitude from the Cascade Range across the Yellowstone Plateau area. Porter et al. (1983) found that glaciation threshold elevations increased, and present snow accumulation decreased eastward at comparative rates, except in the Yellowstone area. The Yellowstone area has both lower glaciation threshold elevations and higher present snow accumulation than surrounding glaciated areas. From these observations, Porter et al. (1983) concluded that Pleistocene and present snow accumulations in the Yellowstone area are enhanced by Pacific air masses that flow relatively unimpeded via the Snake River Plain to the Yellowstone Plateau.

Present snow accumulation in the Uinta Mountains decreases to the northeast, and because the present wind direction also heads to the northeast, it is thought that the anticyclonic circulation that presently occupies the central Great Basin during the winter months (Mitchell, 1976) strongly influences air flow and convergence over the Uinta Mountains. The Pleistocene ELAs and projected snow accumulation in the Uinta Mountains decrease to the east, and it is thought that a more zonal winter air flow prevailed over the Uinta Mountains during the Pleistocene. Thus, it can be argued that the zonal Pleistocene ELAs were influenced primarily by the location of Bonneville Basin paleolakes to the west of the Uinta Mountains, rather than a zonal air flow. However, as illustrated in Figure 19, the north to south distribution of the paleolakes extends well beyond the latitudes of the Uinta Mountains. If a northwesterly, or as in the present case, a southwesterly air flow prevailed over the Uinta Mountains, a substantial distance of lake fetch would still have been encountered, and resultant ELA surface directions would have developed. Furthermore, as illustrated in Figure 20, the height and gradient of the Uinta Mountain ELAs are both substantially higher than the mountains within or directly east of the Bonneville Basin. These observations lead to the conclusions that during the glacial episodes the Uinta Mountains were not subjected to wintertime anticyclonic forces originating from the Great Basin, and that a predominantly zonal air flow is likely to have prevailed over the Uinta Mountains during the snow accumulation season.

Synthesis Of Paleoenvironments

The stage six glaciation is estimated to have been from 9.6° C to 12.2° C colder than present with 71% of present precipitation. Where the stage six glaciation is presumed to have been drier than the present, it is thought to have been more moist and warmer than the stage two episode. The stage six glaciation is believed to have been more moist and warmer than the stage two glaciation because the stage six ELA trend surface has a steeper

gradient and a more southerly oriented direction than the stage two episode. This conclusion is based on observations of present snow accumulation and climate records which demonstrate that present snow accumulation trend surface gradients are steeper and more southerly oriented during more moist and warmer winters. Considering the stage six episode would have been warmer than the stage two episode, it is likely that mean temperature reduction for the stage six episode would be closer to the lower end of the estimate range, closer to the 9.6° C temperature reduction estimate.

The differences between the ELA trend surface gradients of the two episodes in the Uinta Mountains suggest substantially different precipitation and temperature regimes. The cause for the differing precipitation and temperature regimes might be related to regional climatic differences, local climatic differences, or a combination of regional and local climatic differences. Although it cannot be demonstrated, the stage six glaciation is thought to have been influenced by a paleolake body that may have been larger than the stage two Stansbury level in the Bonneville Basin. A Little Valley cycle lake level as high as 1,493.5 meters may have coincided with the maxima of the stage six glaciation. Thus, temperatures would have been moderated and the moisture supply enhanced by the larger water body. Because the ELA heights for both glacial episodes in the Uinta Mountains are substantially higher than the ELA heights in the nearby Bonneville Basin, paleolake enhancement of snow accumulation is thought to have had a more minor influence in the Uinta Mountains, as opposed to the Wasatch Mountains.

Temperatures during the stage two glaciation are also estimated to have been from 9.6° C to 12.2° C colder than present with precipitation reduced as much as 68% of present. The stage two glaciation is believed to have been colder and drier than the stage six episode. Because the stage two episode is postulated to have been colder than the stage six episode, it is likely that mean temperature reduction for the stage two episode would be

closer to the higher end of the estimate range, closer to the 12.2° C temperature reduction estimate.

Temperature reduction estimates from a number of studies for the region (Galloway, 1970; Gates, 1976; McCoy, 1977; McCoy, 1981; Mears, 1981; Meierding 1982; Péwé, 1983; Mulvey, 1985) generally collaborate the 9.6° C to 12.2° C estimate from this dissertation. Whereas stage two precipitation for the region was estimated higher or unchanged from present (Galloway, 1970; Brackenridge, 1987; Leonard, 1984; Zwick, 1980; Locke, 1990), others have found that precipitation was substantially reduced (Wells, 1979; Gates, 1976; Spaulding and Graumlich, 1986; Zielinski and McCoy, 1987; Burbank, 1991). The results from this dissertation indicate that full-glacial precipitation was less than present conditions in the Uinta Mountains.

Where substantial differences in ELA height and inferred precipitation exist between two closely located sites such as the Uinta Mountains and Little Cottonwood Canyon in the Wasatch Mountains (McCoy, 1977), suggest that strong local climate variations might have existed during the glacial episodes. For example, the stage two ELA for the Little Cottonwood glacier was estimated to have been 2,400 ±20 meters (Madsen and Currey, 1979), which is on the order of 637 meters lower than the mean stage two ELA for the Uinta Mountains. If the present ELA for Little Cottonwood Canyon is estimated using the same methods outlined in Chapter 3, the mean 1961 to 1985 April 1 snow accumulation of 87.4 cm (U.S. Dept. Agriculture 1990) that falls in the canyon would yield ELA estimates of 4,051 meters to 4,513 meters. These estimates range from 456 to 394 meters lower than the present mean ELA estimates of 4,507 meters to 4,907 meters found in the Uinta Mountains. The ELA height discrepancy between these two closely located areas illustrates that local climate variations are also likely to have occurred during the Pleistocene.

Air flow during the stage six episode is estimated to have been more zonal than present, but slightly more southerly oriented than the stage two episode. The stage six

wind direction is estimated to have been from $253^{\circ} \pm 9.2$. The stage two wind direction is estimated to have been from $256^{\circ} \pm 9.2$, and the present from 241° . The more zonal orientation suggests that both glacial episodes were not influenced by winter time anticyclonic circulation that is believed to influence present air flow and convergence, and that a more zonal flow as described by Gates (1976) dominated the study area during the glacial episodes. Because air flow direction differences were not detected or mentioned at other sites (Leonard, 1984; Meierding, 1982; Dohrenwend, 1984; Mulvey, 1985; Locke, 1990), it is hypothesized that the primary air low difference between the glacial episodes and the present is the result of the absence of winter time anticyclonic circulation originating from the Great Basin.

To gain an understanding of how the ELA of the Uinta Mountains corresponds to the general pattern of ELA across the Eastern Great Basin, the data from this dissertation were combined with data from selected Eastern Great Basin sites. The median altitudes of stage two reconstructed glaciers in the Uinta Mountains and the Eastern Great Basin are given in Table 28. The median altitude measurement is equivalent to a THAR of 0.50 (Meierding, 1982). The median altitudes of the Uinta Mountains were estimated from Table 13, and the median altitudes for the Eastern Great Basin sites are from Mulvey (1985). The locations of the sites and generalized median altitude contours are shown in Figure 21. The contour pattern shown in Figure 21 was plotted using linear interpolation and triangulation functions with SURFER[®] software.

A comprehensive interpretation of the climatic and paleoenvironmental influences dominating the region during the stage two episode can be seen from the contour pattern. The most apparent trend in the contour pattern is the general south to north decline in median altitude height. The general south to north decline is probably a response to a general northward decline in temperature. A second trend that can be observed from Figure 21 is that sites on the east side of the Bonneville Basin have substantially lower median

altitudes than sites on the west side of the basin. This difference strongly suggests that paleolake distribution influenced the height of glaciation on the east side of the basin. A third trend apparent in Figure 21 is the steep west to east increase in median altitudes across the central Wasatch Range and the Uinta Mountains. The steep increase is interpreted to indicate a strong zonal air flow pattern across the two mountain systems. Furthermore, the eastward increase across the Uinta Mountains is interpreted as indicating that the primary moisture source for the Uinta Mountains originated from the Bonneville Basin.

Table 28
 Median Altitude Of Reconstructed Oxygen Isotope Stage Two
 Glaciers In The Uinta Mountains And The Eastern Great Basin

Site ^a	N Latitude	W Longitude	Median Altitude of Reconstructed Glaciers (m)
1. Eastern Uinta Mountains	40°45'	109°30'	3,222
2. Western Uinta Mountains	40°45'	111°00'	2,993
3. Wasatch Range (South)	40°15'	111°33'	2,616
4. Bear River Range	41°43'	111°43'	2,568
5. Wasatch Range (Central)	40°37'	111°45'	2,647
6. Mount Nebo	39°49'	111°46'	2,954
7. Wasatch Range (North)	41°03'	111°49'	2,475
8. Wellsville Mountains	41°41'	111°52'	2,417
9. Pavant Range	39°00'	112°07'	2,770
10. Oquirrh Range	40°25'	112°12'	2,720
11. Tushar Range	38°22'	112°22'	3,272
12. Stansbury Range	40°25'	112°39'	2,686
13. Brian Head	37°42'	112°51'	3,166
14. Raft River Range	41°55'	113°22'	2,579
15. Deep Creek Range	38°49'	113°55'	2,922
16. Snake Range	39°00'	114°13'	3,092
17. Cache-Harrison Peaks	42°24'	113°41'	2,331
18. Jarbridge Range	41°48'	114°31'	2,714
19. Schell Creek Range	39°22'	114°37'	2,966
20. Ruby-East Humboldt Range	40°30'	115°22'	2,628

^a Sites 1 and 2 this dissertation, sites 3 to 20 after Mulvey (1985). Sites 17 to 20 are located beyond the map limits of Figure 21.

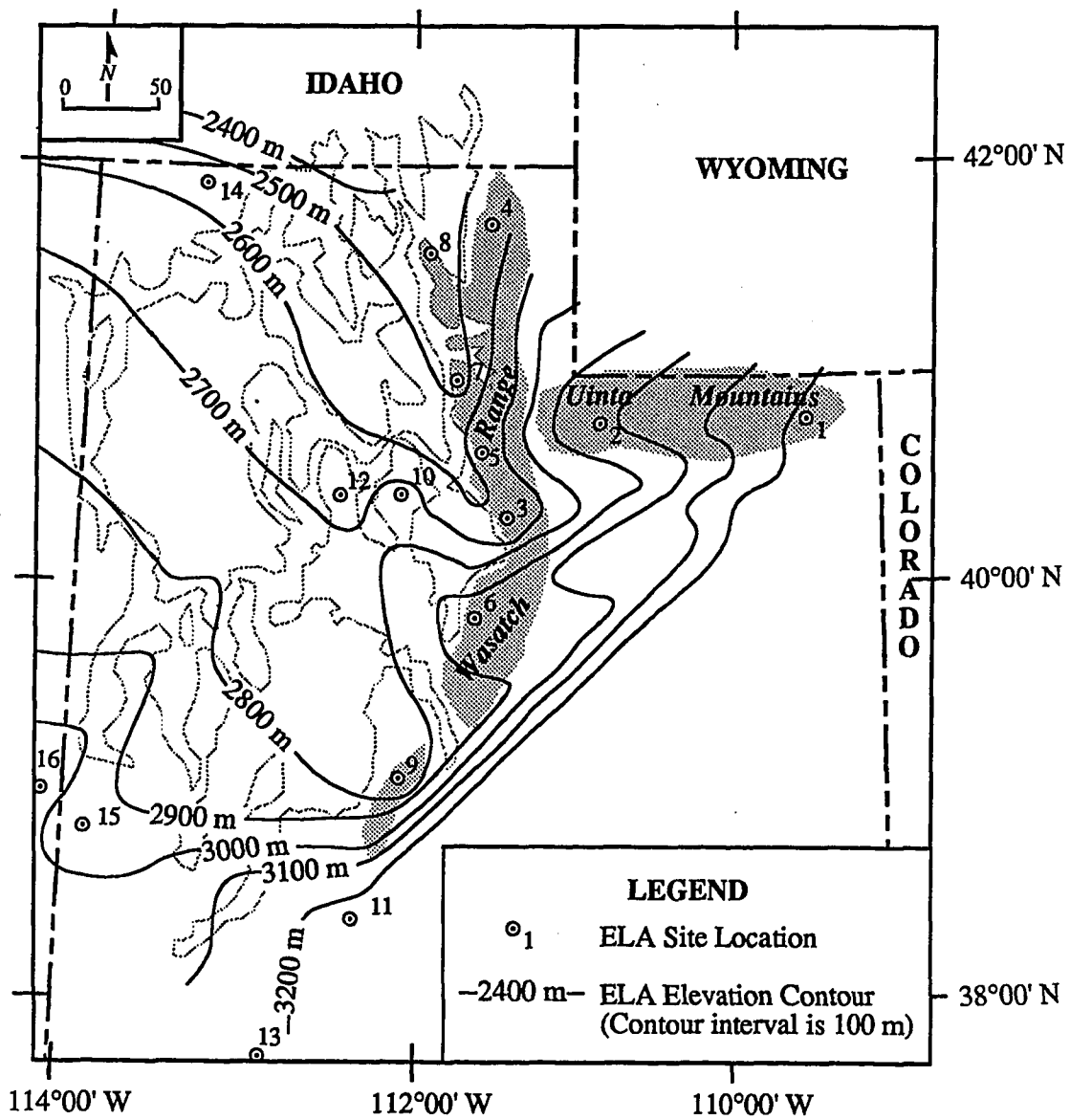


Figure 21. Generalized contours of median altitudes of reconstructed glaciers for sites in the Uinta Mountains and the Eastern Great Basin. Contour interval is 100 meters. Height and location data are listed in Table 29.

CHAPTER VII

CONCLUSION

Summary Of Research Results

From the analyses and discussions in the preceding chapters several findings regarding the Uinta Mountains and surrounding region, both past and present, have been made. The objective of this dissertation was to reconstruct the paleoenvironmental setting of the Uinta Mountains during the last two Pleistocene full-glacial episodes. To focus upon and to accomplish this objective the following question was developed: Can the climate and environmental systems of the late Pleistocene full-glacial episodes in the Uinta Mountains be reconstructed from present climate and environmental systems data, and late Pleistocene glacial geomorphology? To further clarify the objective three research questions regarding the Pleistocene climate of the Uinta Mountains during the last two full-glacial episodes were proposed: (1) How much colder were temperatures during the full-glacial episodes? (2) Was the full-glacial precipitation significantly different from present? (3) If precipitation differed greatly, what environmental conditions would bring about this difference? By reconstructing the full-glacial temperature, precipitation and wind direction for the study area, and drawing comparisons from the surrounding region, the objective(s) of this research was accomplished.

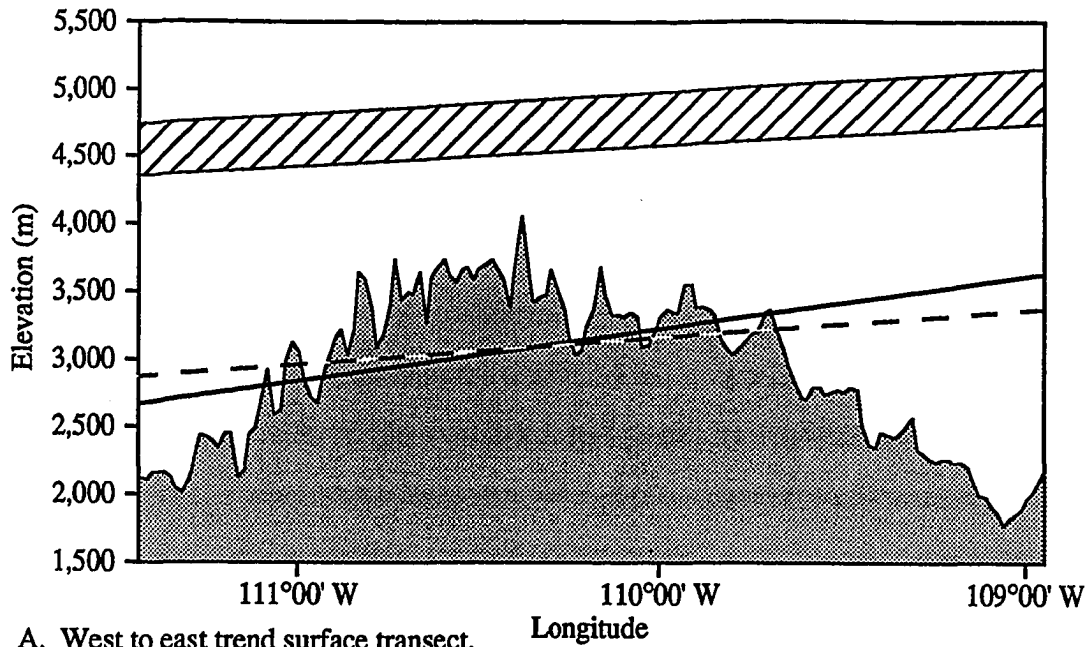
Through the analysis of present snow accumulation and regional climate patterns relationships between snow accumulation patterns and climate variability were identified. The statistical relationships between winter climate parameters and snow accumulation patterns indicate that these variables are closely linked. The analysis of bivariate (i.e., correlation) and multivariate (i.e., regression) relationships revealed that significant

connections exist between region-wide winter precipitation, temperature and upper-level air flow patterns, and snow accumulation and snow accumulation trend surface patterns. This analysis demonstrated that significant correlations (i.e., $r = >0.600$) exist between snow accumulation and regional climate. From numerical models drawn from presently glaciated environments (Leonard, 1989), the present ELA heights were estimated from the snow accumulation and temperature data. The present mean ELA range was estimated to be from 4,507 meters to 4,907 meters in altitude, which is 383 meters above the highest point on the range.

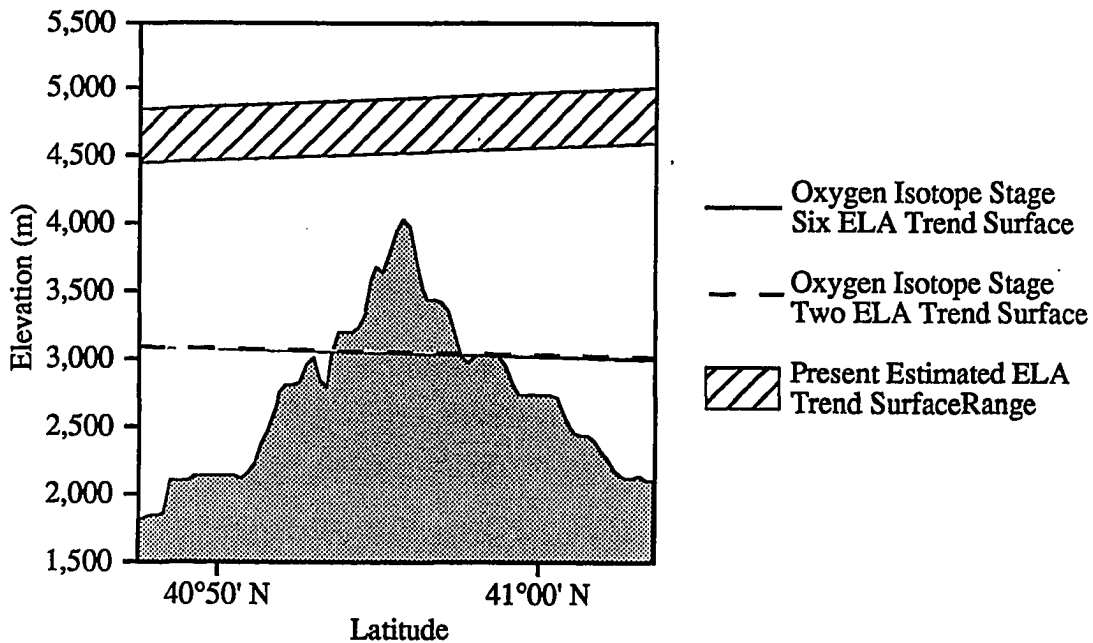
The Pleistocene ELA was estimated from the reconstructed extent of the stage six and stage two episode glaciers. ELA trend surfaces for both glacial episodes were constructed using an AAR of 0.55. The AAR of 0.55 was found to provide the best fit and the lowest over all errors for the two glacial episodes. The mean ELA heights were estimated to be 3,027 meters for the stage six episode and 3,037 meters for the stage two episode.

The Pleistocene ELA trend surfaces were found to differ substantially from the present estimated ELA trend surfaces. The stage six and stage two mean ELA heights were found to be at least 1,480 meters to 1,470 meters, respectively, lower than the present estimated ELA. The directions of the stage six and stage two surfaces ascend from west to east on a nearly zonal axis (276° and 279° , respectively), while the present surface rises from southwest to northeast (230°). The surface gradient of the stage two surface ($2.4 \text{ meters km}^{-1}$) is similar to the present surface gradient (2.8 m km^{-1}), whereas the stage six surface was found to be considerably more steep (4.8 m km^{-1}) than the stage two and present surfaces. The differences between the past and present ELA trend surfaces are shown on figure 22.

From the comparison of the Pleistocene ELA trend surfaces to the present trend surfaces, temperature change, snow accumulation and wind direction for the glacial



A. West to east trend surface transect.



B. South to north trend surface transect.

Figure 22. Transects of past and present ELA trend surfaces. West to east (A) trend surface transect across study area along $40^{\circ}45'$ N latitude; south to north (B) trend surface transect across study area along $110^{\circ}25'$ W longitude, and transect intercept is Kings Peak ($40^{\circ}45'$ N, $110^{\circ}25'$ W). Oxygen isotope stage six (solid lines) and oxygen isotope stage two (dashed lines) are 0.55 AAR ELA surfaces. Present estimated ELA are shown as hatched zones, and shaded area represents ground surface.

episodes were estimated. Temperature change was estimated by measuring the vertical height difference between the Pleistocene and present ELA trend surfaces. Using an assumed normal lapse rate of $0.65^{\circ}\text{C } 100\text{ meters}^{-1}$ the temperatures for both glacial episodes were estimated to have ranged between 9.6°C to 12.2°C lower than present.

The temperature change estimates were used to estimate the snow accumulation for the glacial episodes. The snow accumulation estimates were calculated using the aforementioned numerical models of present glaciated environments (Leonard, 1989). The estimated mean snow accumulation was 40.6 cm for the stage six glaciation and 38.4 cm for the stage two glaciation. The estimates indicate that the Pleistocene accumulations are slightly higher than the present mean of 37.6 cm. However, with the understanding that the present snow accumulation season lasts only six months whereas the Pleistocene snow accumulation seasons were probably nine months or more in length, these estimations indicate that precipitation was probably reduced on the order of 71% during stage six and 68% during stage two. On the basis of trend surface gradient and direction relationships identified in the present snow accumulation climate analysis, the stage six glaciation is projected to have been warmer and more moist than the stage two glaciation.

Using the statistical relationship between the present annual snow accumulation trend surface directions and the upper-level wind directions (i.e., Table 9, equation 15), Pleistocene wind directions were estimated. The stage six direction of 253° and stage two direction of 256° were both found to be more zonal than the present direction of 241° .

By comparing the climate change estimates for the Uinta Mountains to estimates made by others for the region, the paleoenvironmental conditions that prevailed over the region were projected. The temperature reduction estimate of 9.6°C to 12.2°C for stage two is in relative agreement with estimates by others for the region (Galloway, 1970; Gates, 1976; McCoy, 1977; McCoy, 1981; Mears, 1981; Meierding, 1982; Péwé, 1983; Mulvey, 1985). Although some researchers have found that full-glacial precipitation was

similar to or higher than present (Brackenridge, 1987; Leonard, 1984; Zwick, 1980; Locke, 1990), reduced precipitation estimates from this analysis support the theory that precipitation was generally reduced during the Pleistocene (Galloway, 1970; Wells, 1979; Gates, 1976; Spaulding and Graumlich, 1986; Zielinski and McCoy, 1987; Crowley and North, 1991; Burbank, 1991).

Because the full-glacial ELA and snow accumulation trend surfaces are zonally oriented and rise on a sharp gradient from the west, paleolake moisture from the Bonneville Basin is thought to have influenced glaciation in the Uinta Mountains. However, in comparison to the Wasatch Mountains which lie between the Uinta Mountains and the Bonneville Basin, the Uinta Mountains appear to have been substantially dryer. The west to east ELA heights and gradients of the Uinta Mountains (i.e., Figure 20) were found to be more comparable to those of the Colorado Rocky Mountains.

Predominantly zonal wind directions are projected to have prevailed over the Uinta Mountains during the glacial episodes. The lack of a southwesterly orientation on the Pleistocene ELA trend surfaces suggests that the anticyclonic air flow that develops over the Great Basin during present winter seasons (Mitchell, 1976) was probably absent during the Pleistocene. Although general circulation models (Gates, 1976; COHOMAP Members, 1988) and the results of this dissertation research indicate a more zonal full-glacial air flow. Evidence from other studies for the region suggest no significant change to air flow has occurred (Leonard, 1984; Dohrenwend, 1984; Mulvey, 1985; Zielinski and McCoy, 1987; Locke, 1990).

To summarize these results the following conclusions are presented: (1) The full-glacial temperature reduction estimates of 9.6° C to 12.2° C for the Uinta Mountains are in relative agreement with estimates by others for the region. (2) Reduced precipitation estimates from this analysis support the theory that precipitation was generally reduced during the Pleistocene. (3) The Uinta Mountains were influenced by paleolake moisture

from the Bonneville Basin to the west, but were substantially dryer than the ranges located directly to the east of the Bonneville Basin. (4) A predominantly zonal wind direction prevailed over the Uinta Mountains, and the anticyclonic air flow that develops over the Great Basin during present winter seasons was probably absent during the Pleistocene.

Qualification of Findings

The findings made presented in this dissertation are based upon both secondary data resources and primary data derived from secondary data resources. The estimation of the present ELA and climate parameters of the past are established upon rates and relationships observed from present phenomena, whereby it has been assumed that past rates and relationships are consistent with the present. Therefore, the estimations presented here should be considered only first approximations, that require further testing for verification.

Future Research

The findings of this dissertation presents more opportunities for future research. Future research opportunities exist in the further definition of present snow accumulation and climate relationships. The snow accumulation and climate relationships analyzed in this dissertation involve only a 19 year period and could be refined by additional data and analysis. Furthermore, the relationships found to exist in the Uinta Mountains should be explored elsewhere to determine whether these are a consistent phenomenon or only unique to this area.

From the reconstruction and evaluation of the Pleistocene glaciers, several residual cases were identified. The residual cases may represent original mapping errors and may require further verification to determine whether their distributions are valid. A relatively small number of specific geomorphic studies have been conducted (Bradley, 1936; Hansen, 1969; Schoenfeld, 1969; Barnhardt, 1973; Grogger, 1974; Gilmer, 1986;

Schlenker, 1988) since Atwood's original 1907 study of the entire range. A similar reconstruction of the Holocene glacial sequence in the Uinta Mountains, as discussed by Barnhardt (1973) and Grogger (1974), is likely to yield significant hypotheses regarding Holocene climate and paleoenvironmental variations found for the study area.

On a larger scale, a more integrated study focusing on the Uinta Mountains, the Bonneville Basin and adjoining mountain ranges (i.e., Mulvey, 1985) is likely to provide a valuable paleoenvironmental synthesis for a large portion of the Western United States. Furthermore, each of the paleoclimate estimations and paleoenvironmental projections made in this dissertation should be considered hypotheses that require further testing.

REFERENCES CITED

- Atwood, W.W., 1909, Glaciation of the Uinta and Wasatch Mountains: United States Geological Survey Professional Paper 61, 96 p.
- Barnhardt, M.L., 1973, Late Quaternary geomorphology of the Bald Mountain Area, Uinta Mountains, Utah: Salt Lake City, University of Utah, M.S. thesis, 109 p.
- Barry, R.G., 1981, Mountain weather and climate: New York, Methuen, 313 p.
- _____, 1983, Late-Pleistocene climatology, *in* Wright H. E., and Porter S. C., eds., Late Quaternary environments of the United States: Minneapolis, University of Minnesota Press, p. 390-407.
- Blackwelder, E., 1915, Post-Cretaceous history of the mountains of central western Wyoming: *Journal of Geology*, v. 23, p. 307-340.
- Bowen, D.Q., 1978, Quaternary geology: Oxford, Pergamon Press, 221 p.
- Brackenridge, G.R., 1978, Evidence for a cold, dry full-glacial climate in the American Southwest: *Quaternary Research*, v. 9, p. 22-40.
- Bradley, R.S., 1985, Quaternary paleoclimatology: Boston, Allen and Unwin Inc., 472 p.
- Bradley, W.H., 1936, Geomorphology of the North Flank of the Uinta Mountains: U.S. Geological Survey Professional Paper 185-I, p. 163-204.
- Bryant, B., 1990, Geologic map of the Salt Lake 30' x 60' Quadrangle, north-central Utah, and Uinta County, Wyoming: U.S. Geological Survey Miscellaneous Investigations Series Map 1-1944, scale 1:100,000.
- Burbank, D.W., 1991, Late Quaternary snowline reconstructions for the southern and central Sierra Nevada, California and a reassessment of the "Recess Peak Glaciation": *Quaternary Research*, v. 36, p. 294-306.
- Butzer, K.W., 1982, Archaeology as human ecology: Cambridge, Cambridge University Press, 363 p.
- Caine, T.N., 1975, An elevational control of peak snowpack variability: *Water Resources Bulletin*, v. 11, p. 613-621.
- CLIMAP Project Members, 1976, The surface of ice-age Earth: *Science*, v. 191, p. 1131-1137.
- COHMAP Members, 1988, Climatic changes of the last 18,000 years: Observations and model simulations: *Science*, v. 241, p. 1043-1052.
- Coope, G.R., 1974, Interglacial coleoptera from Babbitshole, Ipswich: *Journal of the Geological Society of London*, v. 130, p. 333-340.

- Crowley, T.J., and North, G.R., 1991, *Paleoclimatology*: New York, Oxford University Press, 339 p.
- Currey, D.R., 1990, Quaternary paleolakes in the evolution of semidesert basins, with special emphasis on Lake Bonneville and the Great Basin, U.S.A.: *Paleogeography, Paleoclimatology, Paleoecology*, v. 76, p. 189-214.
- Currey, D.R., and James, S.R., 1982, Paleoenvironments of the northwestern Great Basin and the northeastern Basin Rim region; a review of geological and biological evidence: *Society for American Archeology Papers No. 2*, p. 27-52.
- Currey, D.R., and Oviatt, C.G., 1985, Durations, average rates, and probable causes of Lake Bonneville expansions, stillstands, and contractions during the last deep-lake cycle, 32,000 to 10,000 years ago, *in* Kay, P.A., and Diaz, H.F., eds., *Problems of and prospects for predicting Great Salt Lake levels*: University of Utah Center for Public Affairs and Administration Special Publication, p. 9-24.
- Dohrenwend, J.C., 1984, Nivation landforms in the western Great Basin and their paleoclimatic significance: *Quaternary Research*, v. 22, p. 275-288.
- Fisher, A.G., 1981, Climatic oscillations in the biosphere, *in* Nitecki, M.H. ed., *Biotic crises in ecological and evolutionary time*: New York, Academic Press, p. 103-131.
- Flint, R.F., 1957, *Glacial and Pleistocene geology*: New York, John Wiley and Sons, Inc., 553 p.
- , 1971, *Glacial and Quaternary geology*: New York, John Wiley and Sons, Inc., 892 p.
- Galloway, R.W., 1970, The full-glacial climate in the southwestern United States: *Annals of the Association of American Geographers*, v. 60, p. 246-256.
- Gates, L.W., 1976, Modeling ice age climate: *Science*, v. 191, p. 1138-1144.
- Gifford, R.O., Ashcroft, M.D., Magnuson, M.D., 1967, Probability of selected precipitation amounts in the Western Region of the United States: U.S. Department of Agriculture Western Regional Publication, Climatological data report.
- Graf, W.L., 1976, Cirques as glacier locations: *Arctic and Alpine Research*, v. 8, p. 79-90.
- Grogger, P.K., 1974, *Glaciation of the High Uintas Primitive Area, Utah, with emphasis on the Northern Slope*: University of Utah, Ph.D. dissertation, Salt Lake City, UT, 209 p.
- Hansen, W.R., 1969, *The geologic story of the Uinta Mountains*: U.S. Geological Survey Bulletin 1291, 144 p.
- , 1986, *Neogene tectonics and geomorphology of the Eastern Uinta Mountains in Utah, Colorado, and Wyoming*: U.S. Geological Survey Professional Paper 12356, 78 p.

- Hawkins, F.F., 1985, Equilibrium-line altitudes and paleoenvironment in the Merchants Bay Area, Baffin Island, N.W.T., Canada: *Journal of Glaciology*, v. 31, p. 205-213.
- Hunt, C.B., 1967, *Physiography of the United States*: San Francisco, W. H. Freeman, 480 p.
- Imbrie, J., and Imbrie, K.P., 1979, *Ice ages solving the mystery*: Short Hills, New Jersey, Enslow Publishers, 224 p.
- Jennings, S.A., and Elliott-Fisk, D.L., 1993, Packrat Midden Evidence of Late Quaternary Vegetation Change on the White Mountains, California-Nevada: *Quaternary Research*, v. 39, p. 214-221.
- Johnson, C.M., 1970, *Common native trees of Utah*, Special Report 22, Agricultural Experiment Station, College of Natural Resources: Logan, Utah State University, 109 p.
- Krumbein, W.C., and Graybill, F.A., 1965, *An introduction to statistical models in geology*: New York, McGraw-Hill, 475 p.
- LaMarche, V.C., Jr., 1973, Holocene climatic variations inferred from treeline fluctuations in the White Mountains, California: *Quaternary Research*, v. 3, p. 632-660.
- Leonard, E.M., 1984, Late Pleistocene Equilibrium-line altitudes and modern snow accumulation patterns, San Juan Mountains, Colorado, U.S.A.: *Arctic and Alpine Research*, v. 16, p. 65-76.
- _____, E.M., 1989, Climatic change in the Colorado Rocky Mountains: Estimates based on modern climate at late Pleistocene equilibrium lines: *Arctic and Alpine Research*, v. 3, p. 253-261.
- Locke, W.M., 1989, Present climate and glaciation of western Montana, U.S.A.: *Arctic and Alpine Research*, v. 21, p. 234-244.
- _____, 1990, Late Pleistocene glaciers and climate of western Montana, U.S.A.: *Arctic and Alpine Research*, v. 22, p. 1-13.
- Loewe, F., 1971, Considerations on the origin of the Quaternary ice sheet of North America: *Arctic and Alpine Research*, v. 3, p. 331-334.
- Madole, R.F., 1986, Lake Devlin and Pinedale glacial history, Front Range, Colorado: *Quaternary Research*, v. 25, p. 43-54.
- Madsen, D.B., and Currey, D.R., 1979, Late Quaternary glacial and vegetational changes, Little Cottonwood Canyon area, Wasatch Mountains, Utah: *Quaternary Research*, v. 12, p. 254-270.
- McCoy, W.D., 1981, Quaternary aminostratigraphy of the Bonneville and Lohontan basins: Boulder, University of Colorado Ph.D. Dissertation, 603 p.
- McKay, G.A., 1981, The distribution of snowcover, *in* Gray, D. M., and Male, D. H., eds., *Handbook of snow*: Toronto, Pergamon Press, p. 153-187.

- Mears, B., 1974, Evolution of the Rocky Mountain Glacial Model, *in* Coates D. R., (editor), *Glacial geomorphology*: Allen and Unwin, Binghamton, NY, p. 11-40.
- _____, 1981, Periglacial wedges and the late Pleistocene environments of Wyoming intermontane basins: *Quaternary Research*, v. 15, p. 171-198.
- Meierding, T.C. 1982, Late Pleistocene glacial equilibrium-line altitudes in the Colorado Front Range: A comparison of methods: *Quaternary Research*, v. 18, p. 289-310.
- Miller, G.H., Bradley, R.S., and Andrews, J.T., 1975, The glaciation level and lowest equilibrium-line altitude in the high Canadian Arctic: Maps and climatic interpretation: *Arctic and Alpine Research*, v.7, p. 155-168.
- Mitchell, V.I., 1976, The regionalization of climate in the Western United States: *Journal of Applied Meteorology*, v. 15, p.920-927.
- Mulvey, W.E., 1985, Reconstruction and interpretation of late Pleistocene equilibrium-line altitudes in the Lake Bonneville Region: Salt Lake City, University of Utah, M.S. thesis, 65 p.
- Østem, G., 1966, The height of glaciation limit in British Columbia and Alberta: *Geografiska Annaler*, v.48, p. 126-138.
- Oviatt, C.G., McCoy, W.D., and Reider, R.G., 1987, Evidence for a shallow early or middle Wisconsin-age lake in the Bonneville Basin, Utah: *Quaternary Research*, v 27, p. 248-262.
- Peterson, G.M., Webb, T., Kutzbach, J.E., Van Der Hammen, T., Wijmstra, T.A., and Street, F.A., 1979, The continental record of environmental conditions at 18,000 yr B.P.: An initial evaluation: *Quaternary Research*, v. 12, p. 47-82.
- Peterson, J.A., and Robinson, G., 1969, Trend surface mapping of cirque floor levels: *Nature*, v. 222, p. 75-76.
- Péwé, T.L., 1983, Alpine permafrost in the United States: A review: *Arctic and Alpine Research*, v. 15, p. 145-156.
- Pierce, K.L., 1979, History and dynamics of glaciation in the northern Yellowstone National Park Area: U.S. Geological Survey Professional Paper 729-F, 90 p.
- Pierce, K.L., Obradovich, J.D., and Friedman, I., 1976, Obsidian hydration dating and correlation of Bull Lake and Pinedale Glaciations near West Yellowstone, Montana: *Geological Society Bulletin*, v. 87, p.703-710.
- Porter, S.C., 1975, Equilibrium-line altitude of late Quaternary glaciers in the Southern Alps, New Zealand: *Quaternary Research*, v. 5, p. 27-47.
- _____, 1977, Present and past glaciation threshold in the Cascade Range, Washington, U.S.A.: Topographical and climatic controls, and paleoclimatic implications: *Journal of Glaciology*, v. 18, p. 101-116.

- Porter, S.C., Pierce, K.L., and Hamilton, T.D., 1983, Late Wisconsin mountain glaciation in the Western United States, *in* Wright H.E., and Porter S.C., eds., Late-Quaternary environments of the United States: Minneapolis, University of Minnesota Press, p. 71-111.
- Richmond, G.M., 1965, Glaciation of the Rocky Mountains, *in* Wright H.E., and Frey, D.G., eds., The Quaternary of the United States: Princeton, Princeton University Press, p. 217-230.
- , 1986, Stratigraphy and correlation of glacial deposits of the Rocky Mountains, the Colorado Plateau and the ranges of the Great Basin, *in* Sibrava, V., Bowen, D.Q., and Richmond, G.M., eds., Quaternary glaciations in the Northern Hemisphere: Oxford, Pergamon Press, p. 99-127.
- Ritzma, H.R., 1969, Tectonic resume, Uinta Mountains, *in* Intermountain Association of Geologists, Geologic guidebook of the Uinta Mountains: Salt Lake City, Utah, Publishers Press, p. 57-63.
- Schlenker, G.C., 1988, Glaciation and Quaternary geomorphology of the Blacks Fork Drainage, High Uinta Mountains, Utah and Wyoming: Salt Lake City, University of Utah, M.S. thesis, 87 p.
- Schoenfeld, M.J., 1969, Quaternary geology of the Burnt Fork area, Uinta Mountains, Summit County, Utah: Laramie, University of Wyoming, M.A. Thesis, 75 p.
- Schlenker, G.C., 1988, Glaciation and Quaternary geomorphology of the Blacks Fork Drainage, High Uinta Mountains, Utah and Wyoming: Salt Lake City, University of Utah, M.S. thesis, 87 p.
- Scott, W.E., McCoy, W.D., Shroba, R.R., and Meyer, R., 1983, Reinterpretation of the exposed record of the last two cycles of Lake Bonneville, Western United States: Quaternary Research, v. 20, p. 261-285.
- Shackleton, N.J., and Opdyke, N.D., 1973, Oxygen-isotope and paleomagnetic stratigraphy of equatorial Pacific core V28-238: Oxygen-isotope temperatures and ice volumes on a 10⁵ year and 10⁶ year scale: Quaternary Research, v.20, p. 39-55.
- Spaulding, G.W., and Graumlich, L.J., 1986, The last pluvial climatic episodes in the deserts of southwestern North America: Nature, v. 320, p. 441-444.
- Stokes, W.L., 1969, History of exploration of the Uinta Mountains: *in* Intermountain Association of Geologist, Geologic guidebook of the Uinta Mountains: Salt Lake City, Publishers Press, p.15-21.
- Sutherland, D.G., 1984, Modern glacier characteristics as a basis for inferring former climates with particular reference to Loch Lomand Stadial: Quaternary Science Reviews, v. 3, p. 291-309.
- Trenhaile, A.S., 1975, Cirque elevation in Canadian Cordillera: Annals of the Association of American Geographers, v. 65, p. 517-529.

- Trewartha, G.T., 1968, *An introduction to climate*: New York, McGraw-Hill, 408 p.
- Unwin, D.J., 1979, *An Introduction to trend surface analysis*: Norwich, England, Regency House, 40 p.
- U.S. Department of Agriculture, Soil Conservation Service, 1978, *Summary of mountain precipitation measurements for Utah: 1930-78: Snow survey data report, 1930-1978*.
- _____, 1979-1989, *Utah Annual Data Summary: Snow survey data reports, 1979-1989*.
- U.S. Department of Commerce, National Oceanic and Atmospheric Administration, 1968-1980, *Climatological data, National Summary*: U.S. Government Printing Office, v. 19-31.
- _____, 1972-1989, *Climatological data, Utah*: U.S. Government Printing Office, v. 73-91.
- _____, 1972-1989, *Climatological data, Wyoming*: U.S. Government Printing Office, v. 80-98.
- Wells, P.V., 1979, *An equable glaciopluvial in the West: Pleniglacial evidence of increased precipitation on a gradient from the Great Basin to the Sonoran and Chihuahuan Deserts*: *Quaternary Research*, v. 12, p. 311-325.
- Westbrook, J.K., 1980, *Extrapolation of surface-air temperatures in remote areas using upper-air data*: Utah State University M.S. thesis, Logan, UT, 61 p.
- Zielinski, G.A., and McCoy, W.D., 1987, *Paleoclimatic implications of the relationship between modern snowpack and late Pleistocene equilibrium-line altitudes in the mountains of the Great Basin, Western U.S.A.*: *Arctic and Alpine Research*, v. 19, p. 127-134.
- Zwick, T.T., 1980, *A comparison between the modern and composite Pleistocene snow-lines, Absaroka and Beartooth Mountains, Montana-Wyoming, U.S.A.*: *Journal of Glaciology*, v. 25, p. 347-352.

APPENDIX A
REGIONAL CLIMATE DATA

Mean Regional Winter Precipitation
Data 1972 to 1990^a

Year	Utah Division Five	Utah Division Six	Wyoming Division Three	Regional Average
1972	33.3	9.1	12.0	18.1
1973	33.9	15.0	11.8	20.2
1974	25.2	7.2	8.8	13.7
1975	30.8	10.1	9.9	16.9
1976	25.2	5.9	10.3	13.8
1977	10.5	2.6	3.3	5.5
1978	30.3	10.8	10.8	17.3
1979	24.1	13.9	8.6	15.5
1980	40.7	12.6	12.9	22.1
1981	22.7	6.9	8.4	12.7
1982	42.1	14.9	14.6	23.8
1983	33.3	11.4	11.5	18.7
1984	37.3	10.4	14.3	20.7
1985	30.8	10.1	7.9	16.3
1986	31.1	10.5	15.3	19.0
1987	18.6	10.0	10.3	13.0
1988	19.8	11.0	9.2	13.4
1989	16.4	6.1	5.6	9.4
1990	20.1	6.3	5.6	10.7

^aOctober to March averages reported in cm of precipitation.

Mean Regional Winter Temperature
Data 1972 to 1990^a

Year	Utah Division Five	Utah Division Six	Wyoming Division Three	Regional Average
1972	-1.8	-0.3	-4.7	-2.3
1973	-3.2	-4.7	-6.1	-4.7
1974	-1.4	-2.7	-3.4	-2.5
1975	-1.6	-0.3	-3.3	-1.8
1976	-1.9	-1.9	-3.5	-2.4
1977	-1.3	0.0	-2.6	-1.3
1978	0.6	0.6	-1.4	-0.1
1979	-2.8	-4.8	-5.7	-4.5
1980	-1.1	-0.9	-3.9	-2.0
1981	0.8	2.2	-1.1	0.7
1982	-0.8	0.3	-3.5	-1.4
1983	-1.3	-0.3	-4.0	-1.9
1984	-2.6	-3.8	-5.7	-4.0
1985	-3.5	-3.6	-6.6	-4.6
1986	-0.2	0.3	-3.6	-1.2
1987	-0.9	0.5	-3.4	-1.2
1988	-1.3	-1.8	-3.8	-2.3
1989	-1.6	-1.5	-4.5	-2.5
1990	-0.5	0.6	-3.0	-1.0

^aOctober to March averages reported in °C.

Mean Regional 700 Mb To 800 Mb Winter
Wind Direction Data 1972 to 1989^a

Year	Grand Junction, Colorado WSO	Lander, Wyoming WSO	Salt Lake City, Utah WSO	Interpolated Study Area Direction
1972	205	269	248	241
1973	190	282	228	229
1974	208	268	238	237
1975	208	262	241	237
1976	210	260	251	242
1977	213	288	278	264
1978	217	289	240	244
1979	202	282	238	237
1980	209	252	238	233
1981	200	227	232	223
1982	219	236	236	232
1983	205	236	229	224
1984	200	240	241	230
1985	205	235	228	224
1986	218	224	239	231
1987	185	222	219	272
1988	191	239	233	269
1989	210	233	235	267
1990				

^aOctober to March averages reported in azimuth degrees.

APPENDIX B
SNOW SURVEY DATA

April 1 Snow Survey Measurements
 Uinta Mountain Sites 1972 To 1975^a

Site	Name	1972	1973	1974	1975
1.	Ashley-Twin Lakes	--	--	--	--
2.	Atwood Lake	--	--	--	--
3.	Beaver Creek Divide	--	--	--	--
4.	Blacks Fork Junction	38.9	27.3	34.1	26.1
5.	Brown Duck Ridge	55.0	--	39.1	--
6.	Buck Pasture	--	--	--	--
7.	Burts-Miller Ranch	26.9	29.7	27.8	22.2
8.	Chalk Creek #1	62.6	--	--	--
9.	Chalk Creek #2	45.6	--	--	--
10.	Chalk Creek #3	41.7	38.2	38.2	35.0
11.	Chepeta	--	--	--	--
12.	Chepeta-White R. Lake	--	--	--	--
13.	E. Fork Blacks Fork G.S.	39.3	29.7	34.3	32.1
14.	Five Points Lake	--	--	--	--
15.	Hayden Fork	71.9	51.8	54.9	57.1
16.	Henry's Fork	--	--	--	--
17.	Hewinta G.S.	42.9	30.7	39.0	29.6
18.	Hickerson Park	25.7	--	26.9	30.8
19.	Hole in the Rock	--	--	--	--
20.	Hole in the Rock G.S.	--	--	--	--
21.	Kings Cabin-Upper	36.6	43.2	18.2	25.0
22.	Lake Fork Basin	--	--	--	--
23.	Lake Fork Mountain	41.5	46.2	27.4	42.4
24.	Lake Fork Mountain #3	--	--	--	--
25.	Lightning Lake	--	--	--	--
26.	Lily Lake	44.5	40.5	40.5	--
27.	Middle Beaver Creek	--	--	--	--
28.	Mosby Mountain	37.0	40.8	19.8	33.4
29.	Paradise Park	45.7	47.0	22.9	36.7
30.	Redden Mine Lower	64.3	--	57.0	66.4
31.	Reynolds Park	--	--	--	--
32.	Rock Creek	36.7	41.9	22.1	39.5
33.	Sergeant Lakes	52.5	57.6	49.6	--
34.	Smith and Morehouse	54.0	48.3	47.5	45.2
35.	Smith and Morehouse	--	--	--	--
36.	Soapstone R.S.	49.6	45.1	42.6	46.7
37.	Spirit Lake	44.6	47.7	32.5	33.3
38.	Steel Creek Park	37.5	--	--	--
39.	Stillwater Camp	40.1	34.0	36.6	34.1
40.	Trial Lake	67.0	69.6	59.1	67.9
41.	Trout Creek	--	--	--	18.9

^a Reported in cm of snow water equivalent.

-- Missing Data.

April 1 Snow Survey Measurements
 Uinta Mountain Sites 1976 To 1979^a

Site	Name	1976	1977	1978	1979
1.	Ashley-Twin Lakes	--	--	--	--
2.	Atwood Lake	--	--	--	46.8
3.	Beaver Creek Divide	--	--	--	--
4.	Blacks Fork Junction	29.6	19.9	32.6	--
5.	Brown Duck Ridge	33.0	--	45.7	55.9
6.	Buck Pasture	--	--	--	--
7.	Burts-Miller Ranch	24.2	15.6	22.7	--
8.	Chalk Creek #1	--	--	--	--
9.	Chalk Creek #2	--	--	--	--
10.	Chalk Creek #3	39.0	21.1	34.5	--
11.	Chepeta	--	--	--	--
12.	Chepeta-White R. Lake	--	--	--	48.8
13.	E. Fork Blacks Fork G.S.	28.9	21.4	35.1	--
14.	Five Points Lake	--	--	--	40.3
15.	Hayden Fork	51.4	29.2	57.7	--
16.	Henry's Fork	--	--	--	--
17.	Hewinta G.S.	32.7	21.1	36.2	--
18.	Hickerson Park	23.7	20.7	19.2	--
19.	Hole in the Rock	--	--	--	--
20.	Hole in the Rock G.S.	--	--	--	--
21.	Kings Cabin-Upper	30.1	18.2	32.0	--
22.	Lake Fork Basin	--	--	--	50.4
23.	Lake Fork Mountain	27.6	19.7	37.5	32.3
24.	Lake Fork Mountain #3	--	--	--	16.3
25.	Lightning Lake	--	--	--	56.1
26.	Lily Lake	--	--	--	--
27.	Middle Beaver Creek	--	--	--	--
28.	Mosby Mountain	26.8	--	37.8	39.9
29.	Paradise Park	33.4	16.2	38.4	54.6
30.	Redden Mine Lower	61.1	32.2	65.4	--
31.	Reynolds Park	--	--	--	--
32.	Rock Creek	28.5	13.6	33.8	18.5
33.	Sergeant Lakes	--	--	--	--
34.	Smith and Morehouse	48.6	--	50.8	--
35.	Smith and Morehouse	--	25.6	--	--
36.	Soapstone R.S.	40.5	20.0	46.2	--
37.	Spirit Lake	29.5	24.7	31.2	--
38.	Steel Creek Park	--	--	--	--
39.	Stillwater Camp	31.3	20.7	33.9	--
40.	Trial Lake	58.5	27.0	72.0	--
41.	Trout Creek	31.0	--	27.6	--

^a Reported in cm of snow water equivalent.

-- Missing Data.

April 1 Snow Survey Measurements
 Uinta Mountain Sites 1980 To 1983^a

Site	Name	1980	1981	1982	1983
1.	Ashley-Twin Lakes	--	--	--	--
2.	Atwood Lake	--	--	44.5	37.6
3.	Beaver Creek Divide	--	33.5	63.0	52.5
4.	Blacks Fork Junction	40.7	26.7	40.4	28.5
5.	Brown Duck Ridge	55.8	37.9	63.8	49.9
6.	Buck Pasture	--	--	--	--
7.	Burts-Miller Ranch	--	28.2	31.2	24.3
8.	Chalk Creek #1	69.5	--	91.4	63.2
9.	Chalk Creek #2	44.8	--	53.7	40.8
10.	Chalk Creek #3	44.7	31.6	49.9	35.9
11.	Chepeta	--	--	--	--
12.	Chepeta-White R. Lake	--	--	--	--
13.	E. Fork Blacks Fork G.S.	38.4	30.0	41.7	31.8
14.	Five Points Lake	--	--	55.9	52.3
15.	Hayden Fork	--	40.5	71.7	54.9
16.	Henry's Fork	--	--	--	--
17.	Hewinta G.S.	36.6	29.9	43.8	35.3
18.	Hickerson Park	--	25.9	31.3	37.1
19.	Hole in the Rock	--	--	--	--
20.	Hole in the Rock G.S.	--	--	--	--
21.	Kings Cabin-Upper	44.6	26.7	40.5	39.0
22.	Lake Fork Basin	--	--	62.6	59.6
23.	Lake Fork Mountain	--	33.0	48.0	40.7
24.	Lake Fork Mountain #3	47.0	--	--	--
25.	Lightning Lake	--	--	61.5	77.5
26.	Lily Lake	--	--	53.5	38.3
27.	Middle Beaver Creek	--	--	--	--
28.	Mosby Mountain	39.6	30.9	60.3	45.4
29.	Paradise Park	45.5	36.1	56.0	56.7
30.	Redden Mine Lower	53.8	--	74.7	52.9
31.	Reynolds Park	--	--	--	--
32.	Rock Creek	42.2	29.8	42.5	38.8
33.	Sergeant Lakes	--	--	--	--
34.	Smith and Morehouse	55.7	41.2	--	45.2
35.	Smith and Morehouse	--	--	52.2	--
36.	Soapstone R.S.	53.4	25.6	60.4	44.8
37.	Spirit Lake	46.7	40.3	48.8	45.8
38.	Steel Creek Park	--	--	53.1	35.7
39.	Stillwater Camp	--	19.7	46.5	33.5
40.	Trial Lake	83.1	46.1	88.3	70.5
41.	Trout Creek	45.3	33.1	33.9	43.6

^a Reported in cm of snow water equivalent.

-- Missing Data.

April 1 Snow Survey Measurements
 Uinta Mountain Sites 1984 To 1987^a

Site	Name	1984	1985	1986	1987
1.	Ashley-Twin Lakes	--	--	68.6	35.3
2.	Atwood Lake	33.0	37.3	46.5	25.1
3.	Beaver Creek Divide	51.1	40.9	39.1	22.9
4.	Blacks Fork Junction	37.9	26.4	23.6	19.3
5.	Brown Duck Ridge	58.3	44.5	70.9	44.5
6.	Buck Pasture	--	--	64.0	36.8
7.	Burts-Miller Ranch	28.7	22.8	9.1	13.0
8.	Chalk Creek #1	70.5	--	85.1	45.7
9.	Chalk Creek #2	46.5	--	50.5	31.2
10.	Chalk Creek #3	47.6	36.4	14.2	16.0
11.	Chepeta	--	38.4	47.2	32.8
12.	Chepeta-White R. Lake	37.9	--	58.7	37.3
13.	E. Fork Blacks Fork G.S.	40.7	26.5	29.7	20.3
14.	Five Points Lake	56.6	47.5	61.7	36.3
15.	Hayden Fork	60.6	51.8	49.5	28.4
16.	Henry's Fork	--	--	48.0	33.5
17.	Hewinta G.S.	43.2	28.1	24.4	23.6
18.	Hickerson Park	30.4	19.4	17.8	21.3
19.	Hole in the Rock	--	--	15.5	17.8
20.	Hole in the Rock G.S.	--	--	6.6	12.7
21.	Kings Cabin-Upper	41.2	29.8	30.7	20.8
22.	Lake Fork Basin	44.2	45.0	66.3	38.6
23.	Lake Fork Mountain	38.1	38.0	42.7	25.9
24.	Lake Fork Mountain #3	--	--	23.4	14.0
25.	Lightning Lake	77.7	72.6	85.1	51.3
26.	Lily Lake	50.7	37.5	44.7	29.2
27.	Middle Beaver Creek	--	--	5.3	16.3
28.	Mosby Mountain	40.8	32.5	41.7	21.8
29.	Paradise Park	39.6	38.4	51.3	32.0
30.	Redden Mine Lower	48.1	55.4	63.0	28.2
31.	Reynolds Park	--	--	67.8	39.1
32.	Rock Creek	37.2	34.2	24.6	13.5
33.	Sergeant Lakes	--	--	26.7	23.1
34.	Smith and Morehouse	--	47.5	36.1	24.1
35.	Smith and Morehouse	52.8	--	39.9	30.0
36.	Soapstone R.S.	53.2	44.1	38.1	18.3
37.	Spirit Lake	45.3	35.7	35.8	42.7
38.	Steel Creek Park	47.5	33.4	53.1	41.4
39.	Stillwater Camp	43.3	30.5	31.2	19.6
40.	Trial Lake	71.8	64.4	98.3	48.3
41.	Trout Creek	33.8	30.3	30.5	25.1

^a Reported in cm of snow water equivalent.

-- Missing Data.

April 1 Snow Survey Measurements
 Uinta Mountain Sites 1988 To 1990^a

Site	Name	1988	1989	1990
1.	Ashley-Twin Lakes	21.6	33.0	39.5
2.	Atwood Lake	16.5	30.0	35.2
3.	Beaver Creek Divide	15.0	21.3	35.4
4.	Blacks Fork Junction	25.1	24.9	29.0
5.	Brown Duck Ridge	35.6	40.4	48.1
6.	Buck Pasture	29.7	42.7	41.7
7.	Burts-Miller Ranch	13.0	12.4	21.1
8.	Chalk Creek #1	42.9	52.6	63.1
9.	Chalk Creek #2	30.7	37.8	41.9
10.	Chalk Creek #3	17.0	42.7	33.1
11.	Chepeta	24.9	30.5	36.3
12.	Chepeta-White R. Lake	26.4	33.0	40.4
13.	E. Fork Blacks Fork G.S.	22.9	20.8	30.3
14.	Five Points Lake	23.9	34.0	44.8
15.	Hayden Fork	29.2	31.0	48.4
16.	Henry's Fork	30.5	29.7	34.3
17.	Hewinta G.S.	27.4	20.8	31.9
18.	Hickerson Park	26.9	19.3	24.7
19.	Hole in the Rock	20.1	12.2	16.8
20.	Hole in the Rock G.S.	13.5	--	10.9
21.	Kings Cabin-Upper	13.5	22.4	29.7
22.	Lake Fork Basin	36.6	39.4	48.5
23.	Lake Fork Mountain	17.3	24.1	34.3
24.	Lake Fork Mountain #3	7.1	9.1	18.0
25.	Lightning Lake	42.4	44.2	63.2
26.	Lily Lake	29.5	33.0	39.3
27.	Middle Beaver Creek	12.7	--	11.4
28.	Mosby Mountain	13.7	19.8	33.9
29.	Paradise Park	24.4	28.2	39.1
30.	Redden Mine Lower	30.2	33.8	51.5
31.	Reynolds Park	32.3	34.5	43.4
32.	Rock Creek	3.8	8.1	27.4
33.	Sergeant Lakes	19.8	23.4	36.1
34.	Smith and Morehouse	22.6	27.4	42.4
35.	Smith and Morehouse	27.9	34.3	37.0
36.	Soapstone R.S.	17.0	22.6	39.3
37.	Spirit Lake	29.5	28.2	37.8
38.	Steel Creek Park	41.9	36.3	41.2
39.	Stillwater Camp	22.1	24.4	30.9
40.	Trial Lake	41.1	54.4	62.4
41.	Trout Creek	20.1	21.8	31.4

^a Reported in cm. of snow-water equivalent.

-- Missing Data.

APPENDIX C
SNOW ACCUMULATION TREND SURFACE STATISTICS

Annual Corrected Snow Accumulation Trend Surface Statistics 1972 To 1984

Year	Mean SWE (cm) ^a	R	n	p	Standard Error	Trend Surface Equation
1972	45.9	0.753	24	0.001	8.3	-1061.652 + -28.579Lat + 20.053Lon + 0.02Elev
1973	47.7	0.706	18	0.019	8.3	411.55 + -44.504Lat + 12.641Lon + 0.018Elev
1974	36.7	0.848	21	0.000	6.9	-2882.024 + 4.075Lat + 24.443Lon + 0.018Elev
1975	40.7	0.882	19	0.000	7.1	-774.392 + -47.039Lat + 23.846Lon + 0.024Elev
1976	35.5	0.672	20	0.019	8.9	-926.066 + -17.886Lat + 15.144Lon + 0.006Elev
1977	21.6	0.606	17	0.104	4.3	-831.901 + 1.156Lat + 7.066Lon + 0.009Elev
1978	39.5	0.789	20	0.001	9.0	-759.017+ -36.766Lat + 20.342Lon + 0.018Elev
1979	41.8	0.847	11	0.025	9.0	120.370 + 9.107Lat + -5.097Lon + 0.037Elev
1980	49.3	0.678	18	0.031	9.4	-685.259 + -25.995Lat + 15.74Lon + 0.020Elev
1981	30.8	0.577	21	0.084	5.7	-310.610 + -7.805Lat + 5.657Lon + 0.013Elev
1982	54.0	0.731	29	0.000	10.7	-941.371 + -38.327Lat + 22.619Lon + 0.020Elev
1983	45.2	0.704	29	0.001	9.2	327.344 + -40.06Lat + 11.686Lon + 0.021Elev
1984	46.9	0.687	30	0.001	9.2	-1319.575+ -18.208Lat + 18.627Lon + 0.017Elev

^aApril 1 mean of all reporting sites.

Annual Corrected Snow Accumulation Trend Surface Statistics 1985 To 1990

Year	Mean SWE (cm) ^a	<i>R</i>	<i>n</i>	<i>p</i>	Standard Error	Trend Surface Equation
1985	38.9	0.787	28	0.000	7.9	$-386.376 + -38.509Lat + 17.569Lon + 0.019Elev$
1986	43.1	0.821	41	0.000	13.1	$-1004.652 + -49.699Lat + 26.304Lon + 0.059Elev$
1987	27.8	0.634	41	0.000	6.4	$-1115.959 + 1.388Lat + 9.066Lon + 0.030Elev$
1988	24.3	0.770	41	0.000	6.3	$-2287.318 + 21.329Lat + 12.389Lon + 0.026Elev$
1989	29.2	0.675	39	0.000	8.3	$-1996.124 + 7.487Lat + 14.915Lon + 0.025Elev$
1990	29.5	0.700	29	0.001	8.7	$-421.305 + -13.838Lat + 8.44Lon + 0.029Elev$
1972 to 1990	36.7	0.791	41	0.000	7.6	$-1240.72 + -21.835Lat + 18.898Lon + 0.028Elev$

^aApril 1 mean of all reporting sites.

APPENDIX D
RECONSTRUCTED GLACIER PARAMETERS

Stage Six Reconstructed Glacier Parameters

Basin	N Lat.	W Lon.	Toe Elev. (m)	Head- wall Elev.(m)	Median Altitude (m)	Area (km ²)
1. Swifts Canyon	40°41'	111°12'	2,360	3,100	2,730	3.7
2. Shingle Mill Creek	40°43'	111°12'	2,400	2,840	2,620	1.6
3. Ledge Fork Canyon	40°42'	111°10'	2,390	3,060	2,725	12.5
4. Smith and Morehouse	40°42'	111°04'	2,270	3,360	2,815	56.8
5. Weber River	40°43'	110°59'	2,330	3,480	2,905	112.6
6. Whitney	40°47'	110°55'	3,040	3,060	3,050	2.8
7. Bear River	40°45'	110°48'	2,510	3,680	3,095	211.8
8. Blacks Fork	40°55'	110°35'	2,410	3,810	3,110	320.5
9. Smiths Fork	40°52'	110°25'	2,730	3,960	3,345	92.3
10. Henrys Fork	40°52'	110°21'	2,720	3,810	3,265	62.5
11. West Fork Beaver Creek	40°53'	110°15'	2,610	3,670	3,140	30.4
12. Middle Fork Beaver Creek	40°53'	110°12'	2,670	3,640	3,155	36.8
13. Burnt Fork	40°52'	110°52'	2,420	3,710	3,065	54.8
14. White Rocks	40°45'	110°00'	1,660	3,690	2,675	150.7
15. Uinta River	40°45'	110°13'	2,100	3,980	3,040	295.2
16. Yellowstone River	40°42'	110°42'	2,170	4,040	3,105	222.6
17. Lake Fork	40°42'	110°34'	2,160	3,910	3,035	245.1
18. Rock Creek	40°38'	110°46'	2,220	3,790	3,005	286.3
19. Duchesne River	40°41'	110°51'	2,150	3,670	2,910	151.4
20. Soapstone	40°32'	110°59'	2,730	2,860	2,795	5.4
21. Provo River	40°39'	111°03'	2,350	3,460	2,905	188.6
22. Left Fork Beaver Creek	40°40'	111°12'	2,280	3,080	2,680	15.6

Accumulation Area Ratio Altitudes
Of Stage Six Reconstructed Glaciers

Basin	N Lat.	W Lon.	0.65 AAR (m)	0.60 AAR (m)	0.55 AAR (m)
1. Swifts Canyon	40°41'	111°12'	2,880	2,910	2,940
2. Shingle Mill Creek	40°43'	111°12'	2,650	2,680	2,700
3. Ledge Fork Canyon	40°42'	111°10'	2,710	2,720	2,730
4. Smith and Morehouse	40°42'	111°04'	2,690	2,730	2,750
5. Weber River	40°43'	110°59'	2,830	2,900	2,960
6. Whitney	40°47'	110°55'	3,040	3,040	3,040
7. Bear River	40°45'	110°48'	2,920	2,980	3,010
8. Blacks Fork	40°55'	110°35'	2,770	2,880	2,960
9. Smiths Fork	40°52'	110°25'	3,030	3,030	3,030
10. Henrys Fork	40°52'	110°21'	3,030	3,040	3,070
11. West Fork Beaver Creek	40°53'	110°15'	3,020	3,030	3,030
12. Middle Fork Beaver Creek	40°53'	110°12'	3,020	3,030	3,060
13. Burnt Fork	40°52'	110°52'	3,030	3,040	3,040
14. White Rocks	40°45'	110°00'	3,050	3,090	3,150
15. Uinta River	40°45'	110°13'	3,120	3,200	3,260
16. Yellowstone River	40°42'	110°42'	3,030	3,090	3,170
17. Lake Fork	40°42'	110°34'	3,010	3,060	3,060
18. Rock Creek	40°38'	110°46'	2,990	3,020	3,030
19. Duchesne River	40°41'	110°51'	2,820	2,900	2,980
20. Soapstone	40°32'	110°59'	2,740	2,740	2,740
21. Provo River	40°39'	111°03'	2,740	2,760	2,790
22. Left Fork Beaver Creek	40°40'	111°12'	2,360	2,370	2,390

Toe To Headwall Altitude Ratios
Of Stage Six Reconstructed Glaciers

Basin	Lat.	Lon.	0.45 THAR (m)	0.40 THAR (m)	0.35 THAR (m)
1. Swifts Canyon	40°41'	111°12'	2,693	2,656	2,619
2. Shingle Mill Creek	40°43'	111°12'	2,598	2,576	2,554
3. Ledge Fork Canyon	40°42'	111°10'	2,692	2,658	2,624
4. Smith and Morehouse	40°42'	111°04'	2,760	2,706	2,652
5. Weber River	40°43'	110°59'	2,848	2,790	2,732
6. Whitney	40°47'	110°55'	3,049	3,048	3,047
7. Bear River	40°45'	110°48'	3,036	2,978	2,920
8. Blacks Fork	40°55'	110°35'	3,040	2,970	2,900
9. Smiths Fork	40°52'	110°25'	3,284	3,222	3,160
10. Henrys Fork	40°52'	110°21'	3,210	3,156	3,102
11. West Fork Beaver Creek	40°53'	110°15'	3,087	3,034	2,981
12. Middle Fork Beaver Creek	40°53'	110°12'	3,106	3,058	3,010
13. Burnt Fork	40°52'	110°52'	3,000	2,936	2,872
14. White Rocks	40°45'	110°00'	2,574	2,472	2,370
15. Uinta River	40°45'	110°13'	2,946	2,852	2,758
16. Yellowstone River	40°42'	110°42'	3,012	2,918	2,824
17. Lake Fork	40°42'	110°34'	2,948	2,860	2,772
18. Rock Creek	40°38'	110°46'	2,926	2,848	2,770
19. Duchesne River	40°41'	110°51'	2,834	2,758	2,682
20. Soapstone	40°32'	110°59'	2,788	2,782	2,776
21. Provo River	40°39'	111°03'	2,850	2,794	2,738
22. Left Fork Beaver Creek	40°40'	111°12'	2,640	2,600	2,560

Stage Two Reconstructed Glacier Parameters

Basin	N Lat.	W Lon.	Toe Elev. (m)	Head- wall Elev.(m)	Median Altitude (m)	Area (km ²)
1. Swifts Canyon	40°41'	111°12'	2,880	3,100	2,880	2.1
2. Red Pine Creek	40°43'	111°10'	2,390	2,980	2,390	3.1
3. Ledge Fork Canyon	40°41'	111°90'	2,390	3,060	2,390	8.1
4. Smith and Morehouse	40°42'	111°03'	2,370	3,360	2,370	49.1
5. Weber River	40°42'	111°00'	2,300	3,410	2,300	75.8
6. Gold Hill	40°46'	110°55'	2,640	3,390	2,640	14.8
7. Hayden Fork Bear River	40°44'	110°52'	2,690	3,560	2,690	48.8
8. Stillwater Fork Bear River	40°44'	110°48'	2,680	3,680	2,680	65.7
9. East Fork Bear River	40°46'	110°43'	2,660	3,680	2,660	66.2
10. Mill Creek	40°52'	110°43'	3,030	3,380	3,030	3.0
11. Blacks Fork	40°52'	110°36'	2,450	3,800	2,450	253.2
12. Smiths Fork	40°52'	110°26'	2,730	3,960	2,730	86.8
13. Henrys Fork	40°50'	110°23'	3,000	3,810	3,000	43.6
14. West Fork Beaver Creek	40°52'	110°16'	2,710	3,670	2,710	27.6
15. Middle Fork Beaver Creek	40°52'	110°13'	2,730	3,640	2,730	32.3
16. Burnt Fork	40°51'	110°05'	2,730	3,710	2,730	48.2
17. West Fork Sheep Creek	40°51'	110°01'	2,760	3,440	2,760	31.2
18. East Fork Sheep Creek	40°51'	109°55'	2,730	3,400	2,730	19.9
19. Carter Creek	40°49'	109°52'	2,620	3,390	2,620	51.0
20. Leidy Peak	40°46'	109°46'	2,650	3,380	2,650	27.0
21. Ashley Fork	40°44'	109°49'	2,910	3,500	2,910	30.6
22. Marsh Peak	40°41'	109°48'	3,030	3,350	3,030	2.4
23. Dry Fork	40°42'	109°54'	2,300	3,660	2,300	86.5
24. White Rocks	40°45'	110°00'	2,350	3,680	2,350	141.7
25. Uinta River	40°45'	110°14'	2,360	3,980	2,360	250.4
26. Crow Canyon	40°36'	110°16'	2,650	3,650	2,650	23.2
27. Yellowstone River	40°45'	110°24'	2,440	4,040	2,440	186.4
28. Lake Fork	40°43'	110°36'	2,700	3,890	2,700	186.2
29. Rock Creek	40°39'	110°48'	2,370	3,760	2,370	256.8
30. Hades Canyon	40°34'	110°50'	2,490	3,360	2,490	13.7
31. Granddaddy Mountain	40°36'	110°51'	2,890	3,370	2,890	4.4
32. Duchesne River	40°42'	110°52'	2,540	3,670	2,540	100.2
33. Provo River	40°40'	110°57'	2,460	3,460	2,460	64.4
34. North Fork Provo River	40°39'	111°00'	2,360	3,380	2,360	52.2
35. Shingle Creek	40°39'	111°05'	2,400	3,060	2,400	14.8
36. Slate Creek	40°40'	111°10'	2,420	3,060	2,420	10.7
37. Left Fork Beaver Creek	40°39'	111°11'	2,370	3,080	2,370	5.2

Accumulation Area Ratio Altitudes
Of Stage Two Reconstructed Glaciers

Basin	N Lat.	W Lon.	0.65 AAR (m)	0.60 AAR (m)	0.55 AAR (m)
1. Swifts Canyon	40°41'	111°12'	3,010	3,020	3,020
2. Red Pine Creek	40°43'	111°10'	2,550	2,590	2,620
3. Ledge Fork Canyon	40°41'	111°90'	2,710	2,720	2,720
4. Smith and Morehouse	40°42'	111°03'	2,740	2,770	2,810
5. Weber River	40°42'	111°00'	2,980	3,000	3,020
6. Gold Hill	40°46'	110°55'	2,930	2,970	3,000
7. Hayden Fork Bear River	40°44'	110°52'	2,980	3,010	3,020
8. Stillwater Fork Bear River	40°44'	110°48'	3,020	3,040	3,050
9. East Fork Bear River	40°46'	110°43'	3,030	3,050	3,070
10. Mill Creek	40°52'	110°43'	3,030	3,040	3,050
11. Blacks Fork	40°52'	110°36'	2,980	3,010	3,020
12. Smiths Fork	40°52'	110°26'	3,030	3,030	3,040
13. Henrys Fork	40°50'	110°23'	3,160	3,180	3,210
14. West Fork Beaver Creek	40°52'	110°16'	3,030	3,040	3,090
15. Middle Fork Beaver Creek	40°52'	110°13'	3,040	3,100	3,200
16. Burnt Fork	40°51'	110°05'	3,040	3,080	3,160
17. West Fork Sheep Creek	40°51'	110°01'	3,000	3,020	3,030
18. East Fork Sheep Creek	40°51'	109°55'	2,930	2,980	3,030
19. Carter Creek	40°49'	109°52'	2,890	2,940	2,990
20. Leidy Peak	40°46'	109°46'	3,010	3,020	3,030
21. Ashley Fork	40°44'	109°49'	3,100	3,140	3,180
22. Marsh Peak	40°41'	109°48'	3,210	3,260	3,280
23. Dry Fork	40°42'	109°54'	3,020	3,030	3,070
24. White Rocks	40°45'	110°00'	3,080	3,130	3,190
25. Uinta River	40°45'	110°14'	3,250	3,290	3,310
26. Crow Canyon	40°36'	110°16'	2,930	3,020	3,030
27. Yellowstone River	40°45'	110°24'	3,170	3,240	3,290
28. Lake Fork	40°43'	110°36'	3,110	3,160	3,210
29. Rock Creek	40°39'	110°48'	3,220	3,030	3,040
30. Hades Canyon	40°34'	110°50'	2,900	2,950	2,990
31. Granddaddy Mountain	40°36'	110°51'	3,180	3,210	3,230
32. Duchesne River	40°42'	110°52'	3,010	3,020	3,030
33. Provo River	40°40'	110°57'	2,930	2,970	3,010
34. North Fork Provo River	40°39'	111°00'	2,770	2,800	2,850
35. Shingle Creek	40°39'	111°05'	2,790	2,810	2,860
36. Slate Creek	40°40'	111°10'	2,740	2,750	2,780
37. Left Fork Beaver Creek	40°39'	111°11'	2,770	2,810	2,860

Toe to Headwall Altitude Ratios
Of Stage Two Reconstructed Glaciers

Basin	N Lat.	W Lon.	0.45 THAR (m)	0.40 THAR (m)	0.35 THAR (m)
1. Swifts Canyon	40°41'	111°12'	2,979	2,968	2,957
2. Red Pine Creek	40°43'	111°10'	2,656	2,626	2,596
3. Ledge Fork Canyon	40°41'	111°90'	2,692	2,658	2,624
4. Smith and Morehouse	40°42'	111°03'	2,816	2,766	2,716
5. Weber River	40°42'	111°00'	2,800	2,744	2,688
6. Gold Hill	40°46'	110°55'	2,978	2,940	2,902
7. Hayden Fork Bear River	40°44'	110°52'	3,082	3,038	2,994
8. Stillwater Fork Bear River	40°44'	110°48'	3,130	3,080	3,030
9. East Fork Bear River	40°46'	110°43'	3,119	3,068	3,017
10. Mill Creek	40°52'	110°43'	3,188	3,170	3,152
11. Blacks Fork	40°52'	110°36'	3,058	2,990	2,922
12. Smiths Fork	40°52'	110°26'	3,284	3,222	3,160
13. Henrys Fork	40°50'	110°23'	3,364	3,324	3,284
14. West Fork Beaver Creek	40°52'	110°16'	3,142	3,094	3,046
15. Middle Fork Beaver Creek	40°52'	110°13'	3,140	3,094	3,048
16. Burnt Fork	40°51'	110°05'	3,171	3,122	3,073
17. West Fork Sheep Creek	40°51'	110°01'	3,066	3,032	2,998
18. East Fork Sheep Creek	40°51'	109°55'	3,032	2,998	2,964
19. Carter Creek	40°49'	109°52'	2,966	2,928	2,890
20. Leidy Peak	40°46'	109°46'	2,978	2,942	2,906
21. Ashley Fork	40°44'	109°49'	3,176	3,146	3,116
22. Marsh Peak	40°41'	109°48'	3,174	3,158	3,142
23. Dry Fork	40°42'	109°54'	2,912	2,844	2,776
24. White Rocks	40°45'	110°00'	2,948	2,882	2,816
25. Uinta River	40°45'	110°14'	3,089	3,008	2,927
26. Crow Canyon	40°36'	110°16'	3,100	3,050	3,000
27. Yellowstone River	40°45'	110°24'	3,160	3,080	3,000
28. Lake Fork	40°43'	110°36'	3,236	3,176	3,116
29. Rock Creek	40°39'	110°48'	2,996	2,926	2,856
30. Hades Canyon	40°34'	110°50'	2,882	2,838	2,794
31. Granddaddy Mountain	40°36'	110°51'	3,106	3,082	3,058
32. Duchesne River	40°42'	110°52'	3,048	2,992	2,936
33. Provo River	40°40'	110°57'	2,910	2,860	2,810
34. North Fork Provo River	40°39'	111°00'	2,819	2,768	2,717
35. Shingle Creek	40°39'	111°05'	2,697	2,664	2,631
36. Slate Creek	40°40'	111°10'	2,708	2,676	2,644
37. Left Fork Beaver Creek	40°39'	111°11'	2,690	2,654	2,618

VITA

Greg C. Schlenker was born at Travis Air Force Base, California, on February 20, 1957, to Joseph R. and Eunice M. Schlenker.

Mr. Schlenker attended high school in Germany and Utah, graduating from Weber High School in Pleasant View, Utah, in 1976. Following high school, Mr. Schlenker attended Weber State College in Ogden, Utah, where he graduated with a Bachelor of Science degree in Geography in 1982. In 1984 Mr. Schlenker commenced work towards a Master of Science degree in Geography at the University of Utah in Salt Lake City, Utah. He completed the Master of Science degree in 1988. In the Fall of 1989, Mr. Schlenker enrolled in the Doctor of Philosophy program in Geography at Texas A&M University.

While attending the University of Utah, Mr. Schlenker became employed part-time with the Salt Lake City office of Sergent, Hauskins and Beckwith Geotechnical Engineers. In 1992, following completion of residency and course work at Texas A&M University, Mr. Schlenker returned to Salt Lake City to work full-time with Sergent, Hauskins and Beckwith Geotechnical Engineers, now AGRA Earth and Environmental Services, where he is presently employed as a Project Engineering Geologist.

Mr. Schlenker's Doctor of Philosophy program concludes with this dissertation.
His permanent address is:

4091 Juniper Lane

Eden Utah, 84310